Crosstalk between membrane trafficking and cell adhesion: The role of the SNARE protein TI-VAMP in neuronal morphogenesis

I n a u g u r a l - D i s s e r t a t i o n

zur

Erlangung des Doktorgrades

der Mathematisch-Naturwissenschaftlichen Fakultät

der Universität zu Köln

vorgelegt von

Philipp Alberts

aus Coesfeld, Westfalen

2004

Berichterstatter : Professor Jonathan C. Howard, Institut für Genetik, Universität zu Köln

Professor Thomas Langer, Institut für Genetik, Universität zu Köln

Dr Thierry Galli, Institut Fer-à-Moulin, Paris

Tag der mündlichen Prüfung in Form der Disputation: 15.01.2004

Abstract

The membrane trafficking pathway mediated by the SNARE protein Tetanus neurotoxin-Insensitive Vesicle Associated Membrane Protein (TI-VAMP) in neurons is still unknown. In this work, I show that TI-VAMP expression is necessary for neurite outgrowth in PC12 cells in culture. TI-VAMP interacts with plasma membrane and endosomal target SNAREs suggesting that TI-VAMP mediates a recycling pathway. This view is supported by the direct demonstration that TI-VAMP recycles from and to the plasma membrane. L1, a cell-cell adhesion molecule involved in axonal outgrowth, colocalizes with TI-VAMP in the developing brain, neurons in culture, and PC12 cells. Plasma membrane L1 is internalized into the TI-VAMP-containing compartment. Silencing of TI-VAMP results in reduced expression of L1 at the plasma membrane and impaired L1- but not N-Cadherin-mediated adhesion. Futhermore, the TI-VAMP-compartment is specifically recruited to L1 bead-cell junctions in an actin-dependent manner suggesting that axon guidance cues like L1-ligation act by controlling cytoskeletal and membrane dynamics in a coordinated manner. In conclusion, TI-VAMP mediates the intracellular transport of L1 and L1-mediated adhesion controls this membrane trafficking, thereby suggesting that cross-talk between membrane trafficking and cell-cell adhesion plays a central role in coordinating axonal outgrowth and pathfinding.

Zusammenfassung

Die Rolle des vesikulären Transports in Neuronen, welcher von dem SNARE Protein Tetanus neurotoxin-Insensitive Vesicle Associated Protein (TI-VAMP) vermittelt wird, ist unklar. In dieser Arbeit ist gezeigt, das die Expression von TI-VAMP für effizientes Auswachsen von Neuriten notwendig ist. TI-VAMP interagiert mit target SNARE Proteinen der Plasma Membran und des endosomalen Systems. Es kann gezeigt werden, das TI-VAMP-positive Vesikel mit der Plasmamembrane fusionieren. Daher kann davon ausgegangen werden kann, dass TI-VAMP den Austausch von Proteinen und Lipiden zwischen der Zelloberfläche und einem intrazellulären, endosomalen System vermittelt. Das Zell-Zell Adhesionsmolekül L1, welches eine wichtige Rolle in der Gehirnentwicklung spielt, kolokalisiert mit TI-VAMP im embryonalen Gehirn, in *in vitro*-kultivierten Neuronen sowie in der Zellinie PC12. L1 wird von der Plasmamembran in ein intrazelluläres, TI-VAMP-positives Membrankompartiment aufgenommen. Die Inhibierung der TI-VAMP-Expression provoziert eine verminderte Expression von L1 an der Zelloberfläche und selektive Instabilität von L1-vermittelten adhesiven Kontakten. Weiterhin rekrutieren L1-abhängige Kontakte TI-VAMP-positive Vesikel, ein Phänomen, welches von dem Aktincytoskelett abhängig ist. Diese Beobachtungen legen die Hypothese nahe, dass Signale wie zum Beispiel die Aktivierung des Adhesionsmolküls L1, welche das Navigieren von Axonen während der Gehirnentwicklung ermöglichen, die Dynamik des Cytoskeletts und von Membranverkehr in koordinierter Weise kontrollieren. Es lässt sich der Schluss ziehen, dass TI-VAMP den intrazellulären Transport von L1 vermittelt und das gleichzeitig L1-vermittelte Adhesion die Dynamik dieses Membrantransportweges kontrolliert. Der Austausch zwischen Membranverkehr und Zelladhäsion könnte von entscheidender Wichtigkeit für Phänomene wie das koordinierte Auswachsen von Axonen entlang vorbestimmter Pfade während der embryonalen Hirnentwicklung sein.

Abbreviations

ARF	ADP ribosylation factor
ATP	Adenosine 5’-triphosphate
BFA	Brefeldin A
BSA	Bovine serum albumin
CAM	Cell Adhesion Molecule
DMEM	Dulbecco’s modified Eagle’s medium
EDTA	Ethylenediamine-tetraacetic acid
ER	Endoplasmic reticulum
GST	Glutathione-S-transferase
GTP	Guanosine 5’-triphosphate
IgCAM	Cell Adhesion Molecule of the Immunoglobulin Superfamily
IgG	Immunoglobulin class G
kDa	kilo Dalton
MVB	Multivesicular body
MVE	Multivesicular endosome
NSF	N-ethylmaleimide-sensitive factor
oN	over Night
PAGE	Polyacrylamide gel electrophoresis
PBS	Phosphate buffered saline
PCR	Polymerase chain reaction
RT	Room Temperature
SDS	Sodium dodecylsulphate
siRNA	small inhibitory RNA
SNAP	Soluble NSF attachment protein
SNARE	SNAP receptor
Stx	Syntaxin
Syb 2	Synaptobrevin 2
SNAP-25	Synaptosome associated protein of 25 kDa
TBS	Tris buffered saline
TGN	Trans Golgi network
TI-VAMP	Tetanus neurotoxin Insenstive VAMP

TMD	Transmembrane domain
TeNT	Tetanus Neurotoxin
Tris	Tris[Hydroxymethyl]aminomethane
VAMP	Vesicular Membrane Associated Protein

Table of contents

III. Results 39

I. Introduction

The structure of the nervous system is of great complexity. A high number of distinct neuronal cell types interact with each other via a sophisticated network of specific interactions, sometimes over long distances. At the same time, communication points between neurons are not static, but can be modified, which ultimately allows for the fascinating properties of the nervous system, including learning and memory.

For insight into the complex function of the brain, the molecular mechanisms that warrant brain development have to be elucidated. What are the molecular events that mediate the correct wiring of the highly diverse neuronal connections? It is known that the pattern of connections between neurons is organized by guidance cues which are correspondingly of highest diversity. For example Cadherins, which play a fundamental role in brain development, constitute a large gene family (Yagi and Takeichi, 2000). It is most interesting that the genomic organization of a subgroup of Cadherins, the so called protocadherins, shows similarities to the genomic organization of B- and T-cell receptors of the lymphoid system (Wu and Maniatis, 1999). The well known genomic reorganization of B- and T-cell receptors is the fundamental principle by which the almost unlimited diversity within the immune system is generated, and a similar mechanism might be involved in the generation of diversity during brain development.

Yet, inherent to the generation of complexity, a fundamental problem arises; how to establish specificity in an environment which is of highest diversity? Neurons have to grow axons and dendrites to their specific target along specific pathways. Contact formation has to occur at the right place and the right time, and during its journey the growing neurite has to ignore a number of cues, that are recognized by others as their target. Thus, neurons have to be equipped with a highly sensitive apparatus that reads and interprets cues and that allows advance while preventing the premature establishment of contacts.

For all these reasons, studying the molecular mechanisms of neurite outgrowth is of fundamental importance in order to understand the complex wiring of the nervous system. A huge number of studies on the role of attractive and repulsive

cues and their effects on the neuronal cytoskeleton has led to an impressive knowledge as to how these molecules might work during brain development. In contrast, the role of membrane trafficking during neuronal morphogenesis has received little attention, although it is the delivery of membrane which ultimately allows the neuron to grow. Clearly, for site-directed growth to occur, the delivery of membrane has to be tightly connected to the signaling molecules that guide axons and dendrites during brain development

One reason for the poor knowledge about membrane trafficking in neuronal differentiation might be that molecular markers for specific neuronal membrane compartments with a function in membrane trafficking were sparse. This has changed with the discovery of SNARE proteins, which are essential players in membrane trafficking of eukaryotes. Specific SNARE proteins are expressed in specific membrane compartments and thus the study of a given SNARE protein will lead to a deeper understanding of membrane trafficking pathways and their function (see Fig I1). Therefore, the goal of this thesis was to characterize the role of TI-VAMP/VAMP7, a recently discovered SNARE protein, in the differentiation of neuronal cells.

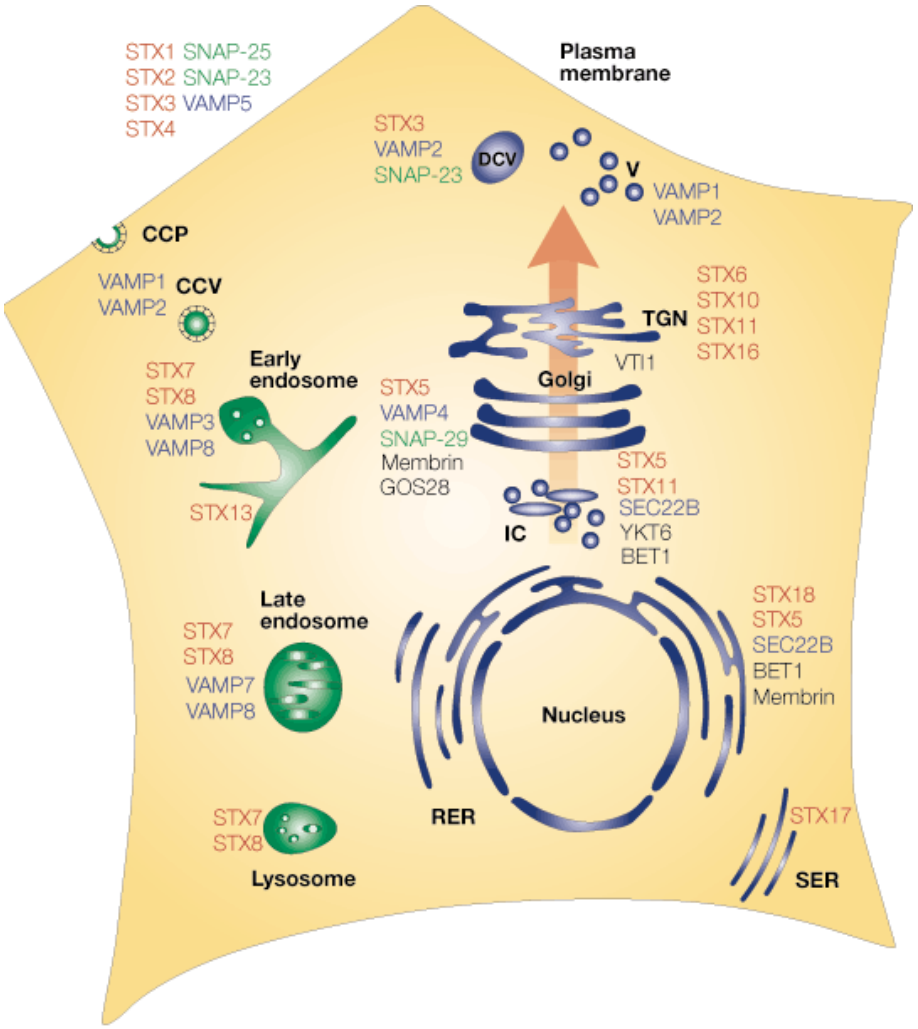

Figure I1) Subcellular localization of mammalian SNARE proteins

The mammalian SNAREs that have been studied so far localize to distinct subcellular compartments in the secretory pathway. (Red, syntaxin family; blue, VAMP family; green, SNAP-25 family; black, others. CCP, clathrin-coated pits; CCV, clathrin-coated vesicles; DCV, dense core vesicles; IC, intermediate compartment; RER, rough endoplasmic reticulum; SER, smooth endoplasmic reticulum; SNAP-25, 25 kDa synaptosome-associated protein; TGN, *trans*-Golgi network; V, vesicles; VAMP, vesicle-associated membrane protein.) (from Chen and Scheller, 2001).

In this introduction, I will first give an overview of the general molecular mechanisms of membrane trafficking, as they can be found from yeast to human. Secondly, I will present the current knowledge of the role of membrane trafficking in neuronal morphogenesis.

I.1 Membrane trafficking in eukaryotic cells: a historical overview

Based on morphological and pulse chase studies on the secretory process in pancreatic cells, George Palade suggested in 1975 (Palade, 1975) that granules release their protein content into the extracellular lumen via a process termed ”exocytosis” or ”membrane fusion”. The membrane of the granule fuses with the plasma membrane and the content is released into the extracellular medium while the diffusion barrier between the cytosol and the extracellular medium is maintained. Moreover, exocytosis was observed to occur in a site-directed and stimulus-dependent way. Thus, granules fuse with the apical, but not the basolateral plasma membrane and hormones can trigger the release of secretory granules in exocrine cells. The astonishing fidelilty by which granules fuse only with the plasma membrane despite the existence of numerous intracellular organelles at similar distance led to the suggestion that ”complementary recognition sites in each membrane may be involved in binding preliminary to fusion” (Palade, 1975). The work on the secretory process in pancreatic cells provided the conceptual framework for later studies: a vectorial flow of proteins and lipids between different compartments of the cell exists, and this flow is mediated by discrete transport carriers or vesicles. The secretion of granules is tightly regulated in space and can be regulated in time by stimulus-secretion coupling indicating a high degree of plasticity in membrane trafficking.

The identification of the key molecular components, that correspond to the ”complementary recognition sites” predicted by Pallade, has been achieved by the convergence of two different approaches, yeast genetics (Novick et al., 1980) and in *vitro* reconstitution of intracisternal transport in the Golgi stack of a mamalian cell line (Balch et al., 1984). Randy Schekman and co-workers took advantage of the fact that yeast cells defective in secretion accumulate newly synthesized proteins and lipids while plasma membrane growth ceases, inducing an increase in cell density. Thus, temperature sensitive mutant cells were selected by simple density gradient centrifugation separating dense and therefore secretion defective cells from non-defective cells. This approach led to the identification of 23 distinct gene products

necessary for secretion and thus cell growth in yeast, called *sec* 1-23 (Novick et al., 1980).

Ultrastructural analysis of the mutant strains grown at the restrictive temperature revealed that the different *sec* mutants could be classified into three different categories: accumulation of ER structures (1), accumulation of so called Berkeley bodies, similar to Golgi (2) or accumulation of vesicles of 80-100 nm in diameter (3) (Novick et al., 1980). To assess the order in which the individual gene products were required for secretion, double mutant strains of the different *sec* mutants were generated and a comparative analysis of the single and double mutant strains was performed. It was observed that defects in genes producing an ER phenotype were always dominant over genes producing a Berkeley body or 80-100nm vesicle phenotype, indicating that the ER mutants are blocked before the Golgi and 100 nm vesicle stage. In turn Golgi mutants were dominant over the 100 nm vesicle stage. This analysis allowed for the establishment of an order of events in the secretory pathway in yeast (Novick et al., 1981). Interestingly, secretion in yeast was essentially identical to the order of events in the secretory pathway in mamalian pancreatic cells (Palade, 1975). Moreover, this work opened the way for the search for key molecules controlling different steps in the secretory pathway in yeast.

Jim Rothman and colleagues reconstituted intra-Golgi transport *in vitro* to analyze the molecular confinements of this transport mechanism. A thorough analysis of this transport assay led to the discovery of numerous key molecules in membrane trafficking.

Transport between Golgi membranes is mediated by vesicular intermediates (Balch et al., 1984). Fusion of these vesicles with the acceptor membranes could be inhibited when the non-hydrolyzable GTP-analogue GTP-γS was added or by pretreatment of the cytosol with the cysteine alkylating agent NEM (N-ethylmaleimide) (Orci et al., 1989). Both treatments led to the accumulation of vesicles, yet of different morphology. Whereas GTP-γS treatment leads to the accumulation of vesicles carrying a coat, NEM treatment leads to the accumulation of uncoated vesicles. Treatment with both agents leads to the accumulation of coated vesicles only, demonstrating that GTP-γS action precedes the function of the NEM-sensitive component in vesicular trafficking (Orci et al., 1989). The accumulation of coated vesicles upon GTP-γS treatment allowed for the biochemical purification of

these vesicles and analysis of the coat components. The target of GTP-γS is a cytosolic GTP-binding protein called ARF (Serafini et al., 1991), whereas the coat seen by electron microscopy is made of seven proteins termed COP (Waters et al., 1991). As will be seen later, ARF-dependent recruitment of coat proteins to the donor membrane is an essential step in the formation of most transport vesicles in the eukaryotic cell (Chavrier and Goud, 1999).

The NEM-sensitive cytosolic component, essential for intra Golgi transport after coat recruitment and vesicle formation, was found to be a 76kDa protein that forms homotetramers and has ATP binding and hydrolyzing activity. The purified protein restored transport in a NEM-blocked transport assay, and was by itself NEM sensitive. (Wilson et al., 1989) Importantly, the NSF protein (for **N**EM **S**ensitive **F**actor) was the mammalian homologue to the *sec*18 gene identified by Novick and Schekman (Block and Rothman, 1992). Thus, the authors were able to test the hypothesis, that a similar fusion machinery might operate in yeast and mammals by replacing mammalian cytosol with cytosol from wildtype or *sec*18 yeast mutants. Indeed, cytosol from WT yeast could restore intra-Golgi traffick *in vitro* and a NEM sensitive factor was required, whereas cytosol generated from *sec*18 mutants failed to restore transport (Wilson et al., 1989).

This was the first direct evidence that a general fusion machinery exists, which is conserved from yeast to mammals. Even plant cytosol could operate in the Golgi transport assay, which extended the generality of the finding to all eukaryotic cells (Paquet et al., 1986). It was surprising that NSF in yeast was essential for protein export from the ER and NSF in mammalian cells for intra-Golgi transport, yet they were functionally interchangeable. This led to the conclusion, that NSF is a general fusion protein which must in some way interact with factors specific for different transport steps (Block and Rothman, 1992).

Whereas NSF could be found associated with membrane, purified NSF would not bind to Golgi membranes, unless cytosol was added. This triggered the search and purification of the **S**oluble **N**SF **A**ttachment **P**roteins or SNAPs. The homologous proteins α-, β-, and γ-SNAP could be purified from bovine brain based on their ability to attach NSF to Golgi membranes and thus restore transport in the *in vitro* assay (Clary et al., 1990). As with NSF, a yeast mutant (*sec*17) identified in the screen of Novick and Schekman failed to restore SNAP activity, but could be rescued

by addition of purified mammalian SNAP further strengthening the view, that a conserved fusion machinery was operating (Clary et al., 1990).

Salt stripped Golgi membranes would bind NSF only when purified α-, or β-SNAP was present indicating the existence of a membrane integral **SN**AP **RE**ceptor or SNARE protein. Purified NSF and SNAP bound to the SNARE could be extracted from Golgi membranes with detergent as a stable 20S particle. Thus, four proteins were isolated from bovine brain as SNAP receptors which had been previously purified and cloned as abundant transmembrane proteins of the presynaptic terminal: Synaptobrevin, Syntaxin 1 and SNAP-25 (Söllner et al., 1993b). Further characterization of the 20S particle revealed that all three SNARE proteins identified from bovine brain were present in a single 20S particle together with NSF and SNAP, and that ATPase activity of NSF dissociates the complex (Söllner et al., 1993a). This finding strongly suggested an important role for SNARE proteins in a late step in membrane fusion, since NSF was known function after vesicle formation. Intriguingly, Synaptobrevin localizes to synaptic vesicles, whereas Syntaxin and SNAP-25 are expressed on the synaptic plasma membrane, thus complex formation between these proteins should occur when the synaptic vesicle has approached the presynaptic membrane (Baumert et al., 1989; Bennett et al., 1992; Oyler et al., 1989; Rothman, 1994). An essential role for SNARE proteins in neurotransmitter release had been proposed shortly before (Schiavo et al., 1992). Clostridial neurotoxins which completely block neurotransmitter release are in fact proteases which cleave the synaptic SNARE proteins Synaptobrevin, SNAP-25 or Syntaxin 1 (Blasi et al., 1993a; Blasi et al., 1993b; Schiavo et al., 1992). Taking all these observations into consideration, Rothman and colleagues suggested a molecular mechanism, which would explain vesicle docking and fusion in molecular terms, the so called SNARE hypothesis (Rothman and Warren, 1994; Söllner et al., 1993a; Söllner et al., 1993b). Each transport step within the eukaryotic cell is mediated by an original pair of SNAREs which reside on the vesicle (the v-SNARE) and the target membrane (the t-SNARE). Complex formation between cognate v- and t-SNAREs would provide the specificity of vesicular docking to the target membrane. Fusion of the vesicle with its target membrane would then be mediated by the concerted action of the general fusion proteins SNAP and NSF.

The predictions of the SNARE hypothesis as they were formulated in 1993 did not hold true in all details, as will be described below. Nevertheless, the

SNARE hypothesis provided the conceptual framework that stimulated and guided studies that aimed at understanding the molecular mechanisms of membrane trafficking.

I.2 SNARE proteins in membrane trafficking: the current view

A common theme of vesicular trafficking is that cargo-loaded transport vesicles are formed in a donor membrane and transported to their specific target organelle. Fusion of the vesicle with its target results in the vectorial transport of cargo. As mentioned above, the step of NSF/SNAP and SNARE dependent vesicle fusion with the target membrane could be distinguished biochemically in the *in vitro* Golgi transport assay from earlier events like vesicle formation. Therefore the intial events in membrane trafficking will be discussed briefly before introducing the function of SNARE proteins in membrane fusion.

I.2.1 The formation of cargo loaded vesicles by coat proteins

The recruitment of cargo proteins destined to leave a donor compartment in transport vesicles is mediated by direct and indirect interactions with cytosolic factors which form a coat. Coat formation ultimately leads to vesicle formation by direct coat-dependent deformation of the membrane or coat dependent recruitment of specialized fission proteins (Farsad and De Camilli, 2003; Kirchhausen, 2000). The ARF-dependent recruitment of coat proteins, as it was described by Rothman and colleagues (see above), is a paradigm for coat formation (Chavrier and Goud, 1999). Eight different coats, which are mainly multi-subunit protein complexes, have been identified in mammalian cells and most of which are conserved from yeast to mammals (Bonifacino and Lippincott-Schwartz, 2003). Different coat complexes serve different trafficking pathways which coincides with their differential localization throughout the cell. Coats forming at the different membrane compartments can be subdivided into two major groups, those that functionally depend upon the structural protein clathrin or those that are clathrin independent. The first group includes the adaptor protein complexes (AP) 1 and 2, which are multisubunit complexes made of

four different polypeptides. GGAs (Golgi-localized, ?-ear-containing, ARF-binding proteins) constitute a protein family of three members (GGA 1, 2 and 3) which form monomeric coats and function via clathrin recruitment like AP1 and 2. AP-3 and AP-4 are homologue to AP-1 and 2, but function in a clathrin independent manner like the complexes COP I and COP II.

Demonstrating the essential role of coat formation in the early secretory pathway several *sec* mutants were later on identified as genes coding for subunits of COPI and II (Kirchhausen, 2000; Novick et al., 1980). Mutants of clathrin in mammalian cells are lethal, (Wettey et al., 2002) whereas yeast mutants show delayed growth, but are still viable (Payne and Schekman, 1985). This is similar with adaptor proteins. Mouse mutants of subunits of AP-1 and 2 are lethal and mutants of AP subunits in Drosophila and Caenorhabditis show a strong phenotype (Zizioli et al., 1999; Gonzalez-Gaitan et al., 1997; Meyer et al., 2000), whereas yeast cells mutant in all AP subunits are still viable (Huang et al., 1999). Thus, in contrast to yeast, in multicellular organisms the efficiency of AP-mediated trafficking pathways seems to be indispensable for proper development.

Coat independent pathways are known to exist in the endocytic pathway, particularly macropinocytosis and phagocytosis (Bonifacino and Lippincott-Schwartz, 2003), but they do not seem to be able to compensate for loss of the major endocytic pathway, which depends on clathrin (Wettey et al., 2002).

I.2.2 The targeted delivery of vesicles by tethering factors and Rab proteins

After coat-dependent cargo selection and vesicle formation, the transport carrier finds its way towards its specific target membrane. Long-range movements of vesicles and organelles are mediated by specific motor proteins of the dynein or kinesin family, which bind to microtubules. Specific members of kinesin interact with their specific cargo organelle to mediate transport to its final destination (Peretti et al., 2000; Setou et al., 2000). For example KIF4, a neuronal motor protein of the kinesin family, mediates long-range anterograde axonal transport of specific transport carriers from the cell body towards the tip of the axon, whereas other vesicles transported in the same direction are apparently independent of KIF4 (Peretti et al.,

2000). Following the microtubule-dependent long-range transport, many vesicles will undergo local movements on F-actin, which are powered by members of the myosin protein family. Again, specific myosin isoforms exist, which mediate movement of specific target organelles on the actin cytoskeleton (Hammer and Wu, 2002).

How do transport vesicles interact specifically with their target membrane? It was originally proposed that specific pairing between SNARE proteins would result in the docking of the vesicle to its target membrane followed by the final fusion reaction (Söllner et al., 1993a). This seems not to be the case. Inactivation of SNARE proteins of the synaptic SNARE complex with botulinum neurotoxins blocks neurotransmitter release in the giant-squid nerve terminal, but the number of vesicles docked to the active zone is in fact doubled, and not diminished (Hunt et al., 1994). Genetic inactivation of synaptic v- and t-SNAREs in Drosophila showed that vesicles were still docked to the presynaptic plasma membrane, but were unable to release neurotransmitter in the perisynaptic cleft (Broadie et al., 1995).

The molecular nature of docking factors which act independently and upstream of SNARE proteins was first described in yeast. *In vitro* reconstitution of ER-to-Golgi transport with purified proteins showed that vesicles can dock to Golgi membranes even in the absence of functional SNARE proteins mediating this transport step. Instead, docking requires the concerted action of two cytosolic proteins: a GTPase of the Rab family, Ypt1p, and another protein called Uso1p (Cao et al., 1998). The active GTP bound form of Ypt1p mediates the recruitment of Uso1p to the target membrane (the Golgi) (Cao and Barlowe, 2000). The following Uso1p-dependent binding of vesicles to the Golgi membrane was termed ”tethering” (Cao et al., 1998). The mammalian homologue of Uso1p, p115, was shown to act in ER to Golgi transport, and its action to be controlled by Rab 1, the mammalian homologue of Ypt1p (Allan et al., 2000).

The importance of tethering factors *in vivo* became clear when the gene products of *sec* 3, 5, 6, 8, 10, 15, together with Exo70 and Exo84, where shown to form a multisubunit tethering complex called the exocyst (Novick et al., 1980; TerBush et al., 1996). Similar to Uso1p and YPT1p, formation of the exocyst at the plasma membrane in yeast is controlled by a Rab protein called Sec 4 (TerBush et al., 1996). A mammalian homologue of the exocyst has been isolated, which plays a role similar to the yeast exocyst in recruiting exocytotic vesicles (Grindstaff et al., 1998). Now, tethering factors, which are recruited by the action of Rab proteins, have

been detected in a number of trafficking steps (Zerial and McBride, 2001). Interestingly, Rab proteins are also involved in the organization of organelle transport along the cytoskeleton, highlighting the importance of Rab proteins in a number of membrane trafficking steps (Hammer and Wu, 2002).

I.2.3 SNARE proteins and membrane fusion

Once docked, a donor vesicle fuses with its target membrane resulting in content mixing or release into the extracellular medium, in the case of exocytosis. SNARE proteins play a critical role in this last step of membrane trafficking. The proteins Synaptobrevin, Syntaxin 1 and SNAP-25 are the founding members of a superfamily of SNARE proteins (Weimbs et al., 1998) which is expressed in all eukaryotic organisms analysed so far. SNAREs are membrane anchored either by a single transmembrane domain like Synaptobrevin and Syntaxin 1 or via cystein linked palmitoylation like SNAP-25. The hallmark of all SNARE proteins is a stretch of about sixty amino acids containing conserved heptad repeat sequences that form coiled-coil structures, wheras N-terminal sequences and the transmembrane domains show very little homology (Fasshauer et al., 1998). The crystal structure of the synaptic core complex revealed that the coiled-coil domain of synaptobrevin, syntaxin and two coiled coil domains provided by SNAP-25 form a bundle of four α-helices aligned in parallel (See Figure I2) (Sutton et al., 1998). The bundle of α-helices forms sixteen layers of interacting amino acid side chains, which are hydrophobic except the central or zero layer. The central layer is made of hydrophilic amino acids, which are three glutamines (Q) contributed by SNAP-25 and syntaxin 1 and one arginine (R) contributed by synaptobrevin (Sutton et al., 1998). Based on the crystal structure and sequence comparisons, SNARE proteins were reclassified from t- and v-SNAREs into Q-SNAREs which contribute the glutamine to the central ionic layer and R-SNAREs which contribute the arginine (Fasshauer et al., 1998). Four distinct subgroups of SNARE proteins can be distinguished based on homologies of their coiled-coil domains: a syntaxin family of Qa-SNAREs, a SNAP-25 family of Qb-SNAREs homologous to the N-terminal coiled coil of SNAP-25, a SNAP-25 family of Qc-SNAREs homologous to the C-terminal coiled-coil, and a synaptobrevin family of R-SNAREs.

The detailed analysis of a SNARE complex operating in endosomal fusion showed that the N- and C-terminal coiled-coil domain provided by SNAP-25 for the synaptic core complex can be provided by two different polypeptides (Antonin et al., 2000). Furthermore, the crystal structure of this endosomal complex consisting of the R-SNARE VAMP-8 and the Q-SNAREs Syntaxin 7, Syntaxin 8 and Vti1b showed striking similarity to the structure of the synaptic core complex (Antonin et al., 2002). Based on the analysis of a number of SNARE complexes from different fusion steps within the cell, the current model predicts that the structure and function of SNARE complexes is conserved and consists of one R-SNARE and three Q-SNAREs (Chen and Scheller, 2001)(see Figure I2).

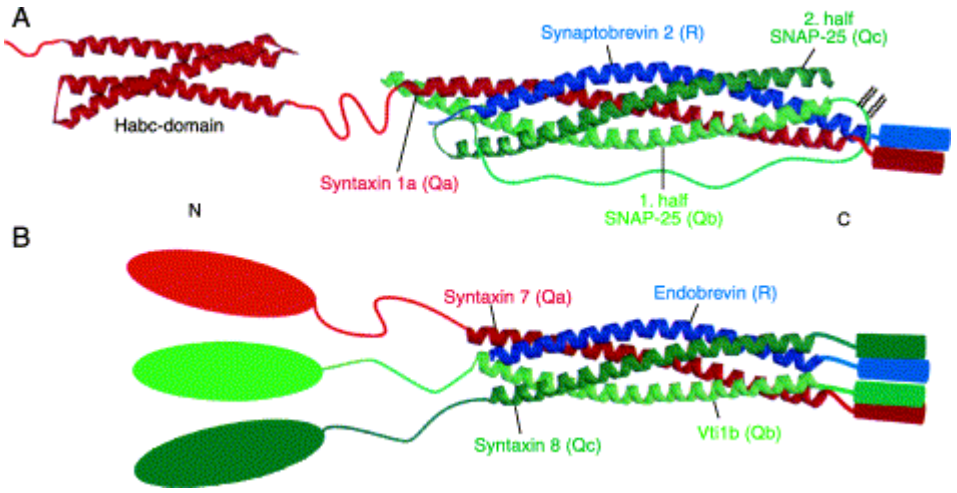

Figure I2) Conserved Structure of SNARE complexes

(A) The core of the synaptic SNARE complex consists of an extended four-helix bundle structure that contains one helix of Synaptobrevin 2 (R-SNARE), one helix of Syntaxin 1a (Qa-SNARE), and two helices of SNAP-25 (Qb- and Qc-SNAREs). The two SNAP-25 helices, and the N-terminal three-helix bundle Habc-domain and the SNARE-motif of Syntaxin 1a are connected by flexible linker regions. Syntaxin 1a and Synaptobrevin each contain a C-terminal TM domain, whereas SNAP-25 is attached to the membrane by palmitoyl modifications. (B) The core of the endosomal SNARE complex consists of a very similar four-helix bundle structure. It is composed of one helix each of Endobrevin (R-SNARE), of Syntaxin 7 (Qa-SNARE), of Vti1b (Qb-SNARE), and of Syntaxin 8 (Qc-SNARE) . Syntaxin 7, Vti1b, and Syntaxin 8 carry large N-terminal domains, probably all constituting three-helix bundle structures. All four endosomal SNAREs hold a TM domain adjacent to their respective SNARE motif . The cylinders represent the TM regions that are linked by a short sequence of unknown structure to the respective SNARE helices. The curved lines represent extended flexible linker regions (from Fasshauer, 2003).

Genome analysis of yeast, worm, fly and human revealed several interesting points: a set of twenty to thirty related SNARE proteins, that can be detected in yeast, worm, fly and humans seems to be sufficient to mediate the main intracellular trafficking events. Moreover, the closest related members in the different

species reside in similar subcellular compartments. In human, additional SNARE proteins are expressed, which raises the total number of SNAREs detected in the human genome to 35 (Bock et al., 2001). This might indicate the use of tissue-specific SNARE proteins for tissue specific membrane trafficking pathways and a diversification of transport steps in mammals.

The SNARE hypothesis predicts a cognate pair of SNARE proteins for each trafficking step within the cell. Consistent with the prediction, different SNARE proteins can be found on different subcellular compartments, indicating that specific SNARE proteins might indeed be involved in specific transport steps. This view is supported by genetic data. Yeast mutants of the SNARE proteins sec22p and sec9p block the secretory pathway at an early timepoint and late timepoint, respectively (Brennwald et al., 1994; Hay et al., 1997; Novick et al., 1980). Mutations of neuron specific SNAREs involved in the highly specialized pathway of neurotransmitter release in fly, worm and mice lead to a block of evoked synaptic transmission and are lethal (Deitcher et al., 1998; Nonet et al., 1998; Schoch et al., 2001; Washbourne et al., 2002). In contrast, mouse mutants of two ubiquitous SNARE proteins involved in endosomal trafficking, cellubrevin and vti1b, are viable and show normal development without any obvious or only very mild phenotype, respectively (Atlashkin et al., 2003; Yang et al., 2001). Thus certain SNARE proteins are dispensable *in vivo* and lack of these proteins can be compensated. Earlier studies showed that inactivation of cellubrevin leads to reduced but not complete inhibition of Transferrin receptor recycling, already indicating that alternative recycling pathways exist, which are presumably mediated by other v-SNAREs (Galli et al., 1994).

What is the exact function of SNARE proteins? SNARE proteins form *trans* core complexes during membrane fusion (see figure I3). The core complex formation is accompanied by major conformational changes in the coiled coil domains of the SNARE proteins. Whereas SNARE domains are unstructured in solution, combining appropriate SNARE motifs leads to spontaneous formation of four helical bundles which is accompanied by a major release of free energy (Fasshauer et al., 2002; Hayashi et al., 1994; Yang et al., 1999). Formation of SNARE complexes was proposed to proceed in a zipper like fashion from the N-termial end of the SNARE motifs towards the C-terminal transmembrane domain (Hanson et al., 1997; Lin and Scheller, 1997). These results led to a strikingly simple model by which the zipper like formation of the SNARE complex would pull the two

opposing membranes close together. The release of energy during core complex formation would be the driving force needed to overcome the energy barrier in order to fuse the opposing membranes (see figure I3).

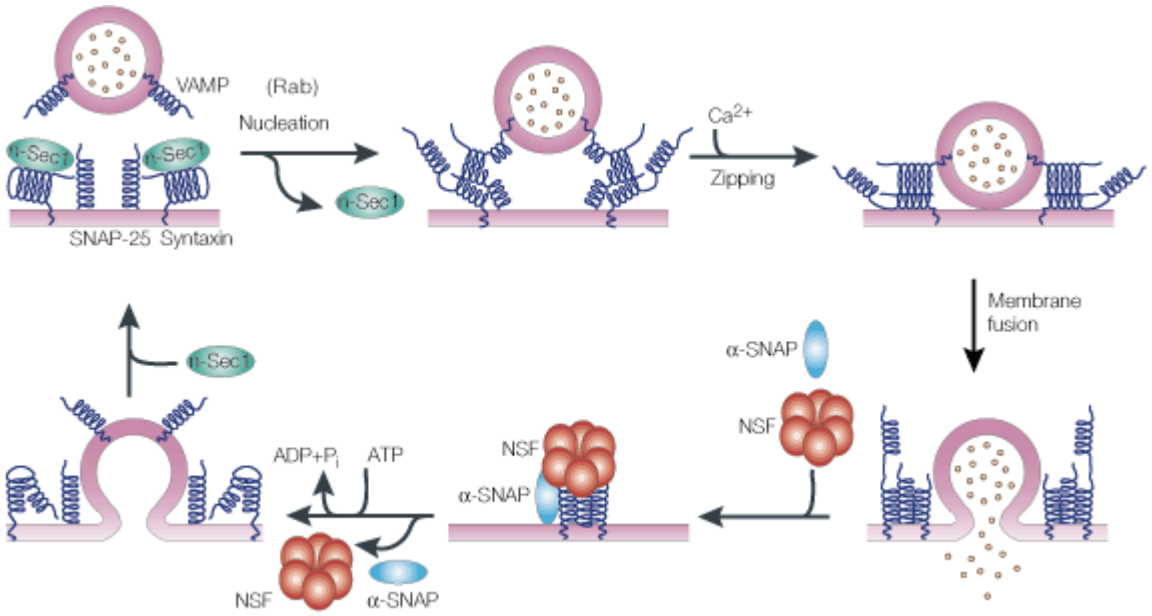

Figure I3) The SNARE cycle
Syntaxin is bound to n-Sec1 before formation of the core complex. Rab proteins might facilitate the dissociation of n-Sec1 from syntaxin, allowing subsequent binding (nucleation) between the three neuronal SNAREs, syntaxin, SNAP-25 and VAMP (for simplicity, only one coil is drawn for SNAP-25). Ca^{2+} triggers the full zipping of the coiled-coil complex, which results in membrane fusion and release of vesicle contents. After the fusion event, recruitment of α-SNAP and NSF from the cytoplasm and subsequent hydrolysis of ATP by NSF causes dissociation of the SNARE complex. Syntaxin, VAMP and SNAP-25 are then free for recycling and another round of exocytosis. (NSF; *N*-ethyl-maleimide-sensitive fusion protein; SNAP-25, 25 kDa synaptosome-associated protein; SNARE, soluble NSF attachment protein receptor, VAMP, vesicle-associated membrane protein) (from Chen and Scheller, 2001).

SNARE proteins are indeed necessary and sufficient to fuse artificial membranes *in vitro*. (Weber et al., 1998) One R-SNARE and three Q-SNAREs have to be present on opposing membranes for fusion to occur *in vitro* (Fukuda et al., 2000), consistent with the conclusions drawn from sequence analysis, where four different subfamilies of SNARE proteins were identified (see above). Cells engineered to express the correct set of cognate SNARE proteins on their plasma membrane facing the extracellular medium will fuse with each other (Hu et al., 2003). Thus it is clear that SNARE proteins are able to fuse artificial and natural membranes.

Yet whether SNARE proteins are the actual fusogens of the cell is still a matter of discussion. In mutants of Synaptobrevin in mice, fly and nematodes, spontaneous release of neurotransmitter is reduced, but clearly detectable, in

contrast to evoked neurotransmitter release, which is essentially abrogated (Deitcher et al., 1998; Nonet et al., 1998; Schoch et al., 2001; Washbourne et al., 2002). A similar result was obtained in mice mutant for SNAP-25 (Washbourne et al., 2002). These results raised the question of whether SNARE-independent membrane fusion events might occur in the cell. Indeed, in an *in vitro* vacuole fusion assay in yeast, the function of *trans* SNARE complex formation was suggested to precede the actual fusion reaction. The final fusion of opposing membranes was suggested to be mediated by the highly hydrophobic, membrane buried V_o subunits of the vacuolar ATPase (Ungermann et al., 1998; Peters et al., 2001).

In conclusion, SNARE proteins fulfill the structural requirements for proteins involved in membrane fusion events, they are necessary for membrane fusion in a large number of trafficking events and they are able to fuse artificial and natural membranes without auxilliary proteins present. It is possible that the transition from *trans*- to *cis*-complexes of SNARE proteins is an essential, but incomplete intermediate in membrane fusion *in vivo*, but the data supporting this view is sparse.

I.2.5 Spatial and temporal control of SNARE dependent membrane fusion

As SNARE complex formation leads to membrane fusion, this event has to be under tight control in order to maintain the integrity of membrane compartments. Specific SNARE complexes mediate specific trafficking events, which led to the proposal that spatial specificity of trafficking events is encoded in SNARE proteins themselves (Rothman, 1994). This may not be true in these general terms since the lack of phenotype of mice carrying null mutations for the SNAREs cellubrevin and vti1b suggests the possibility of functional redundancy (Atlashkin et al., 2003; Yang et al., 2001). Also it was demonstrated *in vivo* that a mutant of fly synaptobrevin, n-syb, can be rescued by driving the expression of the ubiquitous homologue syb in neuronal tissue and vice versa. Yet, each individual mutant shows a strong and specific phentotype (Bhattacharya et al., 2002). Similarly in yeast, mutants of t-SNAREs involved in golgi to endodosome or endosome to vacuole trafficking show specific phenotypes but can be rescued by overexpressing either of the two SNARE proteins (Darsow et al., 1997; Gotte and Gallwitz, 1997).

The isolated, soluble core domains of non-cognate SNARE proteins, i.e. which do not pair *in vivo*, form stable, heat and SDS-resistant core complexes similar to cognate SNARE domains, as long as the QaQbQcR-rule is respected (Fasshauer et al., 1999; Yang et al., 1999). In contrast, combinatorial pairing of all yeast R-SNAREs with a number of yeast Q-SNAREs in an *in vitro* liposome fusion assay revealed a certain degree of specificity encoded in the SNARE proteins themselves (McNew et al., 2000). Thus, certain combinations of SNARE proteins do favour membrane fusion *in vitro* compared to others, but *in vitro* and *in vivo* data suggest, that stability of SNARE complex formation alone cannot account for specificity in membrane fusion.

Since complex formation of non cognate SNARE proteins has not been observed in vivo (Jahn et al., 2003), it seems likely that regulatory mechanisms are superimposed on SNARE complex formation. The existence of individual SNARE proteins for different trafficking steps might enable the cell to selectively aquire regulatory proteins other than SNAREs. In particular, Rab proteins might play an important role in determining fusion specificity. It was shown that activated Rab5 recruits a multiprotein complex containing the SNARE protein Syntaxin 13, the tethering factor EEA1 and the general fusion protein NSF in a functional microdomain, resulting in homotypic endosomal fusion (McBride et al., 1999). Thus, tethering of the membranes and the local activation or priming of the fusion machinery would occur as an integrated mechanism. This is a very attractive model of how specificity of membrane fusion events may occur through several layers of protein-protein interactions.

Temporal control over the final, SNARE mediated fusion reaction is in part encoded in the structure of SNARE proteins. A number of SNAREs have N-terminal extensions which participate directly in the kinetics of membrane fusion by negatively regulating SNARE complex formation (Filippini et al., 2001). The negative regulation of SNARE complex formation by N-terminal extensions is best understood for the synaptic Qa SNARE Syntaxin 1. The N-terminal domain of Syntaxin 1 folds back on the SNARE motif, thus leading to a so called closed conformation, in which the SNARE motif is not accessible for SNARE complex formation (Dulubova et al., 1999). Removal of the N-terminal extension greatly enhances SNARE complex formation and fusion efficiency mediated by Syntaxin 1 (Parlati et al., 1999). A protein called nSec1/munc18, which binds to syntaxin 1, plays an essential role in activating

Syntaxin 1 *in vivo* for SNARE complex formation (Pevsner et al., 1994; Richmond et al., 2001; Verhage et al., 2000). NSec1 is a member of a family of proteins found from yeast to mammals called SM proteins (for**S**ec/**M**unc) which were shown to be crucial in diverse membrane fusion events such as exocytosis and endosomal fusion (Jahn et al., 2003).

Another important family of proteins involved in the temporal regulation of SNARE complex formation and membrane fusion are calcium sensing proteins of the synaptotagmin family, which are found in metazoae (Sudhof, 2002; Littleton, 2001). Synaptotagmin I is most likely the main Ca^{2+}-sensing molecule in fast, Ca^{2+}-triggered neurotransmitter release (FernandezChacon et al., 2001; Geppert et al., 1994), whereas Synaptotagmin VII is implicated in Ca^{2+}-dependent, lysosomal exocytosis mediating plasma membrane repair (Jaiswal et al., 2002). The mechanism by which Synaptotagmins control Ca^{2+} dependent membrane fusion is not understood, but Ca^{2+} dependent lipid binding activity of this protein family seems to play an important role (Shin et al., 2003; Sudhof, 2002).

In addtion, a number of other proteins have been implicated in the regulation of membrane fusion, most of which act via direct binding to SNARE proteins like Nsec1 and Synaptotagmins (Gerst, 2003). As will be seen in the next chapter, the importance for plasticity in membrane trafficking is particularly clear in events like neuronal differentiation.

I.2.6 The role of membrane trafficking in neuronal morphogenesis

The outgrowth of axons and dendrites of neurons is accompanied by a major increase in surface area of the cell. For example, an axon growing at a rate of 20-50µm/h has to incorporate a membrane area corresponding to the size of its cell body every two hours (Futerman and Banker, 1996). To enable axons and dendrites to locate their appropriate synaptic partners and therefore to enable the correct wiring of the nervous sytem, the delivery of membrane to the axon and dendrites has to be integrated into the demands of directed axonal and dendritic growth, respectively. This plasticity in neurite outgrowth is exemplified by the fact that the extent of axonal outgrowth of a neuron in culture can be drastically modified by the substrate that is presented to the neuron (see Fig I4; Lemmon et al., 1989) and signalling cues exist

which preferentially stimulate either axonal or dendritic outgrowth (Higgins et al., 1997; Prochiantz, 1995). Thus, as shown in Figure I4, axonal outgrowth is selectively stimulated by a member of the IgCAM superfamily of cell adhesion molecules called L1, whereas dendritic outgrowth is not affected compared to the control substrate poly-L-Lysine.

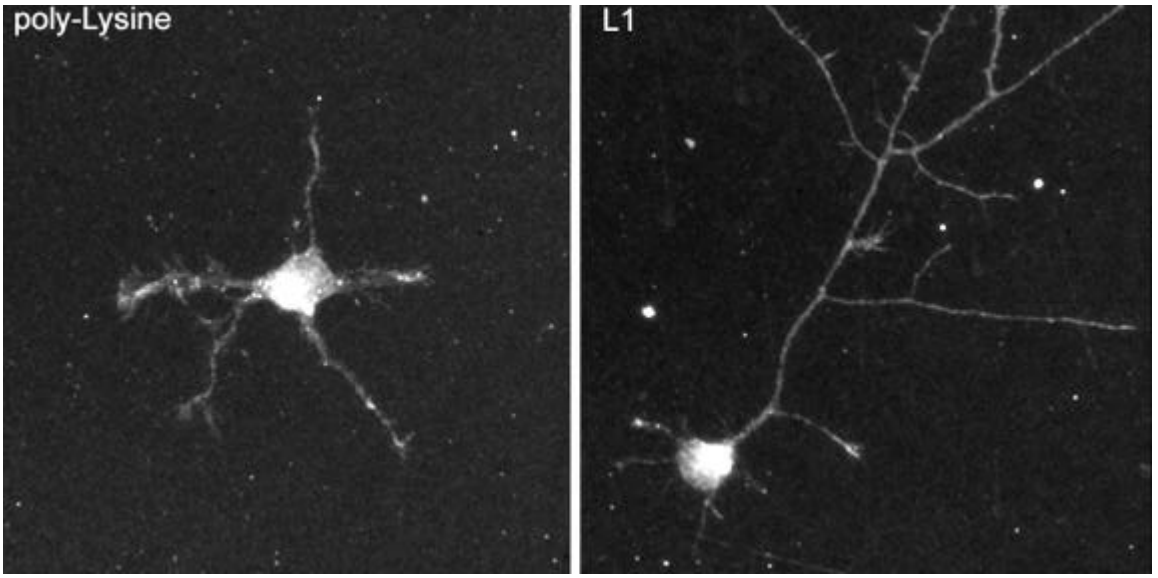

Figure I4) L1 stimulates axonal outgrowth in hippocampal neurons. Poly-L-Lysine-coated coverslips were incubated with anti-human Fc antibodies followed by incubation with (L1) or without (poly-Lysine) L1-Fc fragment. Hippocampal neurons seeded at low density were kept in culture for 24 hours and analyzed by immunofluorescence with pAb to L1.

How do guidance cues, e.g. the ligation of cell adhesion molecules translate into directed growth of the axon? Directed axonal navigation is mediated by growth cones, which are specialized, highly motile structures found at the tip of developing axons. Long- or short-range guidance cues, that can be attractive or repulsive, are recognized by receptors expressed on the growth cone and provoke the classical forms of growth cone behaviour such as advance, turning, withdrawal, and target recognition (Suter and Forscher, 1998). Therefore, by probing and sensing the environment and by translating the information received into motile behaviour, the growth cone ultimately allows for the establishment of the complex pattern of neuronal connexions (Tessier-Lavigne and Goodman, 1996).

The cytoskeleton of growth cones is intimately involved in the axonal response to extracellular cues as drugs interefering with actin dynamics were shown to render neurons “blind” *in vivo* resulting in axons that bypass and extend beyond

normal synaptic partners (Bentley and Toroian-Raymond, 1986; Chien et al., 1993; Kaufmann et al., 1998).

In growth cones, F-actin undergoes a retrograde flow from the peripheral to the central region. This so called retrograde actin flow is the result of constant *de novo*-polymerization of actin at the leading edge of the growth cone and retrograde transport of actin filaments mediated by myosin motors (Forscher and Smith, 1988; Lin et al., 1996). In order for the growth cone to be able to advance, the retrograde actin flow has to be coupled to the substrate. This substrate-cytoskeletal coupling is mediated by surface receptors which link the underlying cytoskeleton to the extracellular matrix and ultimately allows the growth cone to generate force and pull forwards. Thus, cell adhesion molecules of the Integrin-, Cadherin- or IgCAM-family play essential roles in growth cone movement. They all can be linked to the underlying actin-cytoskeleton via distinct adaptor proteins in a stimulus-dependent manner, which is provided by ligation of the respective receptor with its extracellular ligand (Suter et al., 1998).

For the growth cone to advance, substrate-cytoskeletal coupling has to be under tight control. In fact, a gradient of strong adhesion at the leading front and weak adhesion at the rear edge of the growth cone has to exist to allow the cytoskeletal machinery to pull the growth cone forwards. Such a gradient of adhesiveness has been detected for several adhesion molecules, in agreement with the predictions of the substrate-cytoskeletal coupling model of growth cone motility (Kamiguchi and Lemmon, 2000; Kamiguchi and Yoshihara, 2001; Schmidt et al., 1995). As will be explained below, local recycling of cell adhesion molecules via endocytosis at the rear edge and exocytosis at the leading front could be one mechanism in establishing such a gradient of adhesion along the growth cone.

At the same time, ligation of cell adhesion molecules initiates a local signaling cascade (Skaper et al., 2001). The IgCAM L1 induces a complex signaling cascade upon ligation, which includes the non-receptor tyrosine kinase p60src and the MAP kinase pathway (Schaefer et al., 1999; Schmid et al., 2000). The importance of L1-induced signaling for L1-function is highlighted by the fact, that the stimulatory effect mediated by homophilic L1-interaction on neurite outgrowth is abrogated in neurons deficient in p60src. (Ignelzi et al., 1994) Similarly, neurite outgrowth stimulated by L1 or the CAM N-Cadherin are reduced, when the MAP kinase

cascade is inhibited, indicating a conversion of signaling cascades mediated by CAMs of distinct families (Perron and Bixby, 1999; Schmid et al., 2000).

The signaling cascades initiated by CAMs allow for the site-directed rearrangement of cytoskeletal dynamics and the resulting change in growth cone motility (Challacombe et al., 1996; Dent and Kalil, 2001; Suter et al., 1998) and are therefore of greatest importance for neuronal morphogenesis. Yet, the exact molecular mechanisms that link guidance cues to cytoskeletal dynamics are not clear (Skaper et al., 2001).

Whereas adhesion molecules exert their function via direct cell-cell or cell-matrix interaction, other target-derived secreted factors like netrins or the sempahorins exist, which act at a distance to attract or repel axons. Secretion establishes a gradient and thus attracts or repels axons or dendrites along the gradient, if the target neurite expresses the respective receptor (Dickson, 2002). Secreted guidance cues induce motile behaviour of the axon by regulating the growth cone cytoskeleton, similar to what was described above for CAMs (Dickson, 2002). Interestingly, a physical and functional interaction between the receptor for Semaphorin 3a, Neuropillin, and the cell adhesion molecule L1 has been observed. Whereas binding of Sema3a to its receptor induces growth cone turning away from a Sema3a gradient in wild type neurons, repulsion is not observed in L1 knock out cells (Castellani et al., 2000). Thus, adhesion molecules can be functionally linked to soluble guidance molecules and their receptors, illustrating the high plasticity by which growth cones can respond to guidance cues.

In contrast to the well established, important roles for adhesion molecules and secreted guidance cues in axonal navigation, the role of membrane trafficking in axonal and dendritic outgrowth is less clear. Particularly, a possible link between the cytoskeleton, the major target of guidance cues, and the trafficking machinery, which delivers membrane for growth, is not established.

Genetic data which firmly establish a role for exocytotic membrane trafficking in neurite outgrowth *in vivo* were provided very recently in Dorosophila. A mutant of sec5, a subunit of the exocyst complex involved in tethering of exocytotic vesicles, stops growing neurites as soon as the maternal, cytosolic pool of sec5 is exhausted (Murthy et al., 2003). At the same time, accumulation of synaptic vesicles at synapses and neurotransmitter release was not affected. Thus, distinct types of

vesicles with apparently different targeting mechanisms are implicated in neurotransmitter release and neuronal differentiation.

A first description of the SNARE machinery involved in neurite extension came from experiments using clostridial neurotoxins. Clostridial neurotoxins are potent inhibitors of neurotransmitter release by cleaving key components of the synaptic exocytotic membrane fusion machinery. The inactivation of the neuronal plasma membrane target SNARE, composed of SNAP25 and syntaxin 1, by Botulinum Neurotoxin (BoNT) A and C1 leads to a pronounced reduction in axonal outgrowth (Grosse et al., 1999; Osen-Sand et al., 1996) thus suggesting the involvement of SNAP-25/Stx1 dependent exocytosis in neurite outgrowth. In contrast, tetanus neurotoxin mediated cleavage of the synaptic v-SNARE Synaptobrevin has no effect on neurite outgrowth, in spite of its complete abolition of neurotransmitter release (Grosse et al., 1999; Osen-Sand et al., 1996). These findings were confirmed by analysing synaptobrevin 2 knock out mice, which showed a severe impairment in transmitter release, but apparently normal brain development (Schoch et al., 2001). Similarly, mutants for munc-18 and munc 13-1/2, two important regulators of synaptic vesicle exocytosis, showed severe defects in neurotransmitter release without any apparent impairment of brain development (Aravamudan et al., 1999; Verhage et al., 2000). Surprisingly, the knock out of SNAP 25 in mouse shows normal brain development (Washbourne et al., 2002), whereas the experiments mentioned above using clostridial NTs suggested a role for this molecule in neurite outgrowth. This discrepancy could be owing to the expression of SNAP23, a close homologue that may be able to functionally replace SNAP25 in the SNAP25 knock out mice. In any case, these results clearly indicate that the molecules and the membrane compartment(s) mediating neurite outgrowth are, to a large extent, different from those involved in neurotransmitter release.

Whereas the studies mentioned above established a role for exocytosis in neurite outgrowth, the intracellular membrane carriers fusing with the plasma membrane and their molecular composition are only beginning to be characterized. An important regulatory role for the exocytosis of membrane carriers of endosomal origin in the development and plasticity of synaptic contacts has been recently established. The postsynaptic glutamate receptors, NMDA- and AMPA-receptor can undergo a controlled, local cycle of endo- and exocytosis at the synapse through endosomal compartments. This recycling from and to the postsynaptic plasma

membrane directly influences the postsynaptic response to glutamate release at the presynaptic active zone by controling the density of membrane resident receptors (Sheng and Lee, 2003). At least two different membrane trafficking pathways seem to be involved in the recycling of postsynaptic receptors, since membrane carriers could be identified that contained the AMPA-receptor and the SNARE protein Syntaxin 13, but no NMDA-receptor (Lee et al., 2001). Furthermore, whereas NMDA-receptor recycling is independent of Synaptobrevin, recycling of the AMPA-receptor is sensitive to cleavage of Synaptobrevin by clostridial neurotoxins (Lan et al., 2001; Lu et al., 2001).

Less is known about recycling pathways in the development of neurons, but an equally important function for local recycling of membrane receptors can be expected. Early studies on cell adhesion molecules of the Integrin family showed that these molecules do not make immobile glue at the plasma membrane but instead recycle through endocytic compartments to and from the plasma membrane (Bretscher, 1992). In fact, neurons seem to be able to control the density of integrin receptors on the cell surface in response to ligand density by an endocytotic mechanism, in order to maintain growth cone motility (Condic and Letourneau, 1997). Similarly, the cell adhesion molecule L1, which plays an important role in brain development in mice and human, was shown to recycle locally in the growth cone (Kamiguchi and Lemmon, 2000). Therefore, intracellular trafficking of cell-cell or cell-matrix adhesion molecules like L1 and integrins through endosomal compartments is likely to be important in regulating and stabilizing adhesive contacts in the course of neurite outgrowth.

What is the nature of the transport carriers, which deliver newly synthesized lipids and proteins to the growing axons? Brefeldin A, a fungal toxin that blocks post Golgi trafficking of membrane carriers, inhibits neurite outgrowth demonstrating a role for golgi-derived vesicles in neurite outgrowth (Jareb and Banker, 1997). Studies on the chicken homolog of L1, NgCAM, suggest that, when expressed in rat neurons in culture, newly synthesized NgCAM is delivered and inserted in the plasma membrane at the distal end of the growing axon (Vogt et al., 1996). Similar results were obtained when CD8 alpha, a non-neuronal protein, was expressed in neurons in culture and found to be inserted at the tip of the growing axons (Craig et al., 1995). These studies suggest that newly synthesized proteins and lipids may be transported and inserted into the membrane at the sites where growth actually takes place.

Interestingly, a recent study on NgCAM demonstrated that transport carriers delivering newly synthesized molecules and endosomal carriers are not necessarily different. NgCAM can be transported to the axon in an indirect pathway called transcytosis. Newly synthesized NgCAM is first transported to the dendritic plasma membrane followed by immediate uptake and delivery to the axon in endosomal carriers (Wisco et al., 2003).

In summary, multiple membrane compartments of different origin may participate and interact to allow for the highly complex process of neurite outgrowth. Elucidation of the relationship between different post-Golgi compartments involved in neurite outgrowth and the molecular composition including the SNARE proteins expressed in these compartments represents one of the major challenges to understand the role of membrane trafficking in neuronal differentiation.

I.3 Aims of the thesis

The discovery of R-SNAREs insensitive to clostridial neurotoxins opened the way to test the involvement of neuronal, vesicular compartments different from synaptic vesicles in neurite outgrowth (Martinez-Arca et al., 2000a). The first R-SNARE that was demonstrated to be insensitive to clostridial neurotoxins is called TI-VAMP for **T**etanus neurotoxin **I**nsensitive **V**esicle **A**ssociated **M**embrane **P**rotein (also called VAMP7) (Galli et al., 1998; Advani et al., 1998). TI-VAMP is broadly expressed in a variety of tissues, including neurons (Advani et al., 1999; Coco et al., 1999). No true homologue of TI-VAMP exists in yeast, whereas TI-VAMP homologues are found in higher uni- and multicellular organisms like Dictyostelium, C.elegans, Drosophila and humans (Filippini et al., 2001). The structure of TI-VAMP is different from the classical R-SNARE structure found in synaptobrevin and related R-SNAREs in that it carries a N-terminal extension in addition to the SNARE motif and the transmembrane domain (Galli et al., 1998). This N-terminal extension, the Longin domain, is found in a number of R-SNAREs from yeast to human and its sequence shows a high degree of conservation between different R-SNAREs carrying this extension (Filippini et al., 2001). The Longin domain of TI-VAMP and another R-SNARE called Ykt6 were shown to negatively regulate SNARE complex formation

(Martinez-Arca et al., 2000b; Tochio et al., 2001), similar to the structurally unrelated Nterminal extensions of Qa SNAREs like Syntaxin 1 (Gonzalez et al., 2001; Tochio et al., 2001). In addition to its role as negative regulator in SNARE complex formation, the Longin domain of TI-VAMP binds to the adaptor complex AP-3, which is important for the localization of this protein to late endosomal compartments in non-neuronal cells (Martinez-Arca et al., 2003b).

Although a number of studies attempted to elucidate the membrane trafficking pathway(s) mediated by TI-VAMP, its exact nature is still unclear. TI-VAMP localizes to late endosomes/multivesicular bodies and to vesicles scattered throughout the cytoplasm (Advani et al., 1999; Coco et al., 1999; Martinez-Arca et al, 2003a; Martinez Arca et al., 2003b). It forms complexes with SNARE proteins functioning at the plasma membrane and in endosomal compartments (Bogdanovic et al., 2002; Martinez-Arca et al., 2000; Martinez-Arca et al., 2003b; Galli et al., 1998). Function blocking assays have implicated TI-VAMP in the degradative pathway of the EGF receptor and fusion of late endosomes/lysosomes (Advani et al., 1999; Ward et al., 2000), but this function might be redundant with endobrevin/VAMP8, another endosomal v-SNARE (Antonin et al., 2000). Another series of studies implicated TI-VAMP in an exocytotic pathway. In epithelial cells, TI-VAMP plays a role in transport to the apical plasma membrane, a pathway insensitive to Tetanus neurotoxin (Galli et al., 1998; Ikonen et al., 1995; Lafont et al., 1999). In mastocytes, TI-VAMP might be involved in the process of degranulation, another exocytotic pathway insensitive to tetanus neurotoxin (Hibi et al., 2000). The reason for this apparent discrepancy of TI-VAMP function in either endosomal or exocytotic trafficking is not understood, but cell type dependent differences might play a role. In neurons, the TI-VAMP compartment defines a new type of vesicle, which is different from synaptic vesicles and transferrin receptor positive recycling endosomes/early endosomes (Coco et al., 1999). In young neurons developing in culture, TI-VAMP accumulates at the leading edge of growing axons and dendrites, consistent with a role for this protein in neurite outgrowth (Coco et al., 1999). Further studies showed that TI-VAMP indeed mediates neurite outgrowth in PC12 cells and in neurons in culture, which was based on the overexpression of dominant-positive and-negative TI-VAMP variants (Martinez-Arca et al., 2000b; Martinez-Arca et al., 2001).

The goal of this study was to define the role of the TI-VAMP compartment in neurite outgrowth. In particular, the nature of the compartment in

neuronal cells was not well understood and no cargo protein of the TI-VAMP-mediated trafficking pathway in neurons was known. A working hypothesis was that adhesion molecules might be part of the molecules trafficking through the TI-VAMP compartment due to their importance in neuronal development and the fact that these molecules can be regulated by membrane trafficking.

Another important question of this work was to understand the regulation of the TI-VAMP mediated trafficking. As outlined above, the growth cone is the sensor of the axon for attractive and repulsive guidance cues. Profound rearrangements of the cytoskeleton within the growth cone result from guidance cues leading to events like turning, enhanced growth or retraction of the axon (Koleske, 2003). Since the TI-VAMP compartment is highly enriched in the growth cone of axons and dendrites (Coco et al., 1999), a potential relationship between rearrangements of the cytoskeleton triggered by guidance cues and regulation of the TI-VAMP compartment in the axonal growth cone was explored in this work.

II. Materials and methods

II.1. Materials

II.1.1. Antibodies, clones, and reagents

Polyclonal anti-GFP antibody was described earlier (Martinez-Arca et al., 2001). Mouse monoclonal antibodies directed against Syb 2 (clone 69.1) and syntaxin 1 (HPC-1) anti-transferrin receptor (68.4) and the polyclonal antibody against syntaxin 7 were generous gifts from R. Jahn (Max Planck Institute, Goettingen, FRG), C. Barnstable (Yale University, New Haven, CT), I. Trowbridge (Salk Institute, La Jolla, CA, USA) and Dr W. Hong (Institute of Molecular and Cell Biology, Republic of Singapore), respectively. Polyclonal rabbit antibodies against mouse L1 and Fab fragments generated from this antibody were previously described (Rathjen and Rutishauser, 1984). The polyclonal anti-Syb 2 antibody (MC23) was previously described (Chilcote et al., 1995). The following commercial antibodies were used in this study: monoclonal anti-Green Fluorescent Protein (GFP; clone 7.1 and 13.1) from Roche (Indianapolis, IN), monoclonal anti-GluR2 (cl 6C4) from Chemicon (Temecula, CA), monoclonal anti-Vti1b (clone 7) and SNAP25 (clone 20) from Transduction laboratories, monoclonal anti-Syntaxin 13 (clone 15G2) from StressGen (San Diego, CA), monoclonal anti-phospho-tyrosine antibody (clone 4G10) from Upstate (Lale Placid, NY) and polyclonal anti-phospho-src (pT^{418}) from Biosource International (Nivelles, Belgium). Affinity-purified Alexa 488 and Cy3-coupled goat anti-rabbit and anti-mouse immunoglobulins, phalloidin coupled to Alexa 564 or 488, Streptavidin coupled to Rhodamine, affinity-purified Fc-fragments from mouse and human IgGs were from Jackson ImmunoResearch (West Grove, PA). Biotinylated Goat anti mouse-IgG ?-chain antibody was from Southern Biotechnology Associates (Birmingham, Alabama). Horseradish peroxidase- and Alkaline Phosphatase-coupled streptavidin, sheep anti-mouse and anti-rabbit IgGs were from Promega (Madison, WI). NGF was supplied by Alomone Labs (Rehovot, Israel). Collagen was from Becton Dickinson (Franklin Lakes, NJ). All other reagents were from Sigma unless specified.

II.1.2. **Plasmids**

The cDNA coding for L1-Fc chimera was kindly provided by Dr. T. Brümmendorff (Max-Dellbrück Zentrum für molekulare Medizin, Berlin) and has been described (De Angelis et al., 1999). Eukaryotic expression vectors based on pEGFP-C3 (Clonetech) coding for Green Fluorescent Protein (GFP) and TI-VAMP fused to GFP at the C- or N-terminus were provided by S. Martinez-Arca (Institut Fer-a-Moulin, Paris) and have been described. (Martinez-Arca et al., 2000b)

The prokaryotic expression vector coding for Cyt-TI-VAMP fused to GST was provided by Dr Thierry Galli (Institut Fer-a-Moulin, Paris) and described in (Martinez-Arca et al., 2000b).

II.2. General molecular biology methods

II.2.1. PCR

Each reaction contained the following:

2µl of 10mM dNTP (a mixture of dATP, dTTP, dCTP, and dGTP each at 10mM concentration)

10µl of 10x Pfu DNA polymerase buffer (supplied with the enzyme)

10-100ng of template DNA

2µl of each primer at a concentration of 100ng/? l

2µl of Pfu DNA polymerase

Distilled water to a total volume of 100µl

The PCR was carried out using 25 thermal cycles: 94°C for 1 min, 50°C for 1 min, 72°C for 2 min/kb of template DNA. Following these cycles the reaction was incubated for a further 10 min at 72°C, before being cooled to 4°C.

II.2.2. Restriction digestion

Enzymes and buffers were supplied by New England Biolabs and used according to the manufacturers' instructions.

II.2.3. Agarose gel electrophoresis

All agarose gels were run with a TBE (90mM Tris-borate, 2mM EDTA) buffer system. Sigma 1kb ladder was used as a marker. DNA bands of interest were isolated and purified using the QIAEX II Kit supplied by Qiagen.

II.2.4. DNA Ligation

The vector and insert DNA were mixed with 1µl of T4 DNA ligase and the buffer supplied with the enzyme and incubated at 16°C overnight.

II.2.5. Annealing Oligonucleotides

0.5-1µg of each oligonucleotide were mixed with 5µl 10x annealing buffer (100mM NaCl, 10mM Tris-HCl, pH 7.8, 1mM EDTA) and made up to 50µl with H_2O. The reaction mix was annealed in a PCR machine (2 min at 85°C, then cooled to 25°C by 5°C decrements, 3 min at each temperature). The annealed oligonucleotides were ligated into plasmids using the protocol described above, but the plasmid DNA was heated to 45°C for 5 min and chilled on ice prior to ligation.

II.2.6. **Bacterial culture media**

Bacterial cultures were grown in 2xTY (1.6% tryptone, 1% yeast extract, 0.5% NaCl, pH7.4), supplemented with 50µg/ml ampicillin when required.

II.2.7. Transformation of Competent Bacteria

For each transformation, 50µl of competent bacterial cells (Top Ten, Invitrogen) were transferred to a sterile 14ml Falcon tube and placed on ice. 5-10µl of a ligation reaction (~10ng DNA) was added to the cells and incubated on ice for 15 min. The tubes were then placed in a water bath at 42°C for 90 s and returned to ice for 2 min. 450µl of 2 x TY was added and the tubes were placed in an orbital shaker at 37°C for 45 min. 100µl of cells were plated out on a TYE plate containing the appropriate antibiotic and incubated at 37°C overnight.

II.2.8. **Plasmid Purification**

Plasmid DNA was purified from bacterial cultures using the QIAprep Spin Miniprep Kit or the QIAfilter Plasmid Midi Kit (Qiagen).

II.2.9. **Production of GST-fusion proteins**

E. coli XL-1 Blue cells carrying Cyt-TI-VAMP-GST were obtained from Dr. T. Galli. A 10ml overnight culture containing ampicillin was diluted into 250ml 2TY and grown at 37°C with shaking until the optical density at 600nm was 0.6-0.8. 50µl of 1M IPTG was added and the cells were grown overnight for four hours at 22°C. The cells were pelleted at 4°C, washed in 200ml PBS, pelleted and resuspended in approximately 5ml PBS. The cells were kept at –20°C until required. Upon thawing, protease inhibitors were added and cells were sonicated. Triton X-100 was added to a final concentration of 1% and the cells were incubated for 45 min. Following lysis, cell debris was removed by centrifugation at 30000g for 20 min at 4°C.

For each 1ml of cells, 150µl packed volume of glutathione-Sepharose 4B beads (Pharmacia) were used. The beads were washed twice in PBS, prior to use. The cell lysate was added to the washed beads and mixed gently for 15 min at room temperature. The beads were washed with 1.5ml ice-cold PBS five times. To elute the fusion protein, the beads were incubated 200µl of 50mM Tris-HCl, pH8, plus 10mM reduced glutathione for 10 min. The mixture was spun and the supernatant kept. This elution step was repeated twice and the supernatants were pooled. The fusion protein was quantified and analysed on a polyacrylamide gel.

II.3 Tissue culture

II.3.1 Culture of cell lines

PC12 cells were cultured according to Greene and Tischler (Greene and Tischler, 1976) on round collagen-coated plastic dishes, which were coated oN at 200µg collagen/150mm diameter in 10ml H2O/30% EtOH under sterile conditions. Cells were seeded at low density in RPMI from Invitrogen (Cergy Pontoise), 10% Horse Serum , 5% Fetal Calf Serum from Sigma (Lyon) supplemented with Glutamine (100x) from Invitrogen and the medium was changed every two days. For immunofluorescence, collagen-coated coverslips were prepared with a first layer of

poly-L-lysine (Sigma) followed by incubation at 37°C, 60 min with Collagen at 12.5 µg/ml in PBS. Cos-7 cells were cultured on plastic flasks in DMEM, 10%FCS supplemented with Penicillin/Streptomycin.

II.3.2 Preparation and culturing of primary hippocampal and cortical/striatal neurons neurons

Hippocampal neurons were prepared from E18 rat brain, whereas cortical/striatal neurons were prepared from E16 rat brain. Hippocampi were dissected in HBSS-Hepes 20 mM (Sigma and Invitrogen, respectively) and incubated for 15min in Trypsin-containing solution (Invitrogen) at 37°C. Hippocampi were washed three times with HBSS-Hepes and allowed to pellet by gravity after each wash. Hippocampi were resuspended in 3 ml HBSS-Hepes containing 300 µl DNase I (10mg/ml in HBSS-Hepes) from Roche and incubated at 37°C for 5 min. Hippocampi were dissociated by tituration with a glass pipette were the opening was diminished over the flame. Cells were seeded on pretreated coverslips at 10000-20000 cells/coverslip (Ø 14mm) in Neurobasal medium supplemented with 4% B27 (both Invitrogen). Coverslips were pretreated by chloric and sulphuric acid (1/2) oN at room temperature followed by extensive washes for eight hours and coating with poly-L-lysine oN at 50µg/ml in H_2O at 37°C. Cortical/striatal neurons were prepared by dissecting the cortex and striatum in PBS/4%Glucose. Tissue was chopped in little pieces and dissociated in single cells by tituration. Cells were cultivated in chmically defined medium according to Rousselet et al (Rousselet et al., 1990) on pretreated coverslips (see above) and a layer of collagen: a drop of collagen was spread on the coverslips with a pipette bent over the flame and the collagen was allowed to dry before plating the cells.

II.3.3 Culture of hippocampal neurons on L1-substrate

Neurons were grown on L1-substrate according to (Kamiguchi and Lemmon, 2000). For purification of L1-Fc chimera, Cos-7 cells were transiently transfected with cDNA coding for L1-Fc chimera using Lipofectamine-2000 according to the manufactures instructions. For purification of Fc-coupled fusion proteins, cells were grown in DMEM (Invitrogen) containing 1% IgG-depleted FCs or full synthetic medium AIM V-medium (Invitrogen). Secreted L1-Fc protein was allowed to accumulate for several days. The supernatant was collected and recombinant protein

was purified using ProteinA-sepharose (Pharmacia, Amersham). To coat coverslips with L1-Fc chimera, coverslips were incubated for 2 hrs at 37°C with 20µg/ml goat anti-human Fc specific antibody (Sigma, Saint Quentin Fallavier, France) in Leibovitz Medium, pH 8 (Invitrogen, Cergy Pontoise, France). Coverslips were rinsed and incubated with 3µg/ml L1-Fc fragment in Leibovitz Medium for another 2 hrs at 37°C.

II.4 Biochemical methods

II.4.1 Immunoprecipitation

For immunoprecipitation of TI-VAMP, monoclonal anti-TI-VAMP antibody 158.2 and control mouse IgG were covalently coupled to Protein G-sepharose according to Harlowe and Lane (Harlow and Lane, 1988). Rat brain was homogenized with a glass/teflon homogenizer (9 strokes at 900 rpm) in 10 ml of homogenization buffer containing 0.32 M sucrose, 150 mM NaCL, 1mM EDTA and a protease inhibitor cocktail. All the steps were carried out at 4°C. After 10 min centrifugation at 800 g the supernatant was adjusted to 1% Triton X-100 and incubated for 60 min on ice. Unsoluble material was removed by centrifugation at 40000g for 60 min. Rat brain lysate was incubated with immunobeads overnight and the beads were washed five times in homogenization buffer with 0.1% Triton X-100. Bound material was separated by SDS-PAGE (Schagger and von Jagow, 1987; Laemmli, 1970) followed by Western blotting.

II.4.2 SDS-PAGE

Samples to be analysed by SDS-PAGE were boiled in 1x sample buffer and loaded onto mini-gels of the Hoefer™ SE 260 Mini-Vertical Unit (Amersham-Pharmacia). Buffer compositions for SDS-PAGE were as follows:

SDS running (resolving) gel buffer:

Tris 18.17 gr.

3M HCl 8.20 ml.

SDS 0.40 gr.

dH_2O to 100 ml.

Tris and SDS were dissolved in 73 ml H_2O

and titrated with 3M HCl, then brought to volume. The pH was adjusted to 8.6-8.8
3M HCl= 24.75 ml (conc. HCl 14.6M) + 95.875 H_2O

SDS stacking gel buffer:
Tris 6.05 gr.
SDS 0.40 gr.
2M HCl 29.1 ml. ca.
dH_2O to 100 ml.
Buffer was titrated to 6.8-7.0.

SDS-sample buffer:
glycerol 12.5 gr.
tris 0.76 gr.
2-mercaptoethanol 5.00 ml.
SDS 2.30 gr.
0.5M HCl 12.3 ml.
dH_2O 71.0 ml.
bromophenol blue 10 mg.
Buffer was titrated to pH 6.8-7.0.
Acrylamide concentrations for stacking gels were 5% and for separating gels between 7.5 and 15%.

II.4.3 Western Blotting

Following SDS-PAGE, proteins were transferred onto nitrocellulose by electroblotting at a constant current of 100mA overnight, using a wet blotting method in a Hoefer TE 22 Mini Tank Transfer Unit (Amersham-Pharmacia). Buffer composition for transfer was as follows.
TRANSFER SOLUTION:
tris-base 12.1 gr.
glycine 57.6 gr.
ethanol 800 ml.
dH_2O to 4 l.

After transfer, membranes were blocked in blocking solution. Incubation with primary antibodies at appropriate dilution in blocking solution was performed oN

at 4°C or for two hours at room temperature. In the following, membranes were washed for a minimum of three times 10 min followed by incubation with HRP-conjugated secondary antibodies followed by another round of washes like for primary antibodies. Signals were revealed by chemoluminscence using an ECL-Kit (Pierce) and autoradiography.

Washing Buffer:

Tris 50 mM pH 7,4

NaCl 150 mM

Tween-20 0.1 %

Blocking Buffer:

Washing Buffer supplemented with 5% low fat dry milk powder

II.4.4 Subcellular fractionation

PC12 cells were homogenized with an EMBL-cell cracker in 10 mM Hepes-KOH pH7.2, 250mM sucrose, 1mM EDTA, 1mM MgOAc and protease inhibitors. The homogenate was centrifuged at 800 g for 10 min and 1.5 ml of the supernatant was loaded onto a 0.3-1.2M linear sucrose gradient and spun for 15min in a SW40 rotor at 25000 rpm (velocity-gradient). 1ml fractions were unloaded from the top; membranes were pelleted and resuspended in sample buffer. Equal volumes of each fraction were separated by SDS-PAGE (Laemmli, 1970) and analyzed by Western blotting. For equilibrium gradient analysis the light fractions 1-4 of the velocity gradient were pooled and loaded on a sucrose step gradient of the following composition: 1ml 0.8M, 2ml 1M, 2ml 1.2M, 2ml 1.4 M, 1 ml 1.6M. After centrifugation in SW40 at 25000 rpm overnight, the gradient was unloaded and analyzed as above.
Rat brain was homogenized as described above. The supernatant (S1) was recentrifuged for 15 min at 9250 g to yield a supernatant (S2) and pellet (P2). The S2 fraction was further separated by velocity gradient centrifugation. An aliquot was loaded on top of a sucrose gradient ranging from 0.32 to 1.2 M sucrose and spun for 20 min at 25000 rpm in a SW41-rotor. The gradient was unloaded by upward displacement and 1ml fractions were collected, the membranes were pelleted and resuspended in equal volumes of sample buffer. Equal volumes of each fraction were analyzed by SDS-PAGE and Western blotting. The first two fractions of the velocity gradient were further analyzed by equilibrium gradient centrifugation. The fractions

were adjusted to a sucrose concentration of 0.6 M Sucrose and mixed with 1.4 M Sucrose to yield a linear gradient ranging from 0.6 to 1.4 M Sucrose. Samples were spun overnight at 25000 rpm in a SW41 rotor. Gradients were unloaded as described above. The membranes were pelleted and resuspended in equal volumes of sample buffer and analysis was performed as described above.

II.5 Cell biological methods

II.5.1 SiRNA treatment of PC12 cells

PC12 cells grown on collagen-coated 35mm dishes were transfected (as described above) twice on two consecutive days with 0.5µg GFP plus either 4µg siRNA molecules corresponding to the rat TI-VAMP sequence, bp 486-506: AACCTCGTAGATTCGTCCGTC (siRNAr, Dharmacon, Lafayette, CO), or control siRNA molecules corresponding to the equivalent sequence of canine TI-VAMP: AATCTTGTGGATTCGTCTGTC (siRNAd, Proligo-Genset, Paris, France). The canine TI-VAMP sequence was obtained by rt-PCR of RNA from MDCK cells. The next day, cells were split and aliquots cultured on either collagen-coated coverslips or put back on collagen-coated culture dishes. For the neurite outgrowth assay, the cells were differentiated by the addition of 100nM staurosporine 48 h after the second transfection, fixed the next day (i.e.96 hrs after the first transfection) and processed for immunofluorescence with anti-GFP and anti-TI-VAMP antibodies. 30 randomly chosen images for each condition were taken based on the GFP signal with a MicroMax CCD camera (Princeton Instruments, Princeton, NJ), resulting in the analysis of at least 50 GFP-positive cells. A neurite was defined as a thin process longer than 10 µm. The length of each neurite, from the cell body limit until the tip of the process, was measured in each case using the Metamorph software (Princeton Instruments, Princeton, NJ). Differences were evaluated statistically with the Chi squared test. All the recordings and the Metamorph analysis were done blind.

II.5.2 Antibody uptake assays

PC12 cells were plated on collagen-coated glass coverslips and treated with NGF at a concentration of 50ng/ml for 2 to 3 days for analysis of uptake of L1-specific Fab-fragments. Cells were incubated with Fab-fragments directed against L1 in NGF-containing medium at a concentration of 25 µg/ml for 60 min at 37°C. The cells were fixed after washes in cold PBS with 1 mg/ml BSA and acid stripping with 0.2 M acetic acid/0.5M NaCl for 2 min at 4°C. Antibody uptake on neurons grown on collagen-coated glass coverslips was performed essentially as described for PC12-cells. No acid stripping was performed, but after removal of Fab-fragments and two washes of the cells in medium, neurons were reincubated for 60 min at 37°C.

For analysing uptake of GFP-antibody in PC12 cells expressing TI-VAMP with GFP fused to the C-terminus, PC12 cells were transfected by electroporation. PC12 were trypsinized, washed, and resuspended at a density of 7.5–10 x 106 cells/ml in Optimix (Equibio). Electroporation was performed with 10 µg DNA in a final volume of 0.8 ml cell suspension using a Gene Pulser II device (Bio-Rad) with one shock at 950 µF and 250 V. Immediately after electroporation, cells were washed with 5 ml of complete medium before plating them. 5 h later, the medium was removed and replaced with fresh medium containing 100 nM staurosporine to induce neurite outgrowth. PC12 cells were processed 24 hrs later. For enhanced expression of the exogenous proteins, 5 mM sodium butyrate was added the last 6 h before processing the cells. After transfection, cells were incubated in the presence of 5 µg/ml monoclonal anti-GFP antibody in culture medium for 15 min on ice, followed by 0, 15 or 60 min incubation at 37°C, 24 h after transfection with GFP-TI-VAMP or TI-VAMP-GFP. The cells were then washed twice with culture medium and twice with PBS, fixed with PFA, and processed for immunofluorescence.

II.5.3 Qualitative and quantitative immunocytochemistry

Developmental localisation of TI-VAMP and L1 was analysed in Sprague Dawley rats. Embryos (E13, E15, E19) were extracted from timed-pregnant dams after chloral hydrate anaesthesia (E0=day of mating) and fixed in 4% paraformaldehyde overnight. After 24 hour cryoprotection in 10% sucrose in phosphate buffer, serial cryostat sections (15 µm thick) were taken from the whole head in the sagittal plane for embryos. Sections were incubated overnight at room

temperature in TI-VAMP monoclonal antibody (clone 158.2; 1/500) alone or in combination with the L1 antibody (1/500) and processed for immunofluorescence.

Cells in culture were fixed with 4% PFA/ 4% sucrose and processed for immunofluorescence as follows. Cells were briefly permeabilized in phosphate buffered saline (PBS), gelatine 0.2% and Triton X-100 0.25%. Cells were incubated with primary antibodies in blocking buffer containing PBS and 2% goat serum for 2 hrs at RT or oN at 4°C in a humid chamber. After washes with PBS, cells were incubated with fluorescently labeled secondary antibodies and mounted in PBS containing 90% glycerol.

Optical conventional fluorescence microscopy was performed on an Olympus Provis microscope equipped with a MicroMax CCD camera (Princeton Instruments, Princeton, NJ). Confocal laser scanning microscopy was performed using a SP2 confocal microscope (Leica Microsystems, Mannheim, Germany). Images were assembled using Adobe Photoshop (Adobe Systems, San Jose, CA).

For analyzing the effect of silencing the TI-VAMP-expression in PC12 cells on L1-surface expression, cells treated with siRNAr or siRNAd were incubated on ice with anti-L1 polyconal antibody before fixation. Cells were fixed and processed for immunofluorescence analysis by conventional fluorescence microscopy. Quantification of surface L1 signal was performed with a semi-automatic program based on the MetaMorph software (Universal Imaging, Downingtown, PA). Cells were segmented automatically and the mask obtained by the segmentation procedure was used to compute the average intensity of the fluorescence over each cell. All acquisition and segmentation parameters were kept constant for all images. Differences were evaluated statistically with the Mann-Whitney non-parametric test.

The immunofluorescence intensities of growth cones double-labeled for TI-VAMP and Syb 2 and contacting a L1-coated bead were quantified using the “Region Measurement” function of the MetaMorph software (Universal Imaging, Downingtown, PA). Growth cones were chosen on the basis of TI-VAMP signal thus blind for synaptorevin 2 signal. The average pixel intensity was computed over identical regions of identical basal and apical confocal sections for the TI-VAMP and Syb 2 signals. Differences were evaluated statistically with the Mann-Whitney non-parametric test.

For analyzing immunofluorescence intensities of TI-VAMP- and Synaptobrevin-stained growth cones double labeled with Alexa488 Phalloidin in

contact with L1- or N-Cadherin coated beads, cells were washed and fixed as described above. To block excessive anti-mouse Fc-specific IgGs used to cover beads for coupling N-Cadherin-Fc protein, cells were incubated after fixation with recombinant mouse Fc fragment at 400µg/ml in PBS for four hours at RT. Cells were refixed briefly and processed for immunofluorescence. Signals associated with mAb were revealed by incubating the cells with biotinylated anti mouse-IgG ?-chain-specific secondary antibody followed by incubation with streptavidin coupled to Rhodamine. Single confocal sections were taken based on Actin-fluorescence intensity and thus in blind for TI-VAMP- or Synaptobrevin 2-associated signal and were analyzed and statistically evaluated as above.

For comparing TI-VAMP- or Synaptobrevin 2-expression with F-actin content in growth cones, cells were double labeled with mAbs to TI-VAMP or Synaptobrevin 2 and Alexa564-coupled Phalloidin. Images were aquired by confocal microscopy based on the actin staining and therefore in blind for TI-VAMP- or Synaptobrevin 2-associated immunoreactivity. The fluorescence intensity of single confocal planes within growth cones was analyzed and a regression analysis was performed to evaluate differences stastitically.

II.5.4 Bead-cell adhesion assay

Bead adhesion to PC12 cells was performed according to (Lambert et al., 2000). For coating of L1-Fc chimera, surfactant-free Latex-sulfate microspheres (diameter 6,2 µm for PC12 cells and 4 µm for hippocampal neurons, Interfacial Dynamics Corporation, Portland, Or) were incubated with goat anti-human Fc antibody (Sigma) at a ratio of 1 volume IgGs/ 9 volumes beads overnight at 4°C in 0.1M borate buffer pH 8. Beads were then blocked with borate buffer containg 1% BSA for 15 min at RT in the case of PC12 cells or with BlockAid (Molecular probes, Netherlands) diluted 1/3 in borate buffer in the case of hippocampal neurons. Blocked beads were incubated with L1-Fc (80µg/ml) at a ratio of 1 volume L1-Fc/ 4 volumes beads in borate/BSA buffer for 2 hrs at RT or with Borate/BSA buffer alone (control beads). For hippocampal neurons, beads were incubated with either L1-Fc fragment or with recombinant human Fc fragment at the same concentration (Jackson ImmunoResearch, West Grove, PA). For coupling N-Cadherin-Fc chimera

to beads, anti-mouse Fc antibodies were used (Jackson ImmunoResearch, West Grove, PA).

To test bead cell adhesion, PC12 cells were seeded on collagen-coated coverslips (∅12mm) at intermediate density. The next day, beads were added to the cells (2 µl beads in 200µl complete medium) and left for 45 min at 37°C. Cells were washed with 3ml of prewarmed medium, fixed and analysed by immunofluorescence. Neurons were plated at a density of 2.10^4cells/14mm coverslip and incubated with beads at day three in vitro in Neurobasal media plus 4% B27 containing 1%BSA.

To test the role of TI-VAMP in L1 or N-Cadherin mediated bead cell junctions, PC12 cells were treated with siRNA as described above. The bead cell adhesion assay was performed as above and cells were stained with 158.2 and anti-L1-polyclonal antibody. For L1 beads images were acquired by conventional epifluorescence at a magnification of 40X. The choice of cells was based exclusively on the 158.2-signal thus in blind for the signal corresponding to cell-associated L1-beads. N-Cadherin beads were detected with anti-mouse Cy3 conjugated secondary antibody. In that case, choice of cells was based on the L1 signal thus blind for cell associated Cadherin beads. The number of beads in each image was counted and differences were evaluated statistically with the Mann-Whitney non-parametric test.

II.5.5 Video microscopy

PC12 cells or hippocampal neurons were transiently transfected with TI-VAMP-GFP using Lipofectamine 2000. The next day cells were incubated with L1- or N-Cadherin beads in an appropriate chamber equilibrated to 37°C and 5%CO2. TI-VAMP-GFP positive cells with associated bead were recorded every 10 s (exposure time 300ms) taking images by phase contrast or using filters for GFP-fluorescence over a time period of 20 min using a Leica DMIRE2 microsope equipped with a Cascade camera (Roper Scientific, San Antonio, Texas, USA). Camera and microscope used automatized and driven by the metamorph software (Princeton Instruments). Films and extracts were assembled using the metamorph software (Princeton Instruments).

III. Results

Part 1: TI-VAMP mediates L1 trafficking

III.1 Characterization of the TI-VAMP monoclonal antibody Cl158.2

The specificity of the new monoclonal antibody Cl158.2 was assessed by Western blotting, immunoprecipitation and immunofluorescence. A single band was recognized by Cl158.2, corresponding to the expected size of 25 kDa, by Western blotting of rat brain homogenate. The rabbit polyclonal anti-TI-VAMP antibody TG16 purified on a recombinant fragment of TI-VAMP recognized a band of the same size (Fig. 1a). Cl158.2 immunoprecipitated both in vitro translated TI-VAMP and a protein from lysates of rat brain and PC12 cells that was recognized by TG16 and corresponded in size to in vitro translated TI-VAMP (Fig. 1b). Furthermore, synaptobrevin 2 immunoreactivity was not detected in an immunoprecipitation performed with Cl158.2 from rat brain lysate indicating that Cl158.2 does not cross-react with the vesicular SNARE protein Synaptobrevin 2 (Fig. 1c). By immunofluorescence, Cl158.2 revealed the expected vesicular pattern in PC12 cells, which was completely abrogated when the antibody was preincubated with recombinant TIVAMP-GST (Fig. 1d). Similarly, Cl158.2 associated reactivity with rat brain cryosections was completely abrogated, when the antibody was preincubated with recombinant TIVAMP-GST, but not GST alone (Fig, 1e).

Thus, the monoclonal antibody Cl158.2 specifically recognizes TI-VAMP and was therefore used in this study to analyze the TI-VAMP compartment in the nervous system.

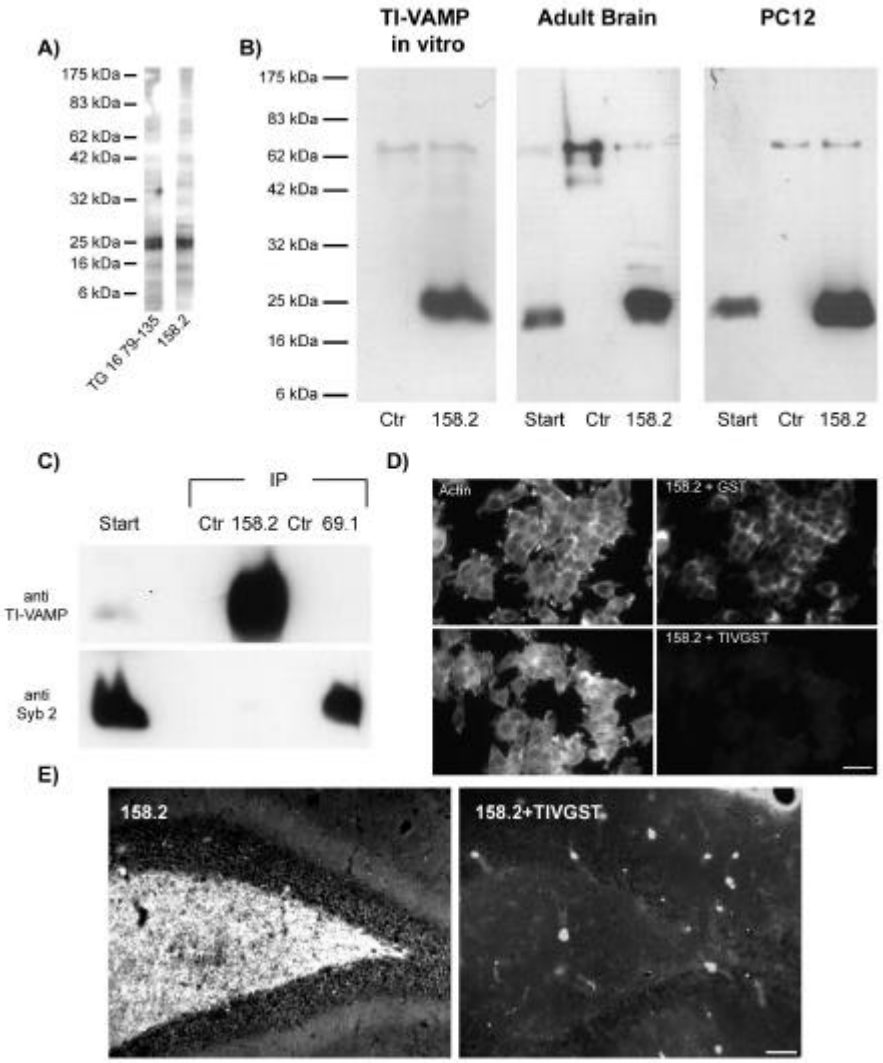

Figure 1) Characterization of the monoclonal anti TI-VAMP antibody 158.2.

a) Rat brain homogenates were separated by SDS-PAGE and transferred to nitrocellulose by electroblotting. Membranes were incubated with polyclonal anti-TI-VAMP-antibody TG16 and monoclonal antibody 158.2. Both antibodies recognize one main reactive band of 25 kDa, which corresponds to the predicted size of TI-VAMP.
b) Cl 158.2 was covalently coupled to Protein G Sepharose and incubated with TI-VAMP and SNAP 25 (ctr) generated by in vitro translation (in vitro translation) or with TritonX-100 extracts from adult rat brain (Adult rat brain) or PC12 cells (PC12 cells). Bound material was analyzed by Western blotting with TG16 79-135. Cl158.2 immunoprecipitates one main band reactive with TG16 79-135 from rat brain and PC12 cells, which corresponds in size to *in vitro* translated TI-VAMP, and is bound to Cl 158.2 immunobeads. The "Start" lanes correspond to 1/10 of the input in each immunoprecipitation experiment.
c) TritonX-100 extracts from adult rat brain were incubated with Cl158.2, anti-synaptobrevin 2 (Cl69.1) or control IgGs covalently coupled to Protein G sepharose. Bound material was tested by immunoblotting for TI-VAMP (pAb TG16 79-135) and synaptobrevin 2 (mAb 69.1). TI-VAMP was specifically precipitated by mAb 158.2 but not synaptobrevin 2, whereas synaptobrevin 2 was found specifically associated with 69.1 immunobeads but not TI-VAMP (compare IP 158.2 and 69.1). Neither TI-VAMP nor synaptobrevin 2 were found associated with control immunobeads (IP Ctr).
d) MAb 158.2 was preincubated with either 100µg recombinant Glutathione S-Transferase (GST) or 100µg recombinant TI-VAMP-Glutathione S-Transferase (TIVGST). Double-immunofluorescence analysis of PC12 cells was performed with pretreated mAb 158.2 ("158.2+GST" and "158.2+TIVGST") and phalloidin coupled to Alexa 568 to label actin filaments. 158.2 preincubated with GST reveals the expected vesicular pattern whereas 158.2-associated immunoreactivity is completely abrogated by preincubation with recombinant TIVGST (bar=20µm).
e) Brain sections through the dentate gyrus were incubated in antibody 158.2 , showing a dense staining of axon terminals in the hilus. The consecutive section incubated with the preadsorbed antibody shows no immunoreactivity in the corresponding area (bar=100 µm).

III.2 The expression of TI-VAMP is developmentally regulated

Functional studies have implicated TI-VAMP in a membrane trafficking pathway necessary for neurite outgrowth (Martinez-Arca et al., 2000b; Martinez-Arca et al., 2001). Since the expression levels of a number of proteins involved in neuritogenesis and synaptogenesis are developmentally regulated (Song et al., 1999), the expression level of TI-VAMP during development of the brain was analyzed. TI-VAMP expression was compared to the expression levels of the cell adhesion molecule L1, involved in axonal outgrowth, pre- and postsynaptic proteins involved in synaptic transmission (AMPA-receptor subunit GluR2 and SNARE proteins SNAP25 and Synaptobrevin 2) as well as a SNARE protein of the endosomal system (syntaxin 7) (Fig. 2). Homogenates prepared from rat brain at embryonic day 16 (E16), 2 days and fourteen days after birth (P2/14) and adulthood were analysed by Western blotting. The TI-VAMP expression level increases from day E16 to a maximum at day P14 followed by a slight decrease to adulthood, whereas the expression level of syntaxin 7 does not change during brain development. The expression pattern of TI-VAMP is very similar to the expression pattern of L1, which also reaches a maximum expression at day P14. The markers of synaptic transmission all reach maximal expression levels at day fourteen, which stay stable to adulthood. Thus, the expression level of TI-VAMP is upregulated during brain development, similar to proteins involved in axonal outgrowth or synaptic transmission.

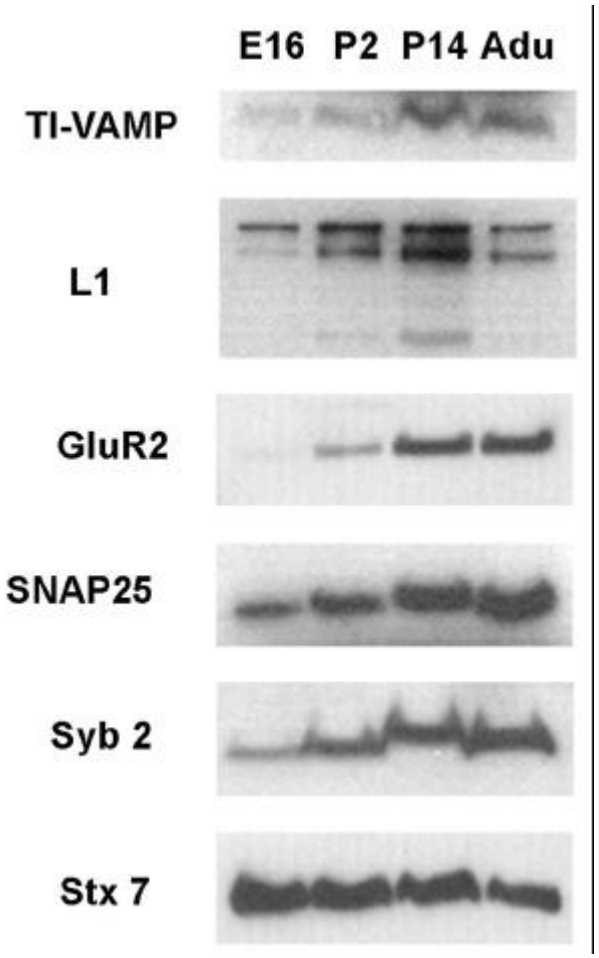

Figure 2) TI-VAMP expression is upregulated during brain development.
Homogenates were prepared from rat brain at embryonic day 16 (E16), 2 days and fourteen days after birth (P2/14) and adulthood. Equal amounts of protein were analyzed by Western blotting for the expression levels of TI-VAMP with mAb 158.2. TI-VAMP expression was compared to the expression levels of the cell adhesion molecule L1 involved in axonal outgrowth, pre- and postsynaptic proteins involved in synaptic transmission (AMPA-receptor subunit GluR2 and SNARE proteins SNAP25 and Synaptobrevin 2) as well as a SNARE protein of the endosomal system (syntaxin 7).

III.3 TI-VAMP forms complexes with SNAP-25, syntaxin 1, syntaxin 7, and vti1b *in vivo* and recycles to the plasma membrane in neuronal cells

The nature of the membrane trafficking pathway mediated by TI-VAMP in neurons is not clear. A function of TI-VAMP in endocytosis has been suggested by several studies in non-neuronal mammalian cells (Advani *et al.*, 1999; Wade *et al.*, 2001) as well as in *Dictyostelium discoideum* (Bogdanovic *et al.*, 2002). We have previously shown that TI-VAMP recycles to the plasma membrane in neuronal cells and forms SNARE-complexes with the plasma membrane t-SNARE SNAP25 (Martinez-Arca *et al.*, 2000). In order to identify the target membranes of TI-VAMP-containing vesicles in neuronal cells, I sought to identify the full catalogue of cognate t-SNARE partners of TI-VAMP. To this end, I searched for t-SNAREs that would co-immunoprecipitate with TI-VAMP from a Triton X-100 extract of rat brain. TI-VAMP was specifically immunoprecipitated by the monoclonal antibody 158.2 but not by control IgGs. Additionally, the plasma membrane t-SNAREs SNAP-25 and syntaxin 1 (Stx 1), and the endosomal t-SNAREs syntaxin 7 (Stx 7) and Vti1b were recovered with the TI-VAMP immunobeads (Fig. 3A). Importantly, no complex formation with another endosomal t-SNARE, syntaxin 13 was observed. The recombinant forms of syntaxin 13 and TI-VAMP are able to interact *in vitro*, (Yang *et al.*, 1999), thus the absence of syntaxin 13 in the assay suggests that the complexes isolated were not formed during the process of detergent solubilization of the tissue. Furthermore, when I determined the subcellular distribution of TI-VAMP and Stx 7 in primary cortico-striatal cultures grown for 1 div, extensive colocalization of both proteins on vesicular structures in the cell body and along the growing neurites was observed (Fig. 3B). These results show that TI-VAMP forms cognate SNARE complexes with the plasma membrane SNAREs SNAP-25 and Syntaxin 1 and the endosomal SNAREs Syntaxin 7 and Vti1b in the adult rat brain. Complex formation between the ubiquitous SNAREs TI-VAMP and Syntaxin 7 is likely to occur in nerve cells, since they colocalize in neurons grown in culture.

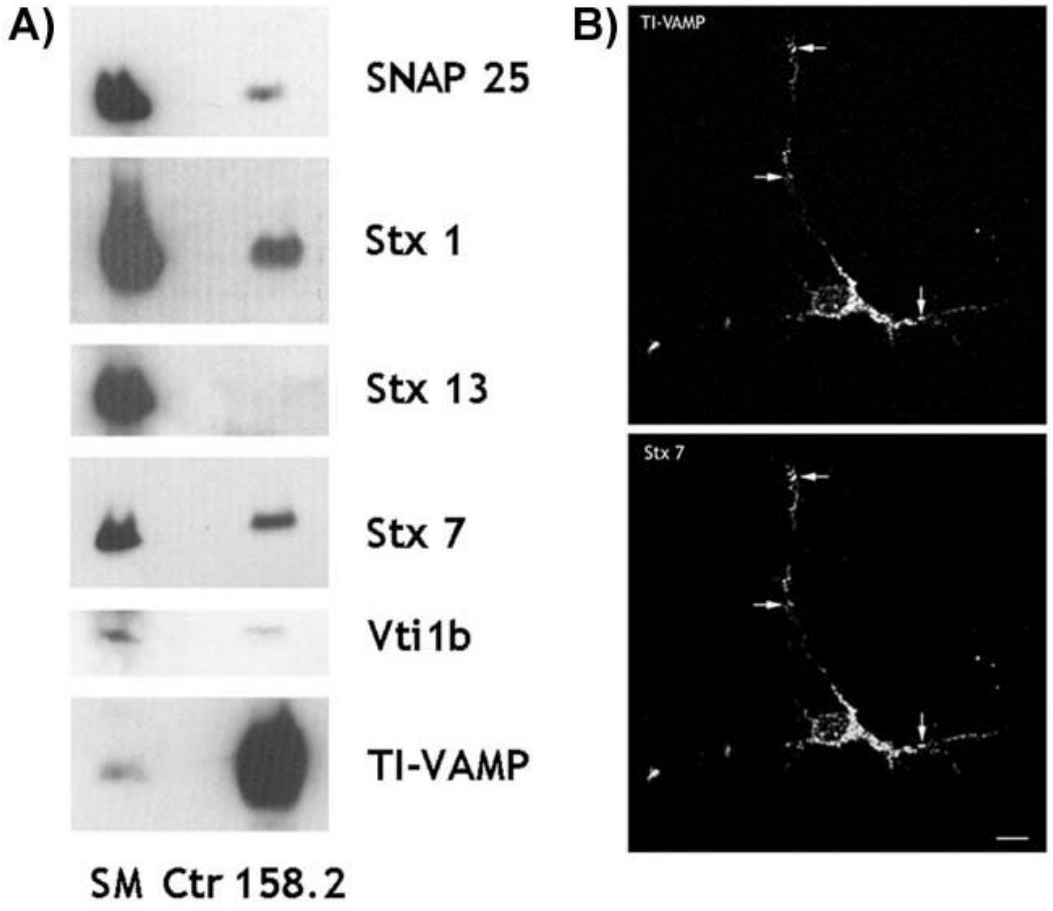

Figure 3) TI-VAMP forms SNARE complexes with plasma membrane and endosomal t-SNAREs and colocalizes with Stx 7.

A) SNARE-complex fomation of TI-VAMP in rat brain. The TritonX-100-soluble fraction of rat brain was incubated with monoclonal antibody 158.2 or control IgGs (Ctr) covalently coupled to proteinG-sepharose. An aliquot of the starting material (SM) and material bound to immunobeads was analyzed by Western blotting with antibodies to TI-VAMP, Vti1b, Syntaxin 7 (Stx7), Syntaxin 13 (Stx 13), Syntaxin 1 (Stx1) and SNAP25.

B) Localization of TI-VAMP and Syntaxin 7 in cortical/striatal neurons in culture. E16 rat cortical-striatal neurons were grown for 1 div, labeled for TI-VAMP and syntaxin 7, and analysed by confocal microscopy. Vesicular structures positive for TI-VAMP and Stx 7 are indicated by arrows (bar: 5μm).

As suggested by the complex formation with plasma membrane SNAREs, TI-VAMP may mediate exocytosis in neuronal cells. To test this possibility, a GFP-tag was fused to the c-terminal and thus luminal part of TI-VAMP (TI-VAMP-GFP). Upon exocytosis, the GFP-tag is exposed to the extracellular medium and is thus accessible to GFP-specific antibodies. PC12 cells transfected with TI-VAMP-GFP were incubated with anti-GFP antibody on ice, before fixation. Antibody labeling was detected at the plasma membrane and was often concentrated at the tip of the growing neurite (Fig. 4). When the cells were allowed to internalize the antibody at 37°C, a fast, time-dependent uptake could be observed. After 15 min at 37°C, the anti-GFP immunoreactivity was seen in peripheral structures, very close to the plasma membrane with a low degree of overlap with the green signal emitted by the bulk of TI-VAMP-GFP. After 60 min, most of the immunoreactivity colocalized with TI-VAMP-GFP, indicating that the anti-GFP antibody had reached the TI-VAMP-GFP compartment. As a control, we transfected PC12 cells with GFP fused to the N-terminal and thus cytosolic part of TI-VAMP (GFP-TI-VAMP). No plasma membrane labeling or GFP antibody internalization was detected in GFP-TI-VAMP–transfected or untransfected cells (Fig 4 GFP-TIVAMP) demonstrating the lack of capture of the antibody by fluid phase uptake. Thus TI-VAMP recycles to the plasma membrane in the course of neurite outgrowth. Taken together with the results in Figure 3, TI-VAMP is likely to mediate a recycling pathway that connects the plasma membrane with an endosomal Stx 7-containing compartment in neurons.

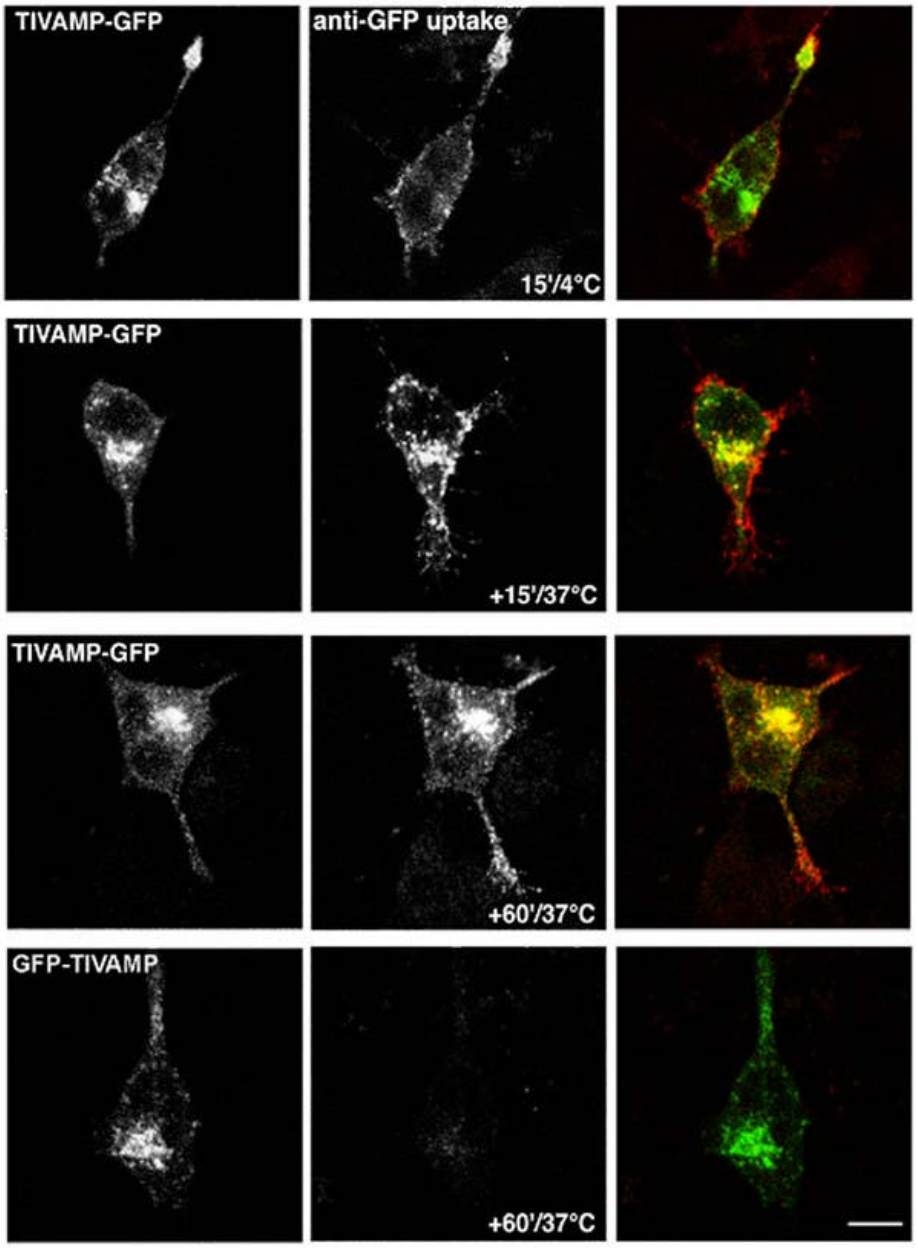

Figure 4) TI-VAMP recycles at the neuritic plasma membrane.
PC12 cells transfected with TIVAMP-GFP or GFP-TIVAMP and treated with staurosporine for 20 h were placed on ice, incubated with monoclonal antibody anti-GFP (5 µg/ml) for 15 min, and then fixed (15'/4°C) or further incubated at 37°C for 15 min (+15'/37°C) or 60 min (+60'/37°C) before fixation. Note the dense labeling of the neuritic plasma membrane in the 15'/4°C and +15'/37°C conditions. Full loading of the GFP-TIVAMP compartment is reached in the +60'/37°C condition (Bar=5 µm).

III.4 TI-VAMP is essential for neurite outgrowth

It was previously proposed that TI-VAMP mediates neurite outgrowth on the basis of the effect of overexpression of dominant-positive and negative forms of the protein in PC12 cells and neurons (Martinez-Arca *et al.*, 2000; Martinez-Arca *et al.*, 2001). A more direct approach is to interfere with the TI-VAMP expression in neuronal cells and analyze its effect on neurite outgrowth. To this end, small interfering double stranded RNA (siRNA,) (Elbashir *et al.*, 2001) were designed equivalent to the sequence of either rat or, as a control, dog TI-VAMP to silence the expression of the TI-VAMP protein in rat cells. Extracts of transfected cells were analysed by Western blotting with antibodies against TI-VAMP, Synaptobrevin 2, the IgCAM L1 and Transferrin Receptor and densitometric analysis of the corresponding signals was performed (Fig. 5B). In rat siRNA (siRNAr) transfected cells, total TI-VAMP expression was reduced to 30% (average over 3 independent experiments) of that of dog siRNA (siRNAd) transfected cells. No difference in the expression level of L1, Transferrin Receptor and Synaptobrevin 2 was observed. To analyze the effect of silencing TI-VAMP expression on neurite outgrowth, PC12 cells were transfected with siRNAr or siRNAd and differentiation of PC12 cells was induced by treatment with staurosporine for 24h. To clearly identify transfected cells, small amounts of EGFP plasmid DNA were cotransfected with the siRNAs. As seen by immunofluorescence, siRNAr-transfected, GFP-positive cells were virtually devoid of TI-VAMP immunoreactivity, whereas no effect on TI-VAMP expression was seen in siRNAd transfected cells (Fig. 5A). Silencing TI-VAMP expression led to a 25% reduction in the average neurite length compared with control. The effect of reduced TI-VAMP expression on neurite length was particularly pronounced when the number of neurites longer than 30, 45, or 60µm was compared to control cells (Fig. 5C).
Thus, TI-VAMP expression in PC12 cells is necessary for efficient neurite outgrowth.

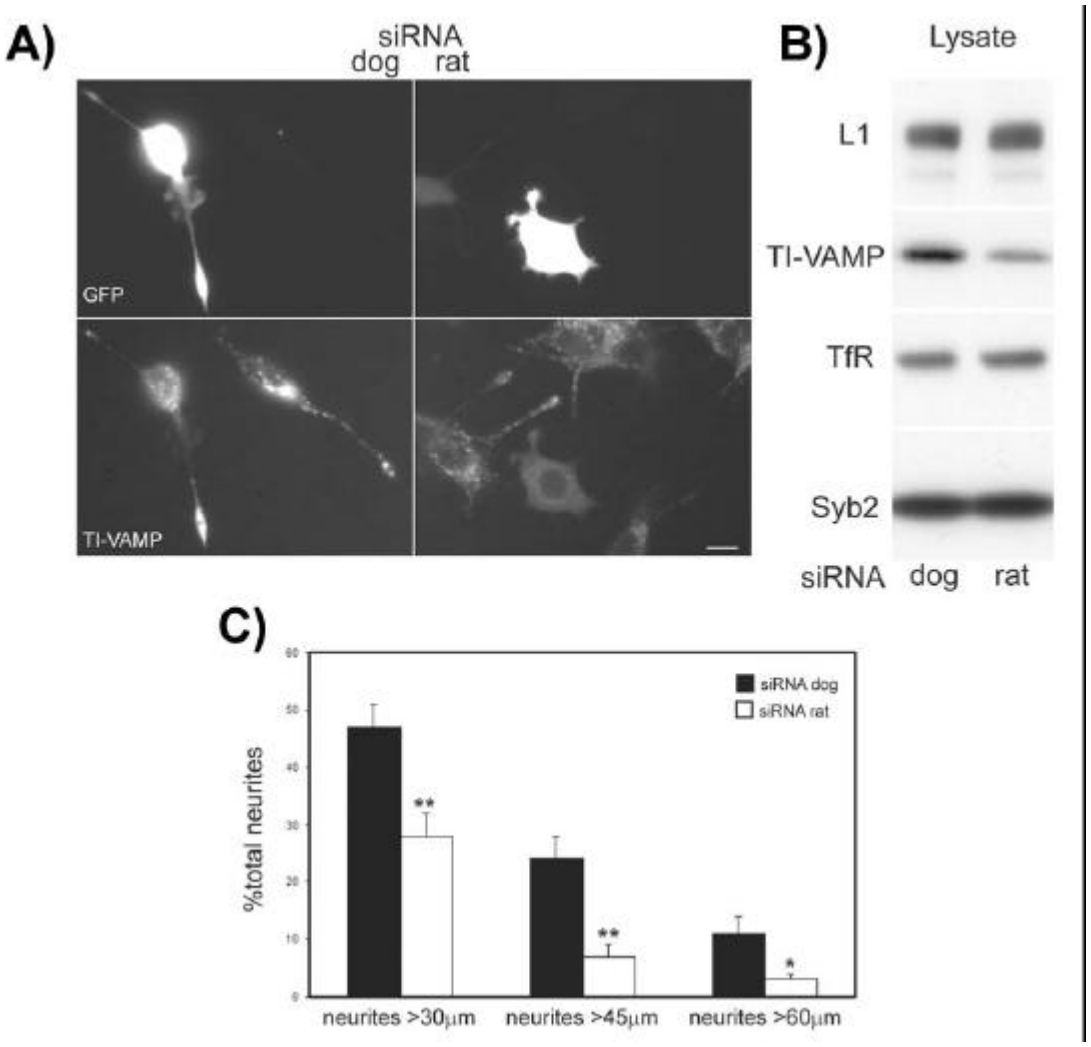

Figure 5) Silencing of TI-VAMP expression impairs neurite outgrowth in PC12 cells.

A) PC12 cells were transfected with siRNAr (rat) or siRNAd (dog) combined with an expression plasmid encoding GFP. After 72 h, differentiation was induced by treatment with staurosporine for 24 h. SiRNAr silenced the expression of TI-VAMP and inhibited neurite outgrowth (GFP-positive cell, right panel) whereas siRNAd had no effect (GFP-positive cell, left panel) (bar: 5µm).

B) Lysates of cells corresponding to A) were analysed by Western blotting for the expression levels of TI-VAMP, L1, Transferrin Receptor (TfR) and Synaptobrevin 2 (Syb 2).

C) The neurite length of GFP-positive cells transfected with siRNAr or siRNAd was quantified. Bars represent the % of the total number of neurites longer than 30, 45, and 60 µm from two independent experiments (*p<0.05; **p<0.01).

III.5. The IgCAM L1 is a cargo molecule of the TI-VAMP compartment

In order to further understand the role of TI-VAMP-mediated trafficking in the differentiation of neuronal cells, I searched for cargo molecules of the TI-VAMP compartment. Candidate molecules included cell adhesion molecules (CAMs) such as integrins, cadherins and CAMs of the Immunoglobulin Superfamily (IgCAMs), owing to their essential role in brain development. The IgCAM L1 is particularly interesting in this context because it actively recycles with the neuronal plasma membrane during axonal outgrowth (Kamiguchi and Lemmon, 2000a) (Nishimura et al., 2003) To investigate the possible relationship between L1-trafficking and TI-VAMP, an analysis of the expression of both proteins in the developing rat brain by confocal microscopy was performed on embryonic brain cryosections. During embryonic life, corresponding to the phases of active axon outgrowth, TI-VAMP labels a large number of axons in cranial nerves such as the olfactory nerve, the trigeminal nerve (Fig. 6A,B,C), and major central axon tracts, such as the thalamocortical tract (Fig. 6D). In all these locations, TI-VAMP-labeled axons co-expressed L1 suggesting that TI-VAMP could indeed play a role in L1 function during active axonal outgrowth.

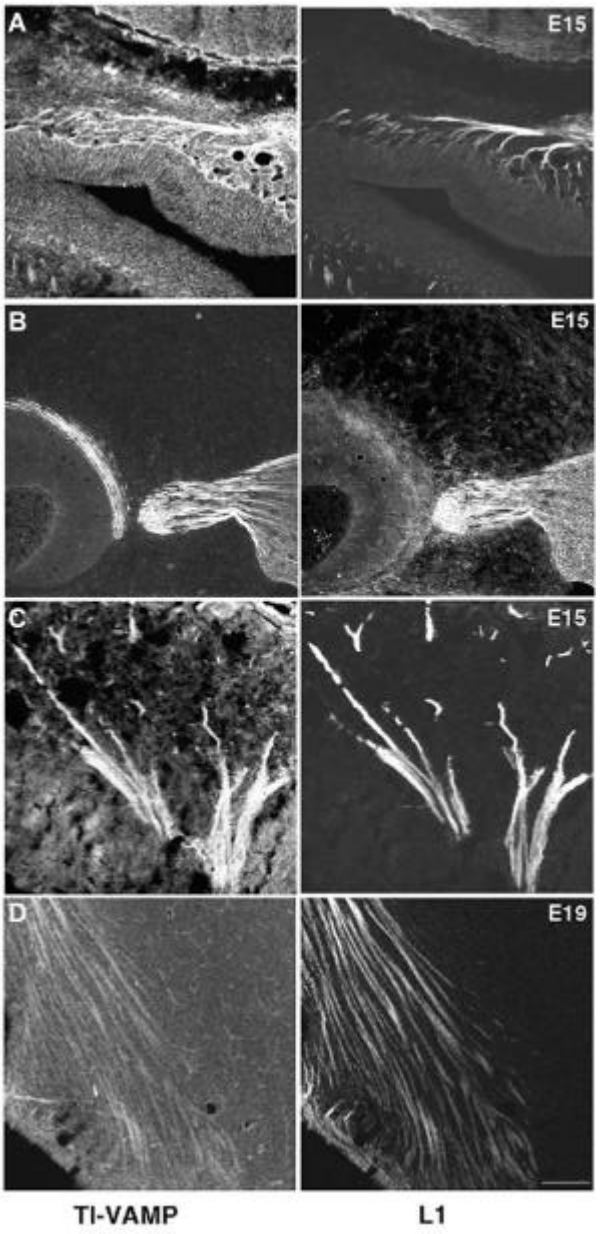

Figure 6) TI-VAMP and L1 are coexpressed in growing axonal tracts in the developing rat brain.

Expression of L1 and TI-VAMP in the developing brain. E15 and E19 embryos were serially sectioned in the sagittal plane and labeled for TI-VAMP and L1 (right column). In all four examples shown there is a high degree of colocalisation: A) Olfactory nerve branching out in the olfactory epithelium; B-C) Trigeminal ganglion and nerve root . B) The trigeminal nerve ganglion contains TI-VAMP labeled neurons. Their labeled axons are seen to converge towards the brainstem and C) Trigeminal nerve branches fan out towards the facial vibrissae; (left part of the figure); D) In the forebrain, TI-VAMP labeled axon tracts are observed, that correspond to corticofugal pathways and to cortical afferent pathways (bar: 100 µm).

Using confocal microscopy, the expression pattern of L1 and TI-VAMP was analyzed at a subcellular level in PC12 cells and hippocampal neurons. In undifferentiated PC12 cells grown at low density, L1-expression was not restricted to the plasma membrane but a considerable intracellular pool of L1 could be detected. This intracellular pool largely coincided with TI-VAMP-positive vesicular structures (Fig. 7A arrows). When L1 is used as a substrate, axonal outgrowth is greatly stimulated in several neuronal cell types (Lemmon *et al.*, 1989). Fig intro), owing to homophilic interactions between L1 on the neurons and on the substrate (Lemmon *et al.*, 1989; Dahme *et al.*, 1997). Therefore I analyzed the subcellular localization of L1 in hippocampal neurons grown on L1, and thus engaged in homophilic adhesion, and compared it to the localization of TI-VAMP. In the growth cone as well as in the cell body, L1 was expressed on the plasma membrane and, in addition, an intracellular pool of L1 could be observed (Fig. 7B,C). Importantly, considerable colocalization could be observed between TI-VAMP and the intracellular pool of L1 at the tip of the growing axon (Fig. 7B) and in cell bodies (Fig. 7C). Occasionally, a striking accumulation of TI-VAMP and L1-immunoreactivity at sites of cell-cell contact could be observed (Fig. 7C arrow, compare also Fig. 13). L1 appeared to be partly vesicular at these sites, which was not the case in varicosities, where L1 was at the plasma membrane (Fig. 7C).

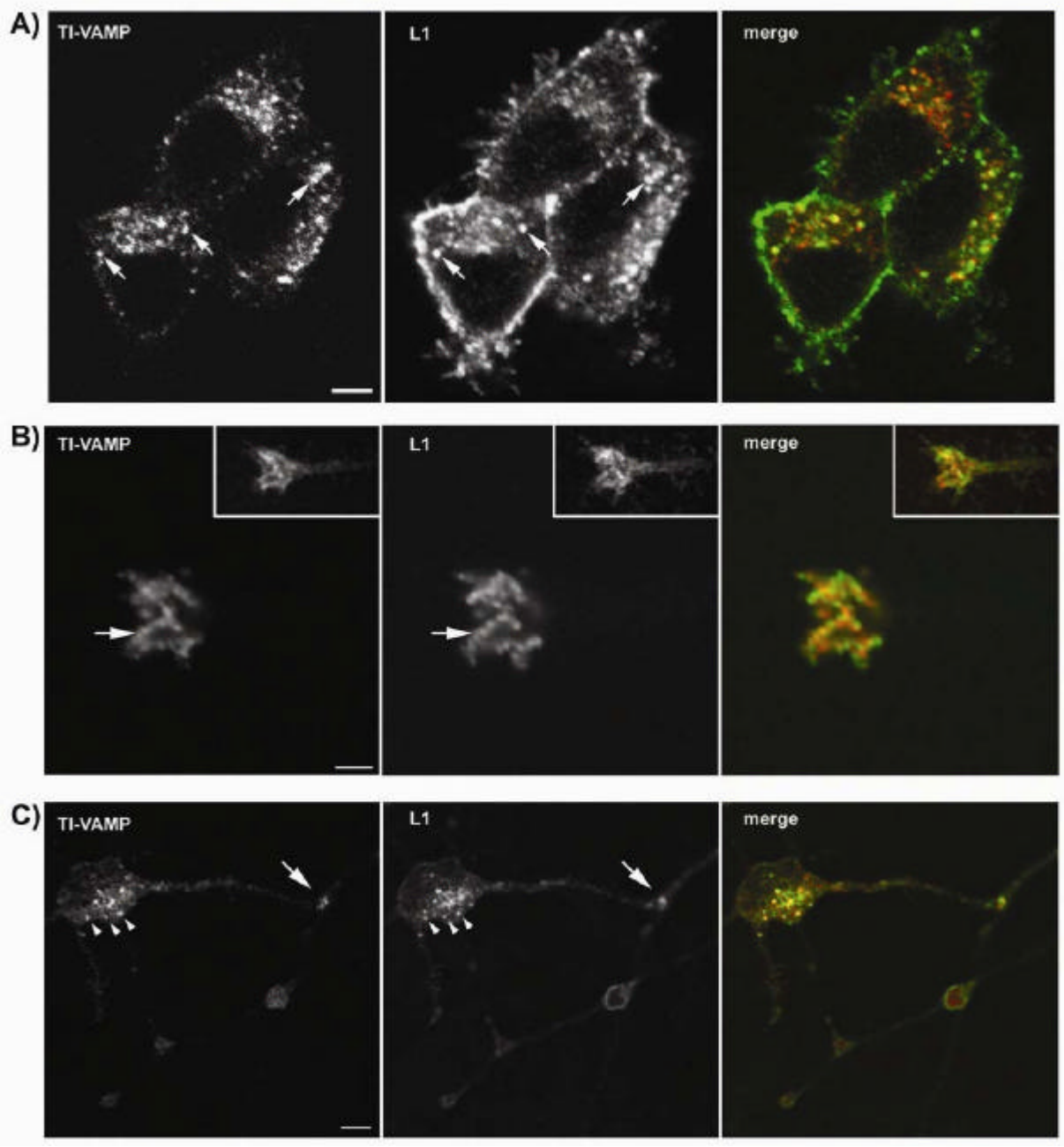

Figure 7) TI-VAMP and L1 colocalize in neurons grown in culture.

A) Localization of TI-VAMP and L1 in PC12 cells. PC12 cells were grown at low density in the absence of NGF and processed for immunofluorescence analysis by confocal microscopy. A considerable pool of L1 immunoreactivity (green) is located on intracellular structures, which largely coincides with TI-VAMP expression (red), as indicated by arrows (bar: 4µm).

B, C) Localization of TI-VAMP and L1 in neurons grown on L1. Hippocampal neurons were grown for 1div on L1 and labeled for TI-VAMP and L1. B) The confocal sections were taken from the apical part of the growth cone shown in the inset. The arrow points to a row of vesicular structures positive for TI-VAMP (red) and L1 (green); most of L1 (green) at the tip of the growth cone accumulates in clusters at the plasma membrane (bar: 3.5µm). C) Two contacting neurons are shown. The arrowheads point at vesicular structures in the cell body of a neuron, which are positive for L1 and TI-VAMP expression. Note also the accumulation of L1 and TI-VAMP-immunoreactivity where a neurite extending from the cell body is forming a contact with a passing axon (arrow) (bar: 7µm).

To further validate the coexpression of TI-VAMP and L1 in the same intracellular compartment, the TI-VAMP compartment was partially purified by subcellular fractionation of PC12 cells and adult rat brain. Velocity gradient analysis of PC12 cells showed that TI-VAMP and L1 immunoreactivity were enriched in the top four fractions of the gradient (Fig 8A Velocity gradient). This pool of membranes did not contain significant amounts of Na/K-ATPase, a plasma membrane protein that does not recycle with endosomal compartments (Le *et al.*, 1999). When these four fractions were pooled and separated by subsequent density gradient centrifugation, we found co-fractionation of L1 and TI-VAMP with membranes of similar density, which were clearly different from plasma membrane (Fig 8A Equilibrium gradient). Then the same approach was applied to fractionate adult rat brain. The supernatant of a low speed centrifugation of rat brain homogenate (S1) was separated by medium speed centrifugation to yield the supernatant S2 and the pellet P2. An antibody directed against the extracellular domain of L1 detected three major reactive species of 220 kDa, 140 kDa and 80 kDa (Fig 8B). These three species correspond to full length L1 (L1-220) and the two cleavage products resulting from a specific proteolysis within the third fibronectin type III domain of L1, extracellular L1-140 and membrane-bound L1-80 (Liljelund *et al.*, 1994; Silletti *et al.*, 2000). Whereas Na/K-ATPase and L1-80 were heavily enriched in fraction P2, a small pool of L1-220 and L1-140 immunoreactivity was detectable in S2. TI-VAMP showed an equal distribution between S2 and P2. Since S2 was poor in plasma membrane proteins, the membrane population of S2 was further analyzed by velocity and equilibrium gradient centrifugation. As in PC12 cells, velocity gradient centrifugation of S2 led to an enrichment of TI-VAMP positive membranes in the upper fractions of the gradient (Fig 8B Velocity gradient), which also contained L1-220, whereas plasma membrane peaked in fraction 3 as seen by L1-80 staining. Subsequent equilibrium gradient centrifugation of these first two fractions clearly separated plasma membrane from TI-VAMP-positive membranes, as shown by the peak of expression of L1-80 and Na/K-ATPase in fractions 3 and 4 (arrowhead and quantification) as compared to the peak of TI-VAMP expression in fraction 9 (arrow) (Fig 8B Equilibrium Gradient and Quantification). Interestingly, L1-220 immunoreactivity was found in a broad distribution from light membranes, presumably corresponding to L1 associated with plasma membrane, to denser membranes where it coincided with TI-VAMP (Fig 8B

Equilibrium Gradient and Quantification). L1-140 showed a distribution indicating a main association with the plasma membrane, but in addition a partial association with intracellular membranes (Fig 8B Equilibrium Gradient and Quantification). The pool of membranes positive for L1 and TI-VAMP expression was different from synaptic vesicles because they were found at lower densities, as seen by expression of Syb 2. Stx 7 showed a broad distribution throughout the gradient, which was very similar to L1-220 and TI-VAMP in fractions 7-11, in agreement with the data in Figure 1 showing complex formation and colocalization of TI-VAMP and Stx 7 (Fig 8B Equilibrium Gradient and Quantification).

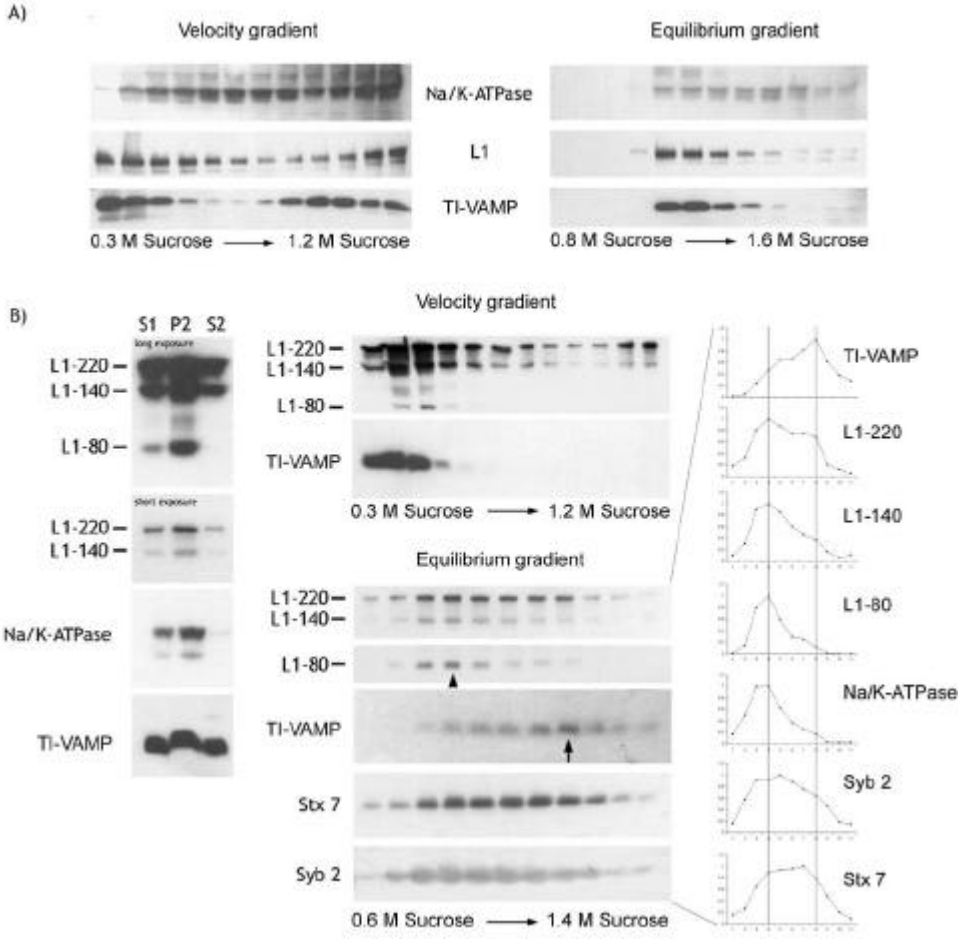

Figure 8) An intracellular pool of L1 cofractionates with TI-VAMP positive membranes in PC12 cells and adult rat brain.

A) Fractionation of membranes from PC12 cells positive for TI-VAMP and L1 in velocity and equilibrium gradients. PC12 cells were homogenized and membranes were separated on a continuous sucrose gradient by velocity gradient centrifugation. The first four fractions of the gradient were pooled and subjected to equilibrium gradient centrifugation on a continuous sucrose gradient. Equal volumes of each fraction were analyzed by Western blotting with antibodies to TI-VAMP, L1 and Na/K-ATPase.
B) Fractionation of membranes from rat brain positive for TI-VAMP and L1 in velocity and equilibrium gradients. Rat brain was homogenized and the supernatant of a low-speed centrifugation (S1) was subjected to a medium speed centrifugation to yield a pellet, P2, and a supernatant, S2. Equal amounts of protein were analyzed by Western blotting for TI-VAMP, L1 and Na/K-ATPase expression. An aliquot of S2 was loaded onto of a continuous sucrose gradient and membranes were separated by velocity gradient centrifugation. Fractions were collected and Western blot analysis of equal volumes of each fraction was performed with antibodies to TI-VAMP, L1 and Na/K-ATPase. The first two fractions were pooled and centrifuged to equilibrium. Analysis was performed as described above with antibodies to TI-VAMP, L1, Na/K-ATPase, Syb 2 and syntaxin 7. The corresponding signals were quantified by densitometry, the peak signal was defined as 1 and the resulting graphs are shown adjacent to the Western blot.

Previous studies (Kamiguchi and Lemmon, 2000b; Kamiguchi and Yoshihara, 2001) suggest that the intracellular pool of L1 that was observed by immunofluorescence analysis (Fig. 7) and subcellular fractionation (Fig. 8) may correspond to molecules that recycle to the plasma membrane. To test this hypothesis, living PC12-cells were incubated with Fab fragments directed against L1. A punctate labeling for L1-specific Fab fragments could be detected along the neurites and within the cell bodies (Fig. 9A) demonstrating that plasma membrane L1 was endocytosed in NGF-differentiated PC12 cells, as described for neurons from dorsal root ganglia (Kamiguchi and Lemmon, 2000b; Kamiguchi and Yoshihara, 2001). The punctate staining of L1 specific Fab fragments did not correspond to fluid phase uptake of the antibody since no uptake of control immunoglobulins used at the same concentration was detected (Fig. 9A). I then asked whether endocytosed L1 would reach, and be restricted to, TI-VAMP's compartment. NGF-differentiated PC12 cells were incubated with L1-specific Fab fragments and co-stained for either TI-VAMP or Syb 2 as a marker for the well-characterized compartment of regulated exocytosis in PC12 cells. Analysis by confocal microscopy, shown in Figure 9B, demonstrated that endocytosed L1 labeled with L1-specific Fab fragments colocalized to a great extent with TI-VAMP in punctate structures scattered around the perinuclear region (arrows). In contrast, no colocalization of endocytosed L1 was observed with the Syb 2-positive compartment in PC12 cells (Fig. 9B). The analysis of the endocytic trafficking of L1 and TI-VAMP was extended to neurons grown in culture. Plasma membrane L1 underwent endocytosis in neurons differentiating in primary culture as confocal microscopy revealed a punctate labeling for L1 Fab fragments along the axon (Fig. 9C). These intracellular structures of endocytosed L1 coincided with structures positive for TI-VAMP expression (marked by arrows).

Altogether, these results show that L1 is specifically endocytosed into the TI-VAMP-containing compartment. This prompted me to investigate the function of TI-VAMP-mediated trafficking in L1-mediated adhesion.

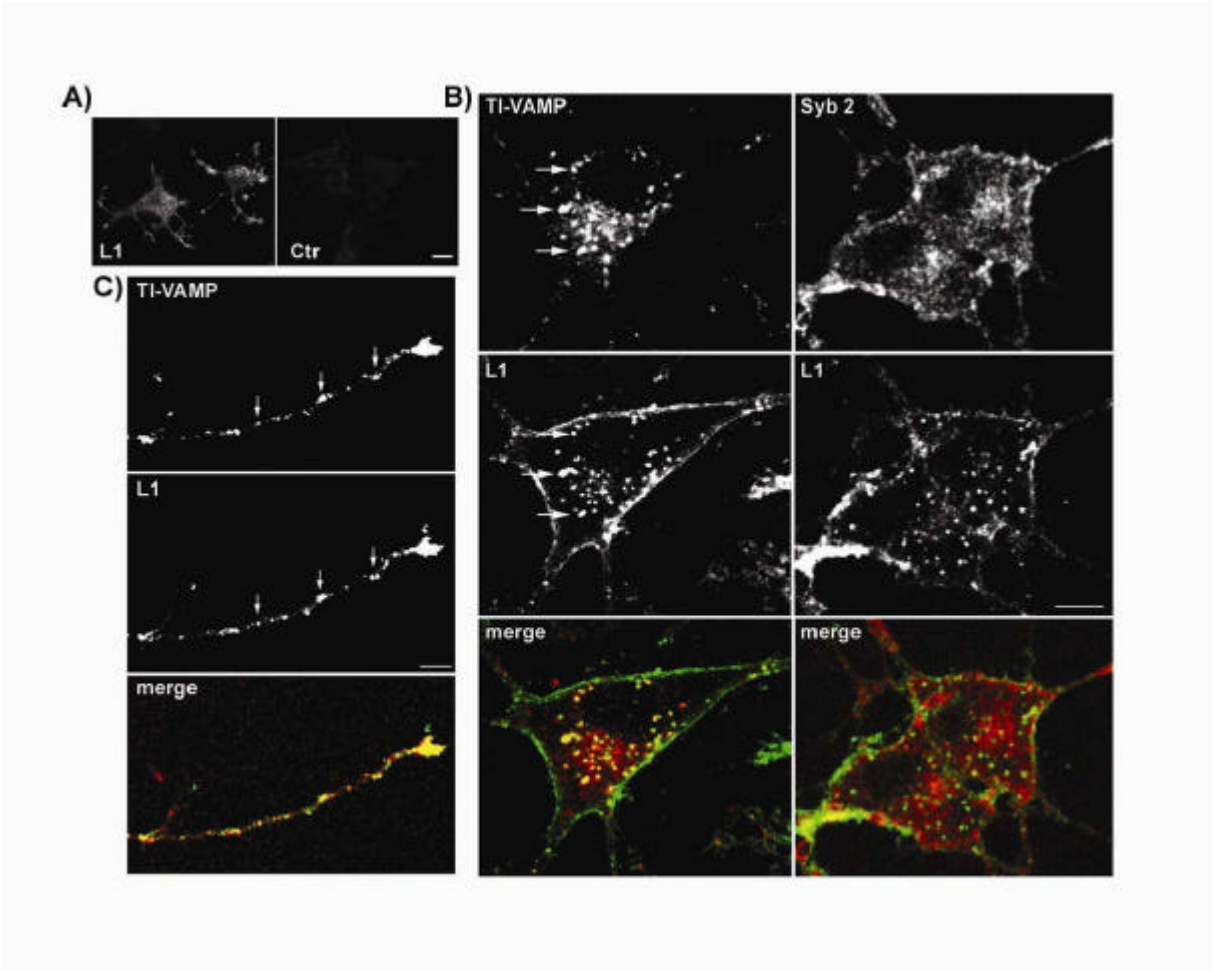

Figure 9) Endocytosed L1 reaches the TI-VAMP compartment, but is absent from the Syb 2-compartment.

A) L1 is endocytosed in NGF-differentiated PC12-cells. PC12 cells were grown in the presence of NGF for 48 h. Cells were incubated with L1 specific Fab-fragments or control IgGs. The cells were "acid stripped" and processed for immunofluorescence analysis (bar: 8µm).

B) L1 is taken up into the TI-VAMP compartment but not into the Syb 2 compartment. NGF-differentiated PC12 cells were incubated with L1-specific Fab fragments (green) as above and labeled for TI-VAMP (red) or Syb 2 (red). Arrows highlight intracellular structures positive for TI-VAMP and endocytosed L1-specific Fab fragments (green) (bar: 5µm).

C) L1 is taken up into the TI-VAMP compartment in neurons in culture. Cortical-striatal neurons grown on collagen were incubated with Fab-fragments directed against L1. After removal of the Fab-fragments, the neurons were further incubated at 37°C, fixed, and labeled for TI-VAMP (red) and endocytosed L1 (green). Arrows point at structures in the growing axon positive for TI-VAMP and endocytosed anti-L1 Fab fragments (bar: 3µm).

III.6. TI-VAMP is required for L1-mediated adhesion

The biological function of L1 as a homophilic adhesion molecule can be mimicked by presenting recombinant L1 on a planar substrate (Fig intro) or coated on beads (Kamiguchi and Yoshihara, 2001; Yip and Siu, 2001). This approach allows the analysis of L1-specific adhesive contacts isolated from the complex situation that occurs when two cells form contacts. Therefore I adapted a bead assay that was successfully used to analyze the functional consequences of N-Cadherin mediated contact formation (Lambert *et al.*, 2000). Stable contact formation of L1-beads with PC12 cells was dependent on the presence of recombinant L1 on the beads, as no beads were found associated with PC12 cells when L1 was omitted during the coating procedure (not shown). For insight into the role of TI-VAMP in L1-mediated adhesion, the expression of TI-VAMP was silenced with siRNA in PC12 cells and the cells were incubated with beads coated with the extracellular domain of L1. N-Cadherin-coated beads were used as a control, since it has been suggested that the function of N-Cadherin is independent of intracellular trafficking in neurons (Kamiguchi and Yoshihara, 2001). A reduction of 50 % in the number of L1-beads associated with cells treated with siRNAr was found when compared with cells treated with siRNAd (Fig. 10 A, B). In contrast, I did not find any effect on the amount of N-Cadherin-beads attached to cells treated with either siRNA rat or dog (Fig. 10 A,B). To analyze the effect of inhibiting TI-VAMP-dependent trafficking on the surface expression of L1, PC12 cells were treated with siRNAr/d and incubated at 4°C with the anti-L1 antibody before fixation. Quantification of L1-associated immunoreactivity revealed that L1 surface expression was reduced to about 80% in siRNAr treated cells compared to control cells ($n=4$, $p<0.02$) (compare also Fig. 10 A L1 panels).
This result demonstrates that TI-VAMP-mediated trafficking is important for surface expression of L1 and the stability of L1-dependent adhesive binding events and thus for the proper function of L1 at the plasma membrane. These results also show that N-Cadherin-mediated adhesive junctions are independent of TI-VAMP trafficking and suggest that the functions of L1 and N-Cadherin at the plasma membrane of PC12 cells are regulated in different ways.

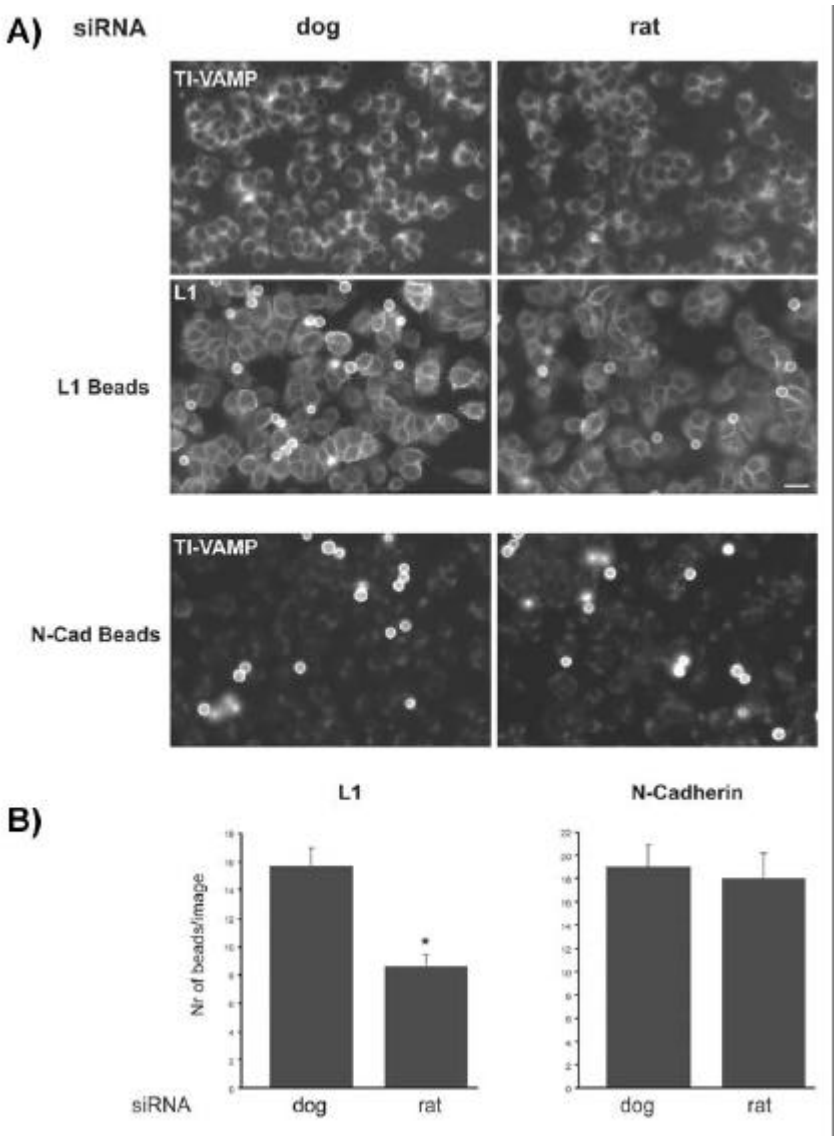

Fig 10) TI-VAMP-mediated intracellular trafficking is essential for L1-dependent adhesive contacts.

A) Binding of L1-coated beads to PC12 cells is inhibited by silencing TI-VAMP expression. PC12 cells were treated with siRNA dog or rat and incubated with beads coated with L1-Fc or N-Cadherin-Fc chimeras. Immunofluorescence was performed with mAb 158.2 and pAb to L1. Note that N-Cadherin beads are labeled by Cy3-coupled anti-mouse secondary antibody owing to the presence of the mouse Fc fragment in the N-Cadherin chimera (bar: 20µm).

B) Binding of L1 and N-Cadherin-coated beads to siRNA treated PC12 cells was quantified by counting the number of beads per image. (*p<0.01).

Part II: L1 controls TI-VAMP-mediated transport

III.7. TI-VAMP accumulation in axonal growth cones is actin dependent

In the first part of this work, it was shown that the TI-VAMP compartment is essential for neurite outgrowth. Then, I demonstrated that TI-VAMP controls transport and function of the cell adhesion molecule L1 at the plasma membrane, which might explain the defects in neurite outgrowth when TI-VAMP expression is inhibited. Yet, a potential regulation of the trafficking pathway mediated by TI-VAMP has not been analyzed. Therefore, the second part of this work aimed at elucidating regulatory mechanisms that control TI-VAMP-dependent trafficking.

During the analysis of TI-VAMP localization in neurons in culture, a striking accumulation of TI-VAMP immunoreactivity in the axonal growth cone was noticed (Coco et al., 1999) Fig. 7). At the same time, labeling intensity in different growth cones was heterogeneous. Some growth cones were strongly labeled, whereas others were virtually devoid of TI-VAMP immunoreactivity (Fig. 11 A). These differences could be observed in processes emerging from the same cell body. Therefore, different types of neurons present in the culture cannot account for variations in TI-VAMP staining intensity seen in different growth cones.

Soluble or membrane bound signaling molecules bind to receptors expressed on the axonal growh cone, which controls the dynamics of the cytoskeleton within the growth cone (Challacombe et al., 1996). Depending on the nature of the signal, the peripheral actin cytoskeleton in the growth cone can be assembled or disassembled leading to advancement or retraction of the growth cone (Song and Poo, 2001). Therefore, one hypothesis was that differences in TI-VAMP staining intensity might be related to different assembly states of the peripheral actin cytoskeleton in the growth cone. To test this, neurons kept in culture for three days were labeled for filamentous actin and TI-VAMP. As shown in Fig 11 A, a high labeling intensity for F-actin in two growth cones coincided with high labeling intensity for TI-VAMP (Fig. 11 A upper pannels, marked with +), whereas another growth cone low in F-actin content showed low labeling intensity for TI-VAMP (Fig11 A, upper pannels, marked with -). In contrast, comparison of F-actin content with Synaptobrevin labeling intensity in growth cones did not coincide (Fig. 11 A, lower pannels). To validate

these observations, the F-actin content of a number of growth cones was quantified and compared with TI-VAMP or Synaptobrevin labeling intensity (Fig. 11 B). Whereas the F-actin content and TI-VAMP labeling intensity are highly correlated (Fig 11 B, R^2=0.818), no correlation between F-actin content and synaptobrevin labeling intensity in growth cones could be observed (Fig, R^2=0.123). Furthermore, the TI-VAMP compartment colocalizes with F-actin rich filiopodial structures in the periphery of the growth cone (Fig. 11 C, upper pannels). In contrast, Synaptobrevin-immunoreactivity seemed to be restricted to the central region of the growth cone by a barrier of F-actin accumulation, separating the central from the peripheral filipodia rich region (Fig. 11 C, lower pannels). In summary, accumulation of TI-VAMP in growth cones coincides with the assembly state of F-actin suggesting that the dynamics of TI-VAMP and actin are coupled. This notion is supported by the observation that TI-VAMP localizes to actin rich peripheral structures of the growth cone.

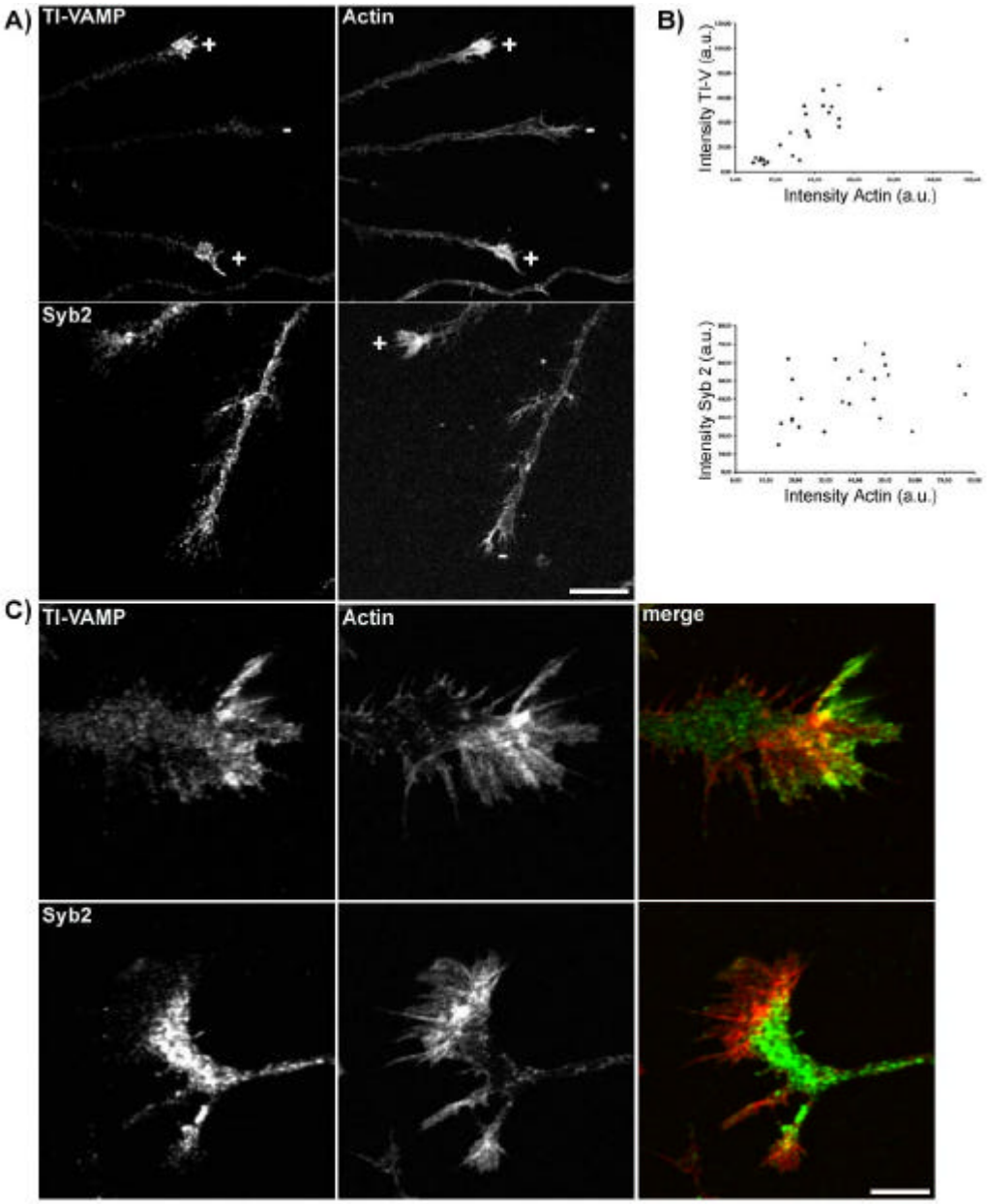

Figure 11) The accumulation of TI-VAMP and F-actin in axonal growth cones is correlated.

A) Hippocampal neurons grown 3 div were stained for F-actin and TI-VAMP or Synaptobrevin 2. Labeling intensity was analyzed by confocal microscopy. High labeling intensity of TI-VAMP (+) coincides with high labeling intensity of F-actin (+), whereas the central growth cone is low in TI-VAMP-and F-actin-staining (-) (Upper panels). The two growth cones in the lower panels show either high (+) of low (-) F-actin staining whereas Synaptobrevin 2-staining shows no variation (Bar=10µm).

B) Confocal images of hippocampal neurons stained for F-actin and TI-VAMP or Synaptobrevin 2 were taken based on F-actin staining, thus blind for associated TI-VAMP or Synaptobrevin 2 labeling (24 images each). Labeling intensity of each marker in the whole growth cone was quantified and F-actin staining was plotted versus associated TI-VAMP (upper panel) or Synaptobrevin 2 (lower panel) labeling intensity. Whereas TI-VAMP and F-actin staining are highly correlated ($Y=-6.771+1.185*X$; $R^2=0.818$; $p<0.0001$), the distribution of Synaptobrevin 2 versus F-actin labelling intensity appears random ($Y=31.269+0.312*X$; $R^2=0.123$; $p=0.093$).

C) High magnification confocal images of axonal growth cones are shown, which were double labeled for F-actin and TI-VAMP (upper panels) or Synaptobrevin 2 (lower panels). TI-VAMP immunoreactivity coincides with F-actin staining in the peripheral region of the growth cone, whereas the central region of the growth cone is low in intensity for both markers. Synaptobrevin 2 staining accumulates in the central region of the growth cone, which is low in F-actin staining (Bar=4µm). Note that synaptobrevin 2 appears to be excluded from the peripheral growth cone area by a barrier of F-actin.

To test the hypothesis that TI-VAMP accumulation in the growth cone is directly dependent on actin dynamics, neurons were treated with low concentrations of F-actin disrupting drugs. As shown in Figure 12 A, treatment of hippocampal neurons with Cytochalasin B led to a redistribution of F-actin to distinct, highly fluorescent foci (Fig 12 A, middle panels, arrows) and a change in growth cone morphology. Interestingly, TI-VAMP immunoreactivity was redistributed to F-actin rich foci (Fig. 12 A, middle panels, arrows). Treatment with the vehicle DMSO alone had no apparent affect on F-actin distribution, growth cone morphology or codistribution of TI-VAMP to actin rich structures Fig. 12 A, upper panels). Treatment of neurons with Latrunculin A disrupted the actin cytoskeleton. At the same time, TI-VAMP immunoreactivity became diffuse and no accumulation of TI-VAMP could be observed following this treatment (Fig. 12 A, lower panels). Localization of Synaptobrevin 2 was not affected by either drug (Fig. 12 B). Therefore, consistent with the observations shown in Figure 11, TI-VAMP localization in growth cones is linked to the assembly state of the actin cytoskeleton, since disrupting the actin cytoskeleton leads to a dramatic redistribution of TI-VAMP immunoreactivity. Localization of the Synaptobrevin 2 compartment in growth cones is apparently independent of the dynamics of the actin cytoskeleton.

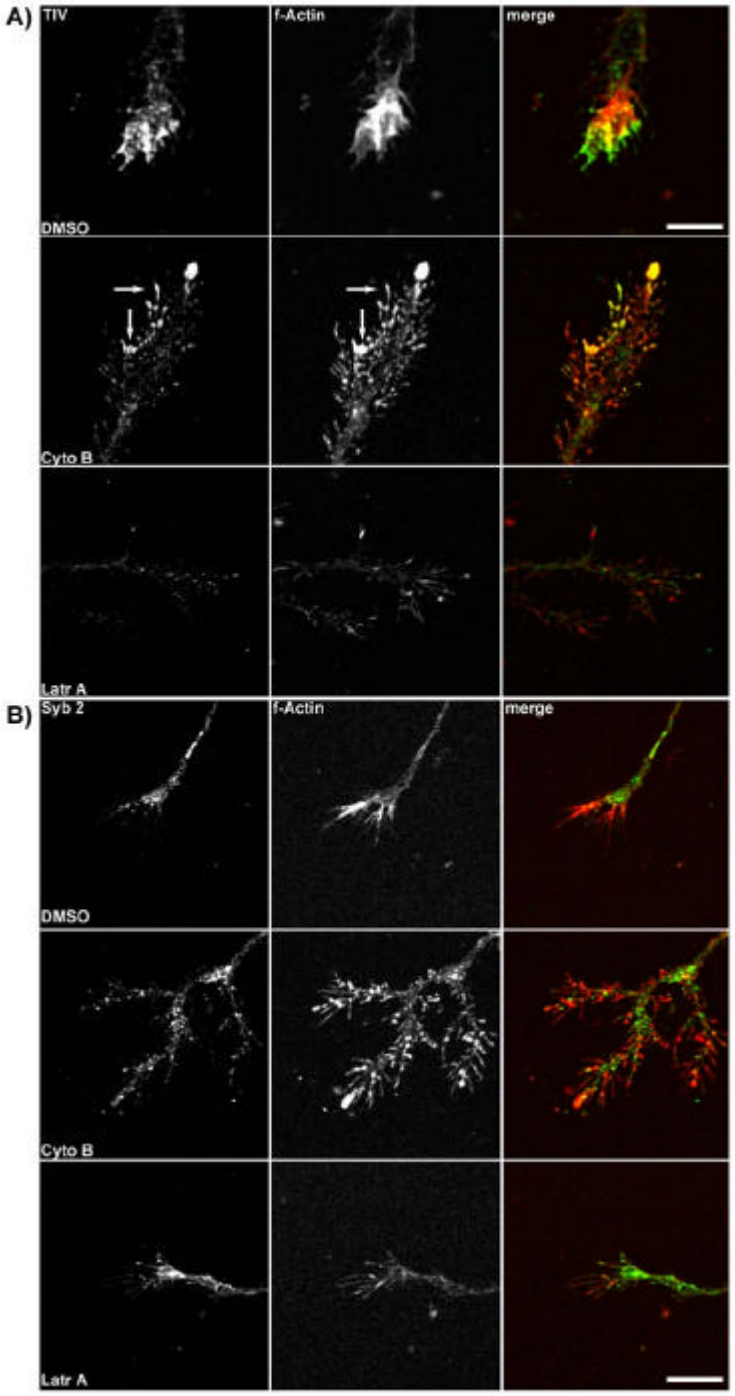

Figure12) TI-VAMP localization in the growth cone depends on actin dynamics.
A) Hippocampal neurons grown on ploy-Lysine 3 div were treated for 30 min with 5µM DMSO, 5 µM Cytochalasin B (Cyto B) or 2,5 µM Latrunculin A (Latr A). Cells were fixed and processed for analysis by confocal microscopy for expression of TI-VAMP and F-actin. Whereas DMSO treated cells show accumulation of actin and TI-VAMP in growth cones, treatment with Cytochalasin B leads to a redistribution of both F-actin and TI-VAMP to highly fluorescent foci (indicated by arrows). Latrunculin A treatment disrupts the actin cytoskeleton and results in diffuse TI-VAMP staining.
B) Hippocampal neurons at 3div were treated with drugs as in A) and analyzed for expression of Synaptobrevin 2 and F-actin by confocal microscopy. Whereas F-actin is redistributed by Cytochalasin B and Latrunculin A as described in A), the distribution of Synaptobrevin 2 appears very similar in all three conditions tested (Bar top panels=4µm, all others=8µm).

III.8. L1-dependent adhesion controls TI-VAMP-mediated trafficking

The correlated accumulation of F-actin and TI-VAMP in growth cones was observed in neurons grown on poly-L-Lysine in a chemically defined medium. Thus, cues leading to an assembly or disassembly of TI-VAMP and F-actin containing structures cannot be easily deduced. This raises the question of what events might induce actin and concomitant TI-VAMP accumulation in the growth cone in a physiological context. As shown in Fig. 7, accumulation of TI-VAMP and L1 was occasionally observed at contact sites between neurites. Furthermore, extensive remodelling of the actin cytoskeleton has been observed when the growth cone establishes contact with a target cell (Lin and Forscher, 1993). Thus, adhesive cues presented to the growth cone might induce the actin-dependent accumulation of TI-VAMP containing vesicles observed in Figures 11 and 12. Therefore, the structure of the actin cytoskeleton was compared to the TI-VAMP distribution at contact sites of neurites. As shown in Fig. 13, contact sites between neurites could be observed which showed a strong accumulation of F-actin (arrows). Similarly, TI-VAMP labeling was heavily enriched in these structures (arrows). Thus, adhesive events might indeed represent a naturally occurring cue which leads to a remodelling of the actin cytoskeleton and concomitant accumulation of TI-VAMP positive vesicles.

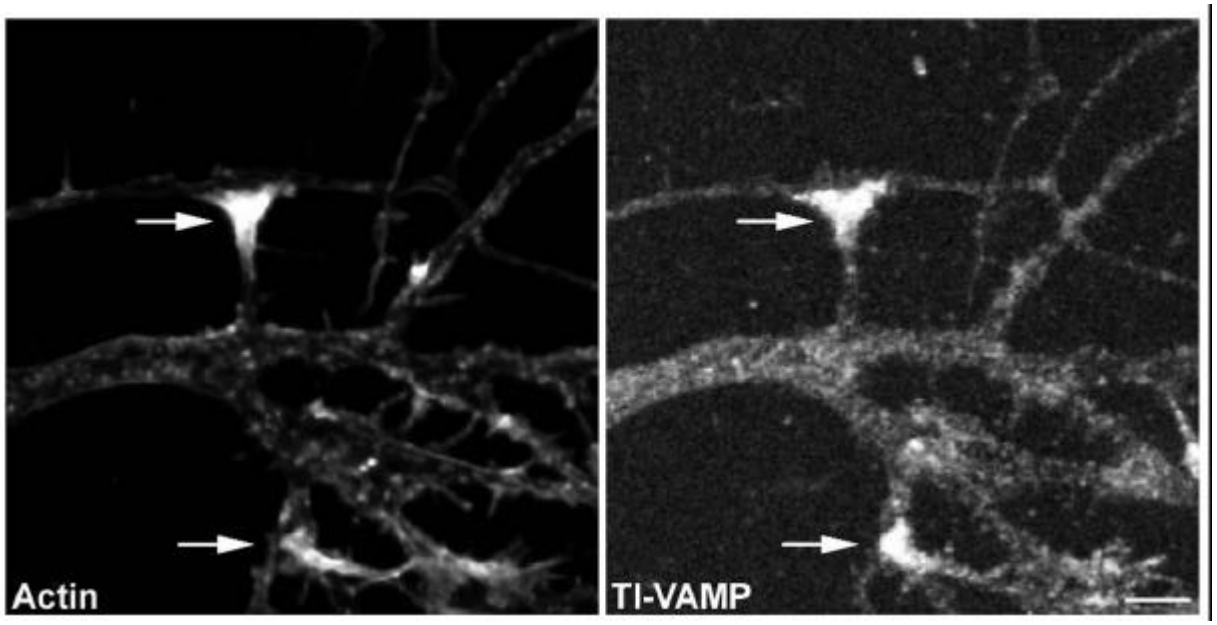

Figure 13) Accumulation of F-actin and TI-VAMP at contact sites between neurites.

Hippocampal neurons at 3div were stained for TI-VAMP with mAb 158.2 (TI-VAMP) and phalloidin for F-actin (Actin). Confocal microscopy analysis reveals accumulation of TI-VAMP and F-actin at sites of contact indicated by arrows (Bar=4µm).

To test this, I made use of the bead assay described above to mimic acutely forming, L1-dependent contacts in PC12 cells and hippocampal neurons. The subcellular localization of TI-VAMP and L1 in PC12 cells incubated with L1-coated beads was analyzed by confocal microscopy. As shown in Figure 14 A, L1-dependent contact formation between cell and bead led to a strong accumulation of plasma membrane L1 at sites of contact, indicating homophilic binding between L1-bead and L1 at the cell surface. Furthermore, vesicles positive for both L1 and TI-VAMP could often be observed in close proximity to the contact site (Fig 14 A arrows). To analyze the dynamics of the recruitment of TI-VAMP vesicles to L1-mediated contact sites, GFP-TI-VAMP was expressed in PC12 cells and the cells were incubated with L1- or N-Cadherin-coated beads. Time-lapsed video-microscopy revealed a recruitment of GFP-TI-VAMP to the L1-bead-cell contact, which was stable for the entire time of recording (20 minutes) (Fig 14 B arrow, video 1). At the same time, GFP-TI-VAMP vesicles more distant to the bead-cell contact showed a dynamic localization with clusters of vesicles appearing and disappearing in several domains of the cytoplasm (Fig 14 arrowhead, video 1). No accumulation of GFP-TI-VAMP close to sites of N-Cadherin bead-cell contact was observed (Fig 14, video 2), indicating that N-Cadherin-dependent outside-in signaling events do not influence TI-VAMP trafficking. Taken together, these results suggest that L1-mediated adhesion promotes a local accumulation of TI-VAMP-containing vesicles at sites of L1-bead-cell contact.

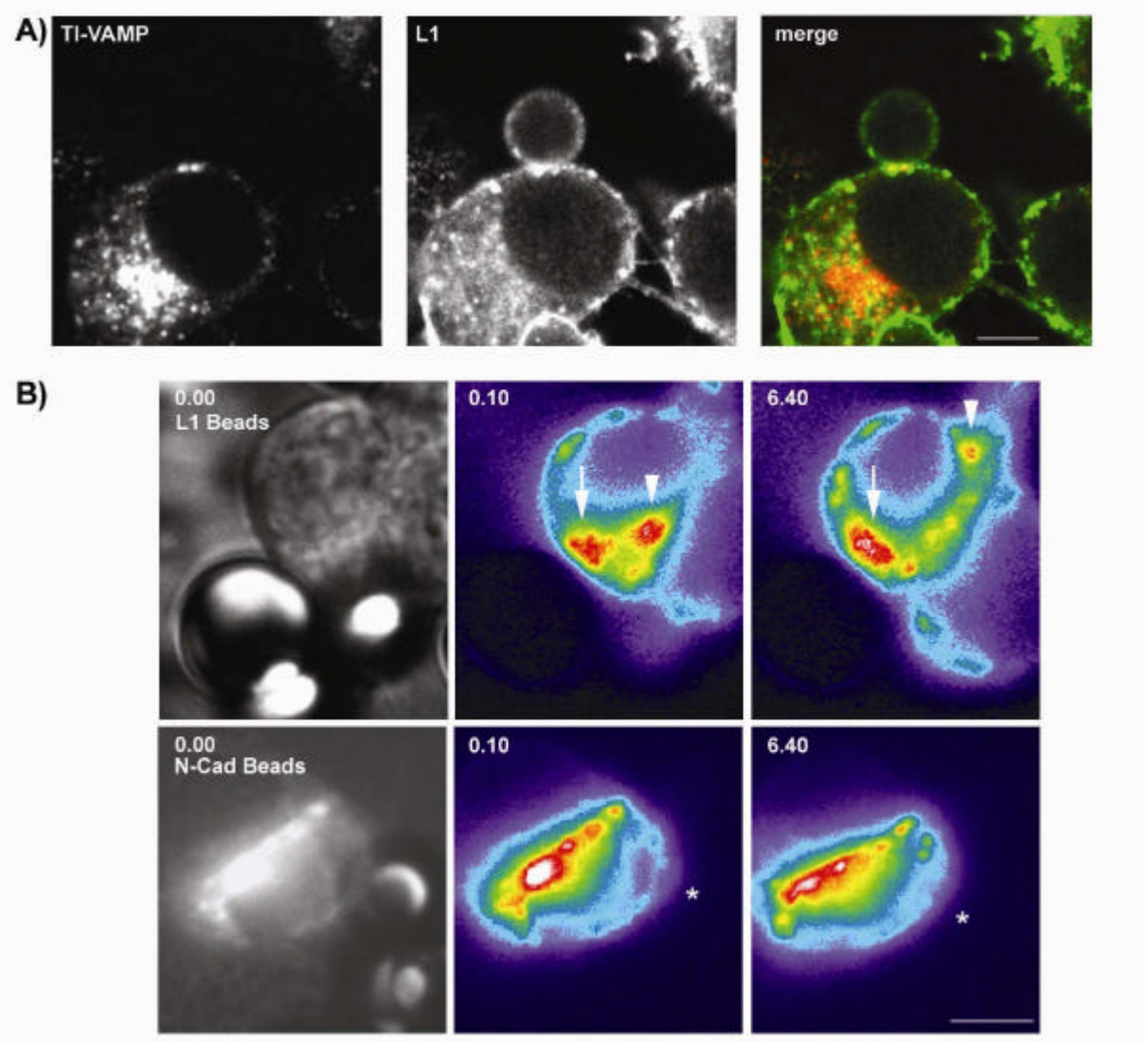

Figure 14) L1-dependent adhesive contacts induce clustering of TI-VAMP-positive vesicles at sites of contact in PC12 cells.

A) TI-VAMP vesicles accumulate at sites of L1-bead contact. PC12-cells were incubated with L1-coated beads, processed for immunofluorescence with mAb 158.2 and pAb to L1 and analyzed by confocal microscopy. Arrows indicate TI-VAMP positive intracellular structures clustered around the bead cell contact, which are also positive for L1 (bar: 5µm).

B) L1-beads induce stable clusters of TI-VAMP-GFP. PC12 cells were transfected with TI-VAMP-GFP and incubated with L1-coated beads (upper panels) or N-Cadherin-coated beads (lower panels). Dynamics of TI-VAMP-GFP were observed by time-lapse video microscopy. Snapshots taken with phase contrast (left) and with GFP-filters (middle and right, shown in false color to highlight concentration of TI-VAMP-GFP signal) are shown. A stable accumulation of TI-VAMP-GFP close to the site of L1-bead-cell contact could be observed during the recording time (indicated by arrow). A second pool of TI-VAMP-GFP signal indicated by an arrowhead showed a dynamic behavior. N-Cadherin-coated beads did not show any influence on the dynamic behavior of TI-VAMP-GFP (position of N-Cadherin bead in false coloured images is indicated with asterisk) (bar: 6µm).

The accumulation of TI-VAMP containing vesicles at sites of L1-bead-cell contact was even more striking when hippocampal neurons were incubated with L1-coated beads. As shown in Figure 15 A, L1-coated beads bound to axonal growth cones induced a strong accumulation of TI-VAMP immunoreactivity at sites of bead-cell contact, as seen by the appearance of bead-shaped structures strongly labeled for TI-VAMP, especially in the apical planes of the confocal sections shown (i.e. where the bead surface is surrounded by the growth cone membrane). As with PC12 cells, the binding of beads to neurons was strictly dependent on the presence of the L1-Fc fragment (not shown). The dynamics of TI-VAMP recruitment to L1-bead-growth cone contact were analyzed by video microscopy in GFP-TI-VAMP transfected neurons (Fig. 15 B, video 3). The recording was started immediately after the bead marked with an arrow had started to contact the growth cone, whereas the other beads shown were already in contact with the growth cone. After contact formation (10 sec), the growth cone seems to wrap a filopodium around the bead surface (phase contrast, 100 sec), which is strongly labeled with GFP-TI-VAMP (GFP-TI-VAMP, 100 sec). The bead is then transported to the more central region of the growth cone, presumably via receptor mediated linkage of L1 present on the bead to the retrograde actin flow (Kamiguchi and Yoshihara, 2001). Accumulation of GFP-TI-VAMP around the bead surface in the central region of the growth cone is weaker (GFP-TI-VAMP, 300 sec). Images taken at a more basal focal plane revealed the presence of GFP-TI-VAMP at all four beads associated with the growth cone (not shown), but to a much lesser extent than the accumulation of GFP-TI-VAMP shown in the peripheral region of the growth cone at 100 sec. Beads present along the neurites or at the cell body did not induce accumulation of GFP-TI-VAMP (not shown). Interestingly, the original region of contact between bead and growth cone was still heavily labeled with GFP-TI-VAMP 300 sec after the initial contact, even after the bead had moved away from the periphery of the growth cone.

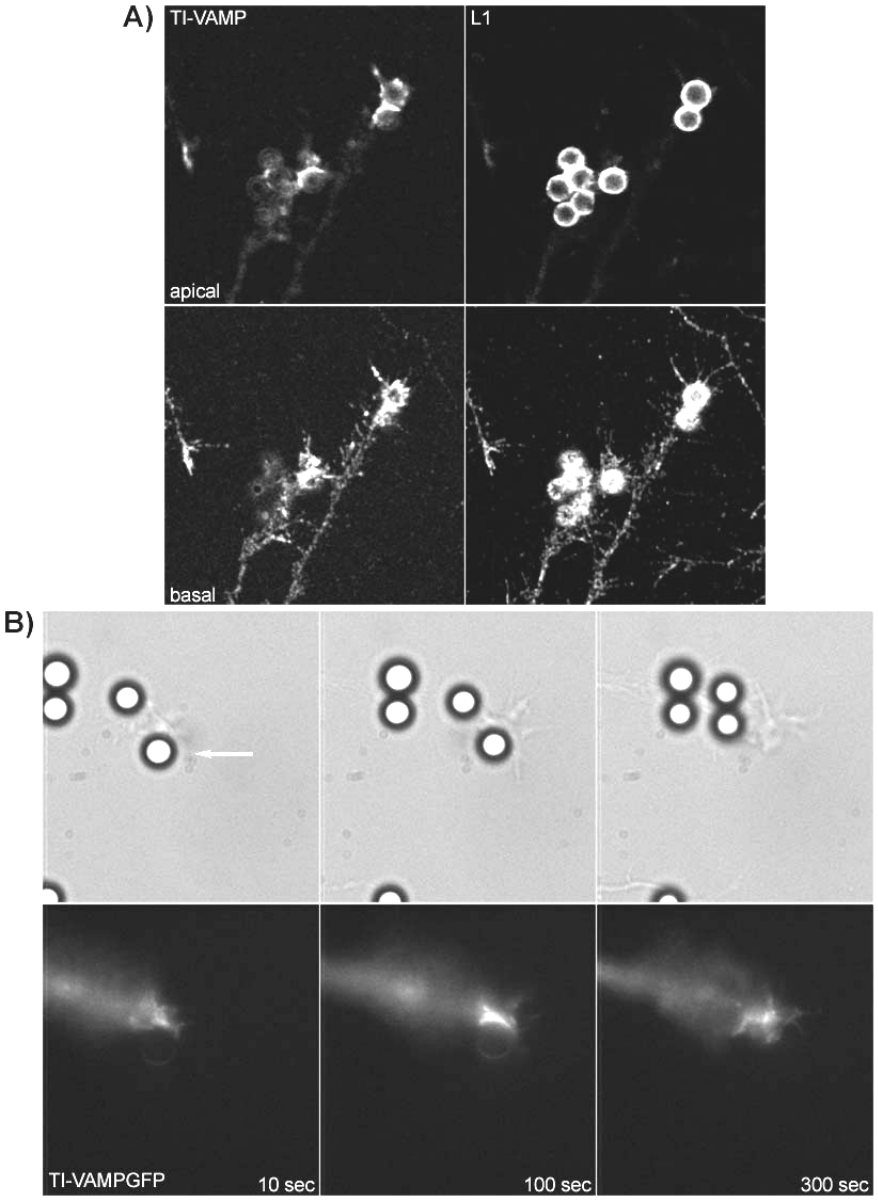

15) L1-dependent adhesive contacts induce clustering of TI-VAMP-positive vesicles in growth cones of hippocampal neurons.

A) Accumulation of TI-VAMP at bead-growth cone junctions. Hippocampal neurons grown for three days in vitro were incubated with L1 coated beads and processed for confocal microscopy analysis with mAb 158.2 and pAb to L1. A basal and an apical section of the same region are shown. Note the formation of bead shaped, TI-VAMP positive structures in the growth cones (Bead diameter: 4µm).

B) Dynamics of TI-VAMP recruitment to L1-coated beads in contact with an axonal growth cone were analyzed by time-lapse video microscopy in hippocampal neurons transfected with TI-VAMP-GFP. Sequential snapshots taken with phase contrast (upper panels) and with GFP-filters (lower panels) are shown. Note that the stage of the microscope was moved slightly to the right during recording time between frames 10 sec and 100 sec. Shortly after the bead touched the growth cone (10 sec, bead touching is marked with an arrow), a filopodium can be recognized in phase contrast wrapping around the upper part of the bead (phase contrast 100 sec), which shows strong accumulation of TI-VAMP-GFP (100 sec; TI-VAMP-GFP). The bead is moving away from the peripheral, filopodium-rich region to the central part of the growth cone (300 sec phase contrast), and TI-VAMP-GFP signal close to the bead is weaker (TI-VAMP-GFP 300 sec). Note that the TI-VAMP-GFP signal remains elevated in the filiopodium rich, peripheral region of the growth cone, where the bead originally touched (Bead diameter: 4 µm).

Thus, signaling events induced by the L1-L1 homophilic interaction seem to persist for a certain time, even after the homophilic engagement is terminated. This analysis revealed, that the recruitment of the TI-VAMP compartment to sites of L1-induced contacts in the growth cone is a transient phenomenon and occurs in the peripheral, actin rich region of the growth cone.

Importantly, the accumulation of TI-VAMP at sites of bead-growth cone contact was a very robust phenomenon as shown in Figure 16. When images were taken based on the L1 signal (i.e. in blind for associated TI-VAMP immunoreactivity), formation of bead shaped structures strongly labeled for TI-VAMP could be observed in six out of eight examples. In summary, L1-coated beads induce a strong, temporary accumulation of the TI-VAMP-positive membrane compartment in the actin rich, filopodial domain of growth cones.

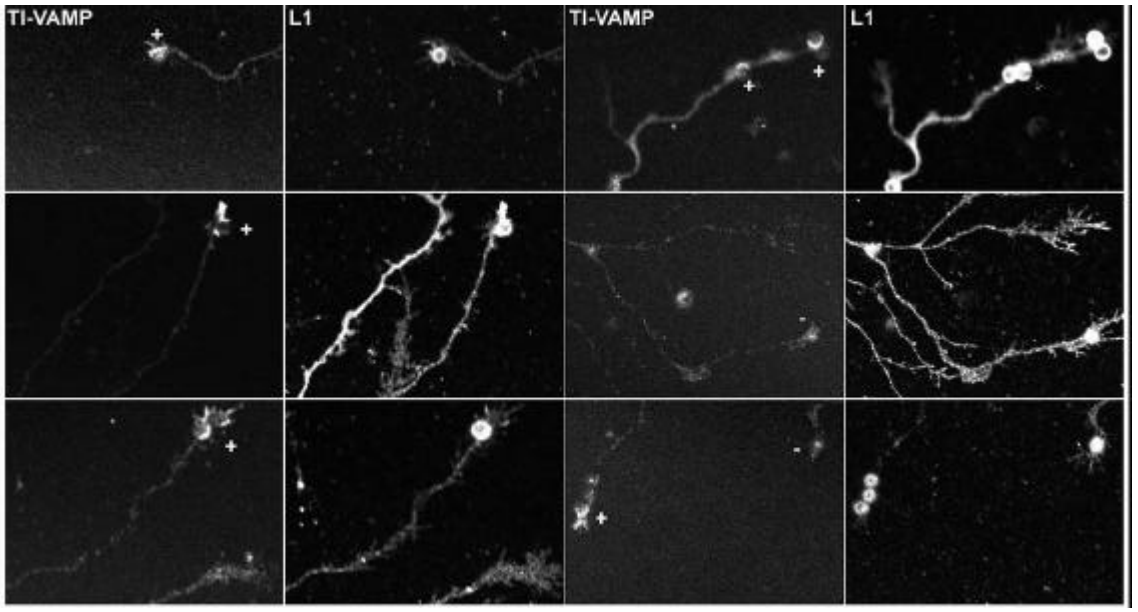

Figure 16) Accumulation of TI-VAMP in growth cones contacting L1 beads is a robust phenomenon.

Hippocampal neurons at 3 div were incubated with L1 coated beads and processed for confocal microscopy analysis with mAb 158 and pAb to L1. Images were taken based on L1 fluorescence, therefore blind for TI-VAMP immunoreactivity. Accumulation of TI-VAMP reactivity at sites of bead contact were scored as positive (+) and no accumulation as negative (-) (Bead diameter represents 4µm).

III.9. L1-, but not N-Cadherin-mediated adhesive contacts induce actin-dependent recruitment of the TI-VAMP compartment

The results obtained in Figures 11,12 and 13 suggested that the recruitment of the TI-VAMP compartment to L1-dependent contacts might involve a remodeling of the actin cytoskeleton around contacting beads. Indeed, beads coated with the cell adhesion molecules of the Cadherin- or IgCAM family actively remodel and recruit F-actin rich structures via outside-in signaling upon engagement in homophilic interaction with receptors (Lambert et al., 2000; Suter et al., 1998). Therefore, the behavior of the TI-VAMP compartment was analyzed with reference to the actin cytoskeleton after incubation of neurons with L1-coated beads. Figure 17 shows that structures enriched for TI-VAMP labeling, which are induced by the L1 beads present on the growth cone, colocalize with F-actin rich structures surrounding the beads. Both the formation of F-actin rich structures and the accumulation of TI-VAMP by L1-beads were completely abrogated in neurons treated with cytochalasin B. The same result was obtained using latrunculin A (not shown). Thus, L1-dependent contact formation in the growth cone leads to the formation of F-actin rich structures, which are necessary for the recruitment of the TI-VAMP compartment to sites of bead-growth cone contact.

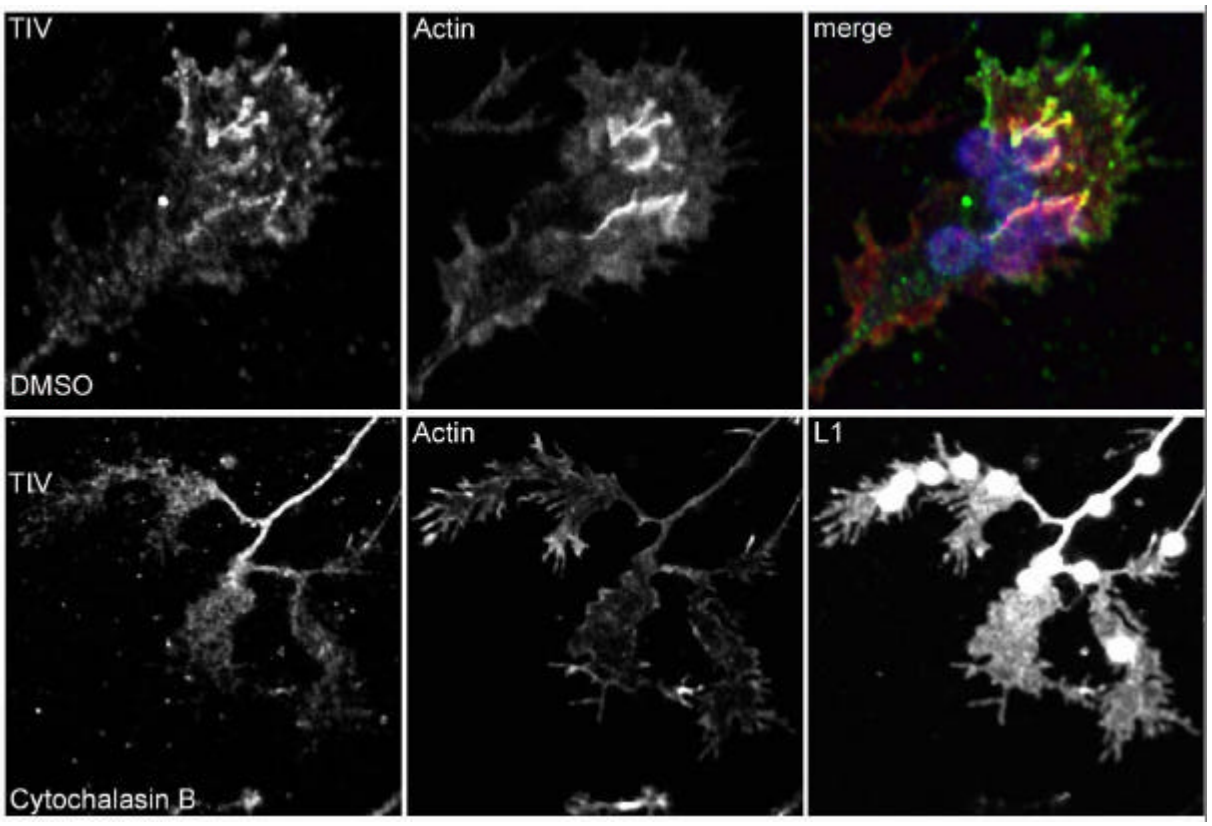

Figure 17) Recruitment of TI-VAMP to L1 beads depends on actin dynamics in the growth cone.

Hippocampal neurons at 3div were incubated with L1 coated beads in the presence of either 5µM DMSO or 5µM Cytochalasin B for 45 min. Cells were processed for confocal microscopy with mAb to TI-VAMP (green), phalloidin (red) or pAb to L1 (blue). Bead shaped structures can be recognized which are positive for TI-VAMP and F-actin and which coincide with L1-coated beads present on the growth cone shown (merge) (upper panels). Low magnification images of Cytochalasin B treated cells demonstrate, that growth cones appear flat and broad (lower panels). A number of L1 coated beads are seen to touch the three neuritic extremities (micrograph L1), but no bead shaped structures appear that are positive for TI-VAMP or F-actin (Bead diameter: 4µm).

As shown above, adhesion of N-Cadherin-coated beads to PC12 cells is independent of the expression of TI-VAMP and does not induce recruitment of the TI-VAMP compartment to bead-cell junctions (Fig. 10 and Fig. 14). Yet, both L1- and N-Cadherin mediated adhesive junctions can induce profound, local rearrangements of the cytoskeleton (Fig 17 and (Lambert et al., 2000). Thus, I tested, whether formation of actin-rich structures independent of the signaling cue is sufficient to induce the accumulation of TI-VAMP-containing vesicles in the axonal growth cone. Therefore, the behavior of the TI-VAMP compartment was compared when either an L1-or N-Cadherin-coated bead contacts a growth cone. As shown in Figure 18 A, both L1- (marked by asterisk) and N-Cadherin-coated beads induced a strong accumulation of F-actin in the growth cones close to the beads. In contrast, F-actin-rich structures close to N-Cadherin beads showed low TI-VAMP immunoreactivity when compared to F-actin-rich structures in proximity to the L1 bead, which were strongly labeled for TI-VAMP. Quantification of the TI-VAMP immunoreactivity in F-actin rich structures showed, that the TI-VAMP signal close to L1-beads is more than twice than that close to N-Cadherin beads. A simultaneous analysis of the Synaptobrevin 2 compartment did not reveal any differences in fluorescence intensity close to either L1- or N-Cadherin beads. Moreover, Synaptobrevin 2 fluorescence intensity showed rather high variation in both cases (not shown), indicating that the localization of the Synaptobrevin 2 compartment is not influenced by either adhesive system.

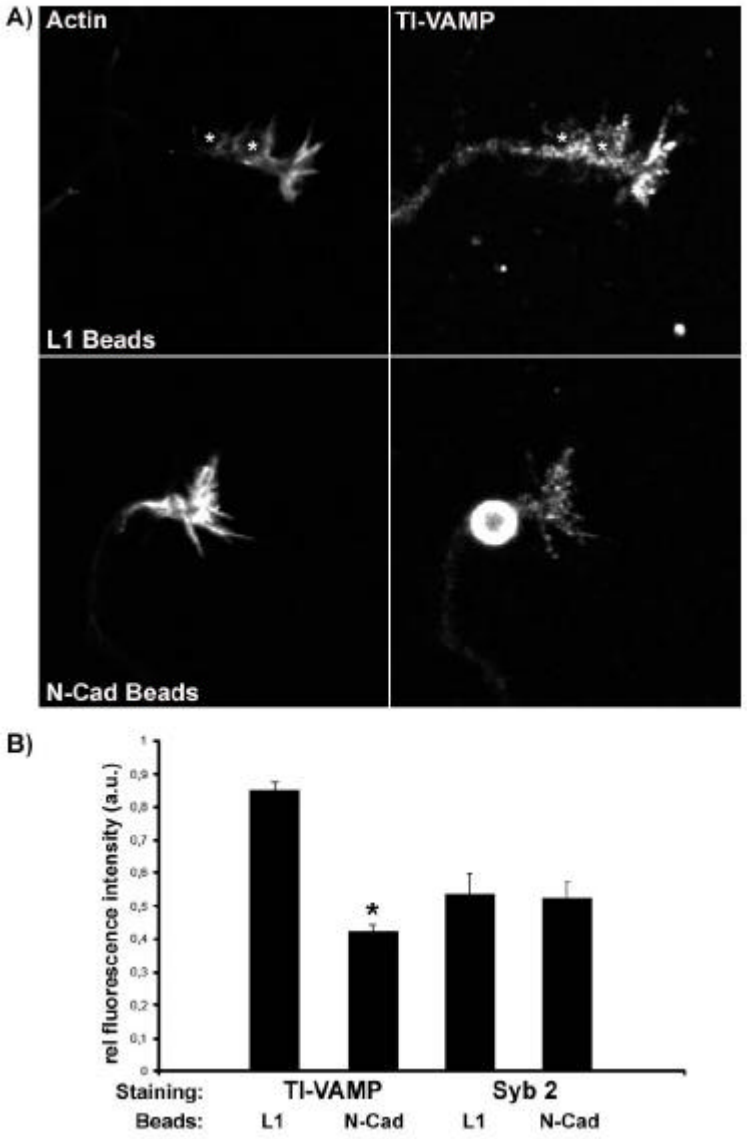

Fig 18) L1-, but not N-Cadherin mediated contacts induce accumulation of TI-VAMP in axonal growth cones

A) Hippocampal neurons at 3div were incubated for 45 min with beads coated with either L1- or N-Cadherin. Cells were processed for immunofluorescence with mAb 158.2 and Phalloidin and analyzed by confocal microscopy. Both L1- and N-Cadherin-coated beads induced a strong accumulation of F-actin in the growth cone close to the bead (upper and lower micrographs, L1 beads are indicated by asterisks). Whereas TI-VAMP-immunoreactivity close to the L1 beads is strong, no particular accumulation for TI-VAMP can be recognized in the growth cone close to the N-Cadherin-bead. Note that anti-mouse Fc-specific antibodies were used to couple N-Cadherin fusion protein to beads. Anti-mouse Fc-binding sites were only partially blocked by preincubation with recombinant mouse Fc fragments before incubation with mAb to TI-VAMP resulting in fluorescent labeling of the N-Cadherin-coated beads (see material and methods) (Bead diameter: 4µm).

B) Neurons were incubated with L1- or N-Cadherin-coated beads and processed for analysis by confocal microscopy with mAbs to TI-VAMP or Synaptobrevin 2. Images were taken based on actin-fluorescence, blind for TI-VAMP- or Synaptobrevin 2 associated fluorescence intensity. Regions in growth cones in close apposition to beads were selected based on high F-actin staining intensity, and the corresponding TI-VAMP- or Synaptobrevin 2-fluorescence was quantified. The mean normalized fluorescence-intensity for TI-VAMP close to L1 beads was more than two times higher than fluorescence intensity close to N-Cadherin beads (L1beads: n=25, N-Cadherin beads: n=17, $p<0.0001$). In contrast, no difference in synaptobrevin 2 staining close to either L1- or N-Cadherin-coated beads could be observed (L1-and N-Cadherin-beads: n=17).

Importantly, this experiment demonstrates, that the presence of beads on growth cones alone is not sufficient to induce accumulation of the TI-VAMP compartment. Moreover, recruitment of the TI-VAMP compartment to adhesive junctions depends on signaling events induced by L1, and not N-Cadherin. Finally, whereas the presence of F-actin was shown to be necessary for the accumulation of TI-VAMP in growth cones (Fig. 12 and Fig. 17), F-actin per se is not sufficient for the recruitment of TI-VAMP, because F-actin-rich structures induced by N-Cadherin-coated beads are low in TI-VAMP immunoreactivity.

III.10. Specific recruitment of the TI-VAMP compartment to the plasma membrane at L1-dependent contacts

Next, I analyzed whether membrane compartments other than TI-VAMP containing vesicles might be recruited to L1-coated bead-growth cone contact. The behavior of the TI-VAMP-compartment was compared to the Synaptobrevin 2-compartment when an L1-bead-growth cone contact. The comparison of these two compartments was of particular interest. Both compartments are expressed in the growth cone and are of similar, vesicular morphology. As seen in Figure 19 A, TI-VAMP immunoreactivity was particularly enriched in the apical plane of the confocal sections of the growth cone shown, where a bead shaped structure was observed. In contrast, Synaptobrevin 2 reactivity decreased from the basal to the apical plane of the growth cone and no formation of a bead like structure was seen. The average pixel intensity was quantified in the basal and apical region of TI-VAMP and Synaptobrevin 2 immunoreactivity in eight growth cones in contact with a bead (Fig. 19 B). In the case of Synaptobrevin 2, the ratio between apical to basal average pixel intensity was found to be 0.4+/- 0.06, indicating a sharp decrease in fluorescence intensity from the basal to the apical plane. In contrast, using the same parameters to analyse TI-VAMP distribution in the same growth cones, a ratio close to 1 was found (0.9+/-0.085). The difference between the apical to basal ratio of Synaptobrevin 2 and TI-VAMP was statistically significant ($p=0.01$; Mann-Whitney non-parametric test). Thus L1-coated beads contacting an axonal growth cone induced a strong and specific accumulation of the TI-VAMP compartment in proximity to the cell-bead contact when compared to the Synaptobrevin 2 compartment.

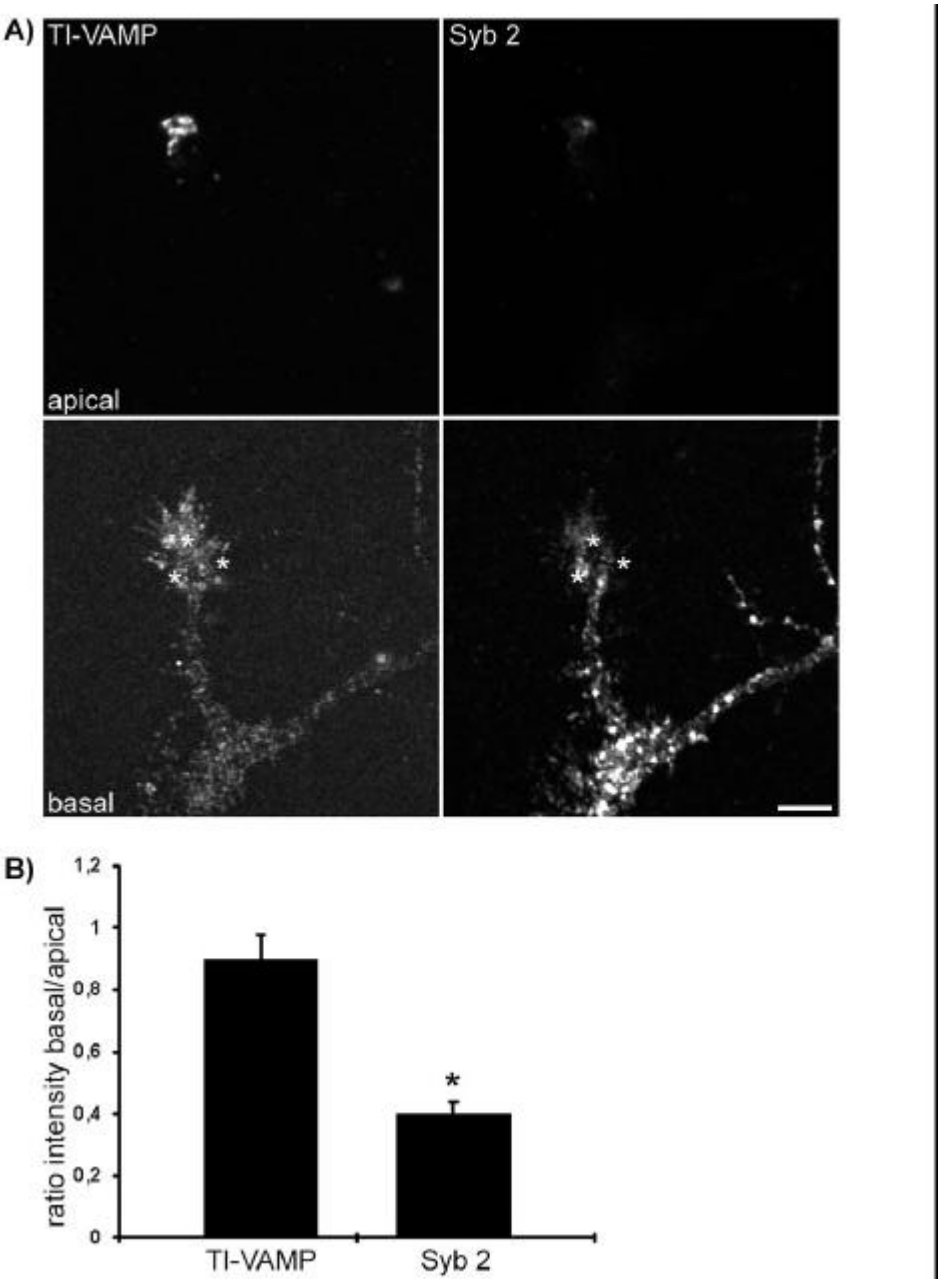

Fig 19) L1-dependent adhesive contacts induce clustering of Tl-VAMP-, but not Synaptobrevin 2-positive vesicles in neuronal growth cones.

A) Comparison between Tl-VAMP and Synaptobrevin 2 (Syb 2) compartment in a growth cone contacting a bead. Hippocampal neurons were incubated with L1 beads and processed for immunofluorescence with mAb 158.2 and pAb to Syb 2. A basal and an apical section of the same region are shown and bead positions are indicated by asterisks. Note the strong Tl-VAMP immunoreactivity in the apical confocal section as compared to the basal section. (Bar=4µm).

B) The average pixel intensity was quantified in the basal and apical region of Tl-VAMP and Synaptobrevin 2 immunoreactivity in eight growth cones in contact with a bead. In the case of Synaptobrevin 2, the ratio between apical and basal average pixel intensity was found to be 0.4+/-0.06, indicating a sharp decrease in fluorescence intensity from the basal to the apical plane. In contrast, using the same parameters to analyse Tl-VAMP distribution in the same growth cones, we found a ratio close to 1 (0.9+/-0.085). The difference between the apical:basal ratio of Synaptobrevin 2 and Tl-VAMP was statistically significant (p=0.01).

Next, the recruitment of other membrane compartments to L1-coated beads was analyzed with specific antibodies to Calreticulin, an ER-resident protein, Syntaxin 7 and VAMP 4, a SNARE protein expressed in the Golgi complex (Fig. 20). The expression of these makers was compared to TI-VAMP specific labeling. Syntaxin 7 and TI-VAMP are both expressed along the neurite including the growth cone, where they partially colocalize, as seen in the basal confocal section (Fig. 20 B, arrows). The apical section shown revealed that the TI-VAMP containing compartment enriched around the bead is devoid of Syntaxin 7 immunoreactivity. The VAMP 4-specific staining showed the typical Golgi shaped staining in the cell body (Fig. 20 C) and was weak along the neurite. No enrichment of VAMP 4 was seen in apposition to the L1 beads, marked by asterisks, although TI-VAMP staining showed high intensity at the same beads. A similar result was obtained with another Golgi marker, GM130, which was not recruited to the beads (not shown). Late endosomes/lysosomes labeled with the marker proteins LAMP1 or CD63 were restricted to the neuronal cell body and thus also absent (not shown). In contrast, the ER, as seen by Calreticulin labeling, seems to be recruited to L1 bead growth cone contacts. Labeling with another ER marker confirmed the presence of the ER at bead growth cone contacts. In summary, L1-mediated adhesive contacts in the growth cone specifically recruit the TI-VAMP compartment and seem to induce enrichment of the ER.

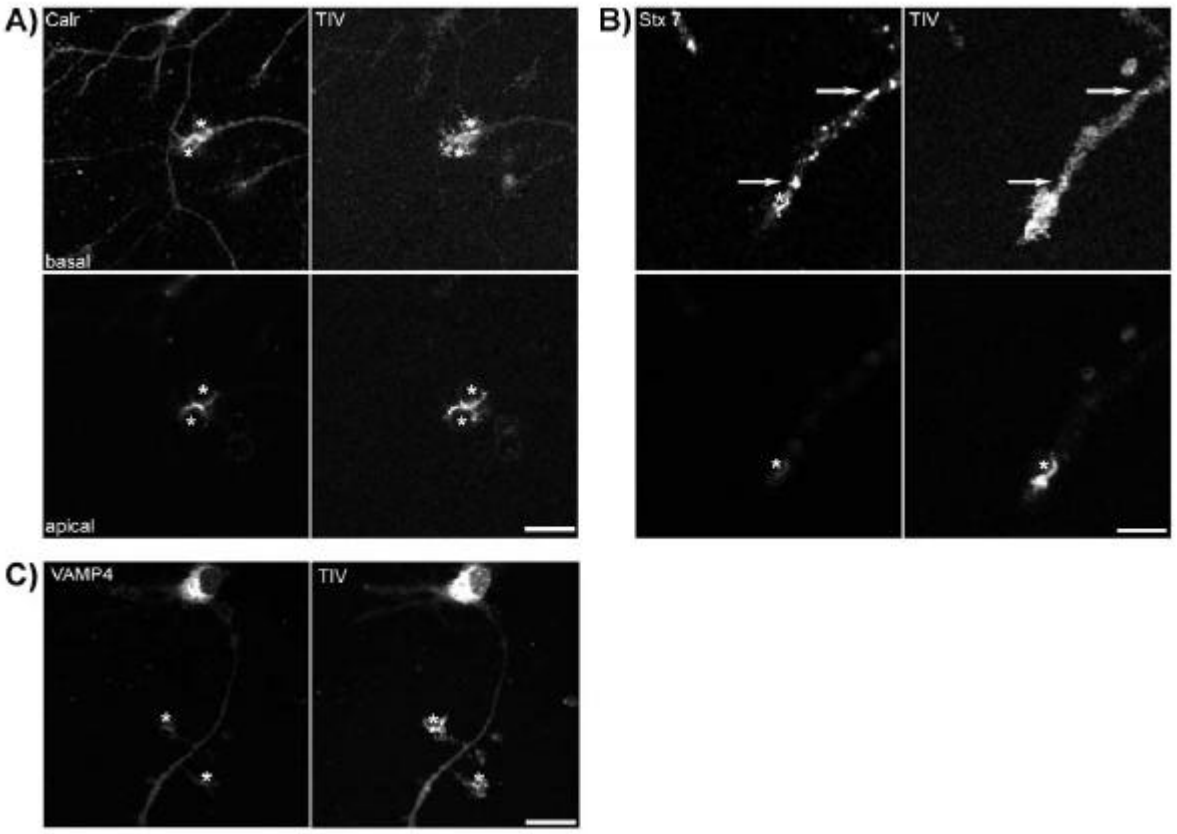

Fig 20) Recruitment of internal membranes to L1 junctions is specific for the TI-VAMP compartment and ER.

Hippocampal neurons 3 div were incubated with L1-coated beads. Membrane compartments were visualized with specific markers to ER (pAb to Calreticulin-Calr), endosomes (pAb to Syntaxin 7-Stx7) or Golgi (pAb to VAMP4) and costained with mAb to TI-VAMP. Comparison between TI-VAMP associated staining and Syntaxin 7 showed that both markers are present in the basal part of the growth cone shown, close to the L1-coated bead marked by an asterisk. In contrast, only TI-VAMP staining can be observed in the apical confocal section of the same growth cone (Bar=8µm). VAMP 4 staining is most intense in the cell body, showing a typical Golgi-shaped staining pattern. In contrast to TI-VAMP staining, no particular enrichment of VAMP 4 can be observed close to the two L1 beads marked by asterisks (Bar=16µm). Calreticulin shows strong labeling intensity in the basal and apical confocal sections close to L1 beads indicated by asterisk, similar to TI-VAMP staining (Bar=8µm).

The accumulation of the TI-VAMP compartment around L1-coated beads implies an outside-in signaling cascade triggered by L1 engaged in homophilic interactions. Indeed, activation of L1 by homophilic interactions is known to trigger signaling cascades such as the MAP kinase pathway (Schaefer et al., 2002; Schmid et al., 2000). In addition, the non receptor kinase p60src plays a crucial role in L1 mediated neurite outgrowth, since stimulation of axonal growth by L1 is abrogated in src deficient neurons (Ignelzi et al., 1994). Activation of outside-in signaling pathways by L1-coated beads was tested by immunofluorescence with specific antibodies to phosphorylated and thus activated kinases of the src-family and to tyrosine phosphorylated proteins (Fig. 21). In A), two beads bound to the growth cone shown (marked by asterisk) induced the formation of bead shaped TI-VAMP positive structures (Fig. 21 A). As seen by the phospho-src immunoreactivity, these structures were also highly enriched in phosphorylated and thus activated p60src (Fig. 21 A). Similarly, binding of L1 beads to growth cones induced high and local activity of tyrosine kinases (Fig. 21 B). The growth cone shown exhibits high immunoreactivity for the pTyr specific antibody compared to the axonal shaft (basal plane). In the apical part of the bead a structure wrapping around half the bead labeled strongly for pTyr (apical plane). Note that pTyr labeling in the apical panel colocalizes with L1 positive structures, that can be recognized by the increased labeling intensity for L1 in the right part of the bead (arrows). In conclusion, engagement of L1 in homophilic interactions leads to the activation of src-family kinases and possibly other tyrosine kinases in axonal growth cones. These events are likely to be involved in the rearrangement of the actin cytoskeleton and recruitment of the TI-VAMP compartment.

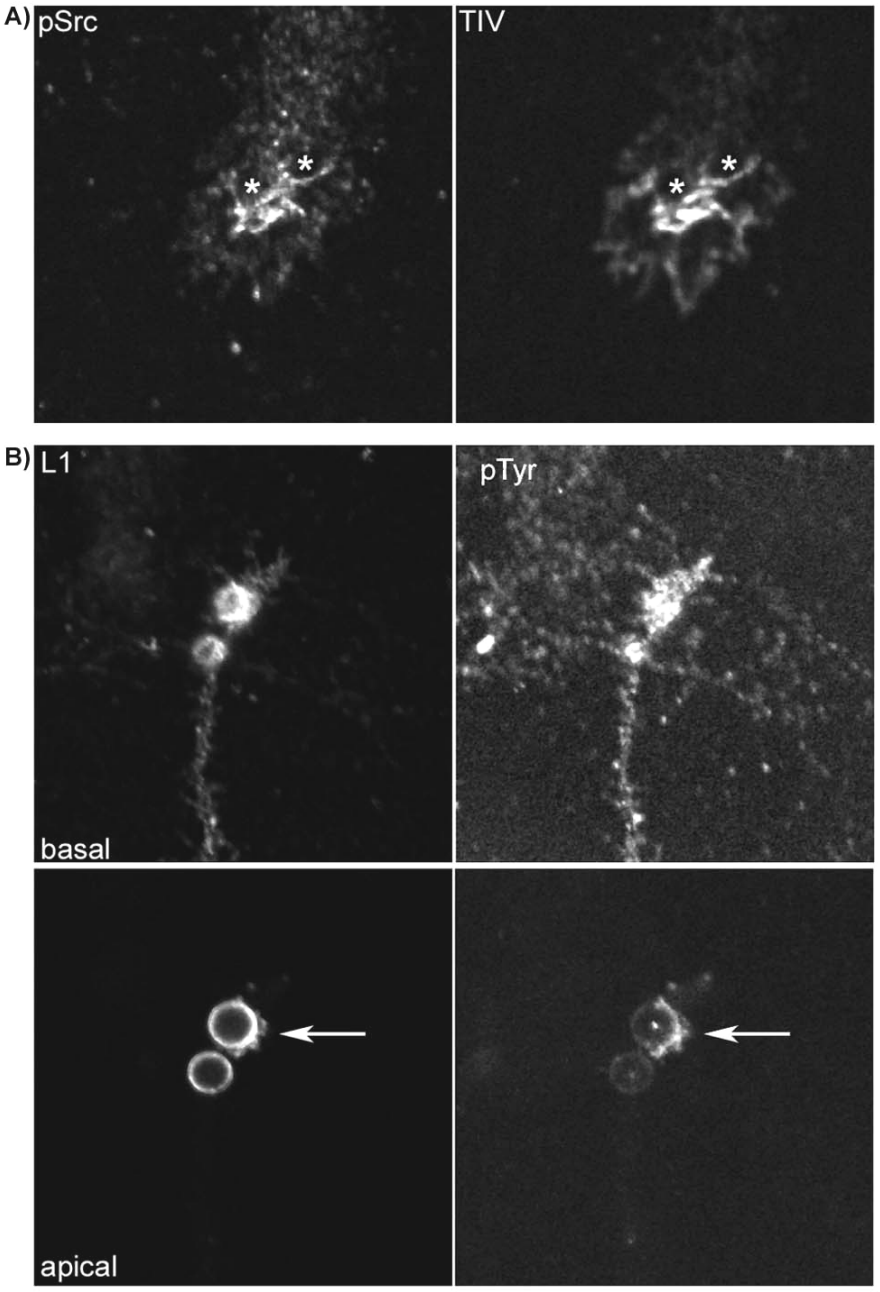

Figure 21) Binding of L1 coated beads to growth cones activates src-kinases and tyrosine kinases.

Hippocampal neurons 3 div incubated with L1-coated beads were analyzed by confocal microscopy for the expression of phosphorylated, and thus activated src-kinases and tyrosine-phosphorylated proteins with specific antibodies. A) Two L1-coated beads (asterisks) bound to the growth cone shown are surrounded by a local accumulation of TI-VAMP immunoreactivity. Phospho-src immunoreactivity coincides with the TI-VAMP staining pattern. B) L1 staining indicates the presence of two beads on the growth cone. PTyrosine staining is strong in the growth cone compared to the axonal shaft (basal). In the apical confocal plane, accumulation of tyrosine phosphorylated proteins around one bead can be recognized (arrow). Note that the side of the bead positive for tyrosine phosphorylation also shows irregular and more intense L1-labeling, indicating the presence of membrane protrusions positive for both, L1-and pTyrosine immunoreactivity (arrow, apical) (Bead diameter: 4µm for all micrographs).

As described earlier, TI-VAMP forms SNARE complexes with the plasma membrane SNAREs Stx1 and SNAP25 (Fig. 3) and undergoes exocytosis in neuronal cells (Fig. 4). Yet, a potential regulation of this exocytotic pathway has not been explored. L1-induced outside-in signaling might represent such a regulatory cue. Figure 22 shows a growth cone contacted by three L1-coated beads. Strikingly, TI-VAMP immunoreactivity is localized close to or in continuity with the plasma membrane of the growth cone. This type of TI-VAMP labeling pattern was observed frequently in larger growth cones where the point of bead-growth cone contact could be clearly distinguished from the plasma membrane outlining the growth cone (see Figures 17 and 21). Thus, L1 mediated adhesive contacts seem to trigger signaling events that lead to a relocalization of the TI-VAMP compartment towards the plasma membrane. To support this notion, the localization of Syntaxin 1, the plasma membrane t-SNARE of TI-VAMP in neurons (Fig. 3), and sec 6, a subunit of the exocyst complex, was analyzed in neurons incubated with L1-coated beads. Syntaxin 1 is localized throughout the axonal plasma membrane including the growth cone (Fig. 22 B, basal). Staining with phalloidin reveals the formation of the typical F-actin rich structure around the L1-coated bead (marked by asterisk) contacting the upper growth cone, which colocalized with Syntaxin 1-positive plasma membrane (Fig. 22 B, apical). A similar result was obtained for the exocyst subunit sec 6 (Fig. 22 C). L1 staining demonstrates the presence of several beads contacting a growth cone. The basal plane shows localization of sec 6 along the plasma membrane of the growth cone. The apical confocal section demonstrates the presence of a bead-shaped structure positive for sec 6 which wraps around a bead.

The presence of Syntaxin 1 in structures forming around the L1-coated bead supports the possibility that the TI-VAMP-compartment undergoes local exocytosis in the growth cone controlled by L1-induced signaling events. The exocyst complex could play a role in determining the site of exocytosis of TI-VAMP vesicles, similar to its role in yeast and epithelial cells (Grindstaff et al., 1998; TerBush et al., 1996).

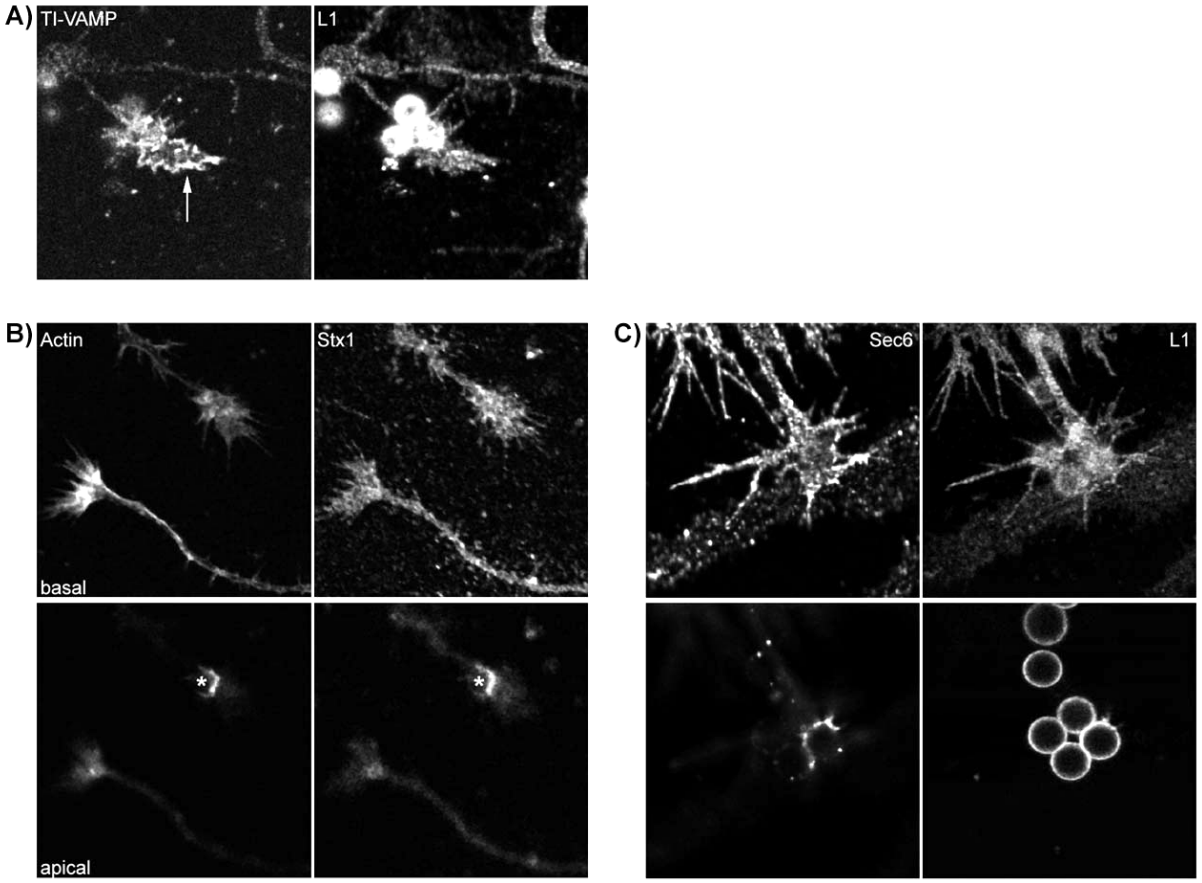

Figure 22) Localization of TI-VAMP, Syntaxin 1 and the exocyst subunit Sec 6 in growth cones contacted by L1 beads.

Hippocampal neurons 3div were incubated with L1 coated beads. The expression of TI-VAMP and two markers of the exocytotic machinery in neurons, Syntaxin 1 and sec 6, was analysed by confocal microscopy. A) A growth cone is in contact with three L1 coated beads, as seen by L1 immunolabeling. TI-VAMP immunoreactivity outlines the shape of the periphery of the growth cone indicating TI-VAMP localization close to, or coinciding with, the plasma membrane (arrow) (Bead diameter: 4µm). B) A basal confocal section of Syntaxin 1 immunolabeling reveals a uniform distribution of this protein throughout the neuritic plasma membrane including the growth cone (Syntaxin 1, basal). An actin rich structure revealed by phalloidin staining, which forms around the L1 bead (indicated by asterisk), is also positive for Syntaxin 1 (apical section). C) Sec 6 is localized to the plasma membrane along the neurite and the growth cone (basal section). L1 staining reveals the presence of four beads on the growth cone shown. On the apical confocal section, a bead shaped structure can be recognized that is positive for sec 6. Note that the L1 staining on the bead positive for sec 6 is irregular and of higher intensity compared to adjacent beads, indicating the presence of L1 positive membrane wrapping around the bead surface (arrow) (Bead diameter: 4µm in both Syntaxin 1 and sec 6 micrographs).

IV Discussion

In this study, I have demonstrated that TI-VAMP expression is necessary for neurite outgrowth and L1-mediated adhesion. Furthermore, L1-mediated adhesion controls TI-VAMP-mediated trafficking via an actin-based mechanism. This model is based on the following evidence presented here: (i) TI-VAMP mediates a recycling pathway in neuronal cells and inhibiting this pathway by TI-VAMP-specific RNAi strongly inhibits neurite outgrowth in PC12 cells; (ii) TI-VAMP co-localizes with L1 *in situ* in the developing brain, PC12 cells and neurons and endocytosed L1 is localized to the TI-VAMP compartment; (iii) impaired TI-VAMP expression affects the surface expression of L1 and reduces the binding of L1-coated beads to PC12 cells; (iv) the TI-VAMP expression in growth cones depends on actin dynamics and L1-dependent adhesive contacts induce local clustering of TI-VAMP in an actin-dependent manner, suggesting that L1-mediated adhesion controls the anchoring of TI-VAMP containing vesicles. Therefore, this report demonstrates that a cross talk exists between TI-VAMP-dependent trafficking and L1-mediated adhesion and between L1-induced signaling and TI-VAMP dynamics.

IV.1. TI-VAMP expression is developmentally regulated and required for neurite outgrowth

The results described show that TI-VAMP expression is upregulated during brain development, similar to other proteins with known function in neurite outgrowth and synaptogenesis (Fig. 2) suggesting an important role of this protein for brain development *in vivo*. Furthermore, a strong decrease of TI-VAMP expression was achieved by RNA interference in PC12 cells (Fig. 5). Similar results were obtained by our group using hippocampal neurons in primary culture providing strong evidence that TI-VAMP expression is essential for neurite outgrowth (Fig. 5 and (Alberts et al., 2003).

These results confirm and extend previous studies from our group (Martinez-Arca *et al.*, 2000; Martinez-Arca *et al.*, 2001), which demonstrated that the TI-VAMP

membrane trafficking pathway is important for axonal and dendritic outgrowth, by using dominant positive and negative forms of the protein. The present finding that TI-VAMP expression is required for normal neurite outgrowth clearly demonstrates that membrane trafficking plays an important role in this process. Also, this underlines the high degree of compartmentalization of neuronal cells and the specificity of v-SNAREs in mediating distinct membrane trafficking pathways. Similar conclusions were drawn from the analysis of another neuronal v-SNARE Syb 2, which was shown to be essential for neurotransmitter release, but, in contrast to TI-VAMP, dispensable for neuronal differentiation (Osen-Sand *et al.*, 1996). *In vivo* confirmation of these observations were obtained by the analysis of mice mutant for Syb 2, which show an almost complete block in neurotransmitter release, but apparently normal brain development (Schoch *et al.*, 2001).

Similarly, the regulators of membrane trafficking involved in neurotransmitter release and trafficking events leading to neuronal differentiation seem to be distinct to a large extent. Mutants for munc-18 and munc 13-1/2, two important regulators of synaptic vesicle exocytosis, show severe defects in neurotransmitter release without any apparent impairment of brain development. (Aravamudan et al., 1999; Verhage et al., 2000) However in contrast, studies describing that SNAP-25 antisense oligonucleotides and botulinum neurotoxin A inhibited neurite outgrowth (Osen-Sand *et al.*, 1993; Osen-Sand *et al.*, 1996), were not confirmed in the knockout mice (Washbourne *et al.*, 2002). Since neurons express several syntaxins and both SNAP23 and SNAP25 (Chen *et al.*, 1999), a level of redundancy can be anticipated and only the genetic invalidation of several plasma membrane SNAREs (at least SNAP25 and SNAP23) could result in defects in the development of the brain.

Taken together with the earlier results provided by our group (Martinez-Arca *et al.*, 2000; Martinez-Arca *et al.*, 2001), the study presented here establishes the important function of the TI-VAMP compartment in neurite outgrowth and will help to define the role of other SNARE proteins and regulators of membrane trafficking involved in neuronal differentiation.

IV.2. TI-VAMP mediates a recycling pathway in neuronal cells

It was important to define the pathway mediated by TI-VAMP in neuronal cells, because conflicting data exist as to whether it is of exocytotic (Galli et al., 1998; Hibi et al., 2000; Lafont et al., 1999) or degradative nature (Advani et al., 1999; Bogdanovic et al., 2002; Ward et al., 2000). The results presented here suggest that TI-VAMP mediates a recycling pathway in neuronal cells, which is based on the following findings: i) TI-VAMP forms SNARE complexes with the plasma membrane SNAREs Syntaxin 1 and SNAP-25 as well as the endosomal SNAREs Vti1b and Syntaxin 7 and colocalizes with the latter (Fig. 3); ii) the IgCAM L1 is endocytosed into the TI-VAMP compartment in both neurons and in PC12 cells (Fig. 8); iii) TI-VAMP undergoes exocytosis in PC12 cells during the course of neuronal differentiation (Fig. 4); iv) importantly, TI-VAMP controls the surface expression of L1, thus clearly indicating that TI-VAMP mediates an exocytotic pathway in neuronal cells (Fig. 10).

It was previously shown, that TI-VAMP defines a new type of vesicle that is different from synaptic vesicles and transferrin receptor positive recycling endosomes/early endosomes in neuronal cells (Coco et al., 1999). A striking feature of the TI-VAMP localization in neurons is its accumulation in the peripheral region of growth cones (Coco et al., 1999) Fig. 7, 11 and 12). In fact, acidic, late endosomal/lysosmal compartments are absent from growth cones and confined to axonal and dendritic regions proximal to the cell body (Overly and Hollenbeck, 1996; Parton et al., 1992). Thus, whereas TI-VAMP might localize to late endosomal compartments in the neuronal cell body similar to non-neuronal cells, this is clearly not the case in growth cones. The majority of endocytic organelles in the growth cone are of a pH typical for recycling/sorting endosomes (Overly and Hollenbeck, 1996) and therefore, in agreement with the observations made in Figures 3, 4 and 9, TI-VAMP is likely to mediate a local recycling pathway within the growth cone.

In non neuronal cells, TI-VAMP colocalizes with late endosomal markers like CD63 (Advani et al., 1999; Coco et al., 1999; Martinez Arca et al., 2003; Martinez-Arca et al., 2003) and TI-VAMP was suggested to mediate late endosomal/lysosomal fusion together with Syntaxin 7 (Bogdanovic et al., 2002; Ward et al., 2000).

Ultrastructural analysis by electron microscopy performed by our group and Advani et al. localized TI-VAMP to multivesicular bodies and a tubulo-vesicular compartment in the neuronal cell line PC12 and in brain (Advani et al., 1999; Coco et al., 1999; Muzerelle et al., 2003). Multivesicular bodies are in fact intermediates of the endosomal pathway and are therefore better referred to as multivesicular endosomes (MVEs) (Raiborg et al., 2003). Since late endosomal/lysosomal compartments in neurons seem to be restricted to cell bodies and the proximal part of neurites (Overly and Hollenbeck, 1996; Parton et al., 1992), proteins and membrane destined to be degraded have to be transported retrogradely to the cell body. Interestingly, the transport carriers mediating this pathway have been identified as large, multivesicular structures (Parton et al., 1992). Thus, TI-VAMP could play a role in retrograde transport along the axon mediated by MVEs as seen by Dotti and colleagues (Parton et al., 1992).

In recent years, however, the detailed analysis of multivesicular endosomes in several cell types has shed new light on possible, additional functions. So called secretory lysosomes in hematopoetic cells are derived from or identical to MVEs. These specialized organelles are of lysosomal nature, but can be exocytosed in response to stimulation (Blott and Griffiths, 2002) and the secretion of secretory lysosomes from mast cells was proposed to be mediated by TI-VAMP. (Hibi et al., 2000) In fact, secretory lysosomes do not seem to be restricted to specialized cell types like hematopoetic cells but, as recently demonstrated, exist in multiple, different cell types, where they mediate plasma membrane repair (Jaiswal et al., 2002). It is tempting to speculate that membrane repair and cell outgrowth could depend on the same exocytotic pathway. Intriguingly, a PC12 cell line was described which lacks the classical, TeNT-sensitive regulated secretion, but specialized secretory vesicles persist, called enlargosomes, which are capable of mediating membrane repair and neurite outgrowth (Borgonovo et al., 2002).

Both membrane repair and cell outgrowth require massive transport to the plasma membrane, and internal vesicles in MVEs could be seen as a reservoir of membrane that could be mobilized upon demand (Blott and Griffiths, 2002). Supporting this notion, it was demonstrated in dendritic cells, that a maturation stimulus leads to fusion of the internal vesicles with the limiting membrane of the MVE resulting in a tubular organelle (Kleijmeer et al., 2001). Transport to the plasma membrane of peptide-loaded MHCII molecules occurs thereafter, in vesicles devoid

of lysosomal markers like LAMP (Amigorena et al., 1994; Turley et al., 2000). Recent results from our group demonstrate, that TI-VAMP is localized to the internal membranes of MVEs in the epithelial cell line MDCK (V.Proux, G. Raposo, T.Galli, unpublished). Thus, the membrane compartment in neurons containing TI-VAMP and Syntaxin 7 could be related to the multivesicular endosomes/secretory lysosomes known from hematopoetic cells. The TI-VAMP-positive vesicles accumulating in growth cones, which are devoid of Syntaxin 7-immunoreactivity, might have originated from this compartment. Ultrastructural analysis of the TI-VAMP-compartment in neurons grown in culture should help to better understand the relation between TI-VAMP-positive membrane carriers expressed in growth cones and in the cell body.

IV.3. TI-VAMP is required for L1 function

The finding that L1-dependent adhesion is impaired by reduced expression of TI-VAMP clearly points to an essential role of TI-VAMP-dependent trafficking in the function of L1 at the plasma membrane (Fig. 10).

L1 is a cell adhesion molecule of the IgCAM family expressed mainly in brain, where it plays a crucial role in development. A human neurological disorder, known as MASA syndrome, is caused by mutations in the L1 gene (Brummendorf et al., 1998). The disease is characterized by malformations of the brain, particularly of the cortico-spinal tract. Similarly, mice mutant for L1 show defects in corticospinal axon guidance (Cohen et al., 1998; Dahme et al., 1997). At the cellular level, purified L1 presented to neurons growing *in vitro* stimulates axonal outgrowth by homophilic L1 interactions (see Fig Intro, (Lemmon et al., 1989), which is abrogated in L1 knock-out animals (Dahme et al., 1997).

Interestingly, neuronal L1 harbours an additional short exon that yields a tyrosine-based motif YRSLE. This motif mediates binding to the AP-2 adaptor complex and clathrin dependent endocytosis and accelerates the recycling of neuronal L1 (Kamiguchi *et al.*, 1998). Thus, a role for intracellular trafficking in L1 function, especially in the course of neuronal development, can be anticipated. In analogy to migrating cells, it was suggested that L1 trafficking in the axonal growth

cone establishes a dynamic gradient of L1 adhesivity necessary to move along the substrate (Kamiguchi and Lemmon, 2000b). Indeed, such a gradient was recently detected and its maintenance was dependent on endocytic trafficking (Kamiguchi and Yoshihara, 2001). The results presented here suggest that the TI-VAMP-dependent intracellular trafficking of L1 may be necessary to stabilize and regulate adhesive contacts of neuronal cells. As mentioned above, TI-VAMP colocalizes with the tetraspanin CD63 (Coco et al., 1999; Martinez-Arca et al., 2003) which has been implicated in Integrin-mediated cell migration, like other tetraspanins (Berditchevski, 2001). Thus, the TI-VAMP compartment could correspond to a specialized recycling endosome to which L1 and tetraspanins like CD63 would be targeted following internalization and from which they would then be recycled to the plasma membrane. Additionally, the YRSLE motif important for L1 trafficking is conserved in other members of the IgCAM family like NrCAM and neurofascin suggesting that these molecules might also travel through the TI-VAMP compartment (Kayyem et al., 1992; Volkmer et al., 1992).

Since decreased neurite outgrowth in TI-VAMP-depleted cells was observed in PC12 cells grown on collagen (Fig. 5) or hippocampal neurons grown on poly-L-lysine (Alberts et al., 2003), neurite extension should not directly depend on homophilic L1-ligation in these systems. In addition to homophilic L1-interactions, a wide spectrum of heterophilic interactions of L1 in *cis* and *trans* with other members of the IgCAM family, receptors of the Integrin family or receptors for secreted guidance cues have been reported (Brummendorf et al., 1998; Castellani et al., 2000). Other IgCAMs have been shown to cooperate in *cis* in promoting axonal outgrowth (Buchstaller et al., 1996) suggesting important functions in neurite outgrowth for the observed *cis*-interactions of L1 with other members of the IgCAM family. Moreover, L1 was shown to enhance β1 integrin-mediated cell migration and this promoting effect seems to depend on L1-mediated endocytosis of β1 integrin (Thelen et al., 2002). Therefore interfering with the TI-VAMP-dependent traffcking of L1 would be expected to affect functional interactions of L1 with other molecules that promote neurite outgrowth. Clearly, the exact consequences of inhibiting TI-VAMP-expression for neurite outgrowth will not be understood until a more complete picture of the cargo proteins of the TI-VAMP compartment exists.

The endosomal nature of the TI-VAMP compartment does not exclude the possibility that newly synthesized L1 is targeted to the axon in a TI-VAMP dependent manner. A very recent study on the biosynthetic pathway of L1 unraveled a specialized, axonal targeting pathway for newly synthesized L1, called transcytosis (Wisco et al., 2003). Transcytosis is an important trafficking pathway particularly well described in epithelial cells, where it mediates targeting to the apical plasma membrane (Tuma and Hubbard, 2003). Newly synthesized L1 is first transported to, and inserted in, the dendritic plasma membrane followed by immediate uptake into endosomal compartments, which then mediate axonal targeting (Wisco et al., 2003). The transcytotic targeting depends on the YRSLE motif of L1, further underlining the importance of intracellular trafficking in the function of neuronal L1 (Kamiguchi and Lemmon, 1998; Wisco et al., 2003). Interestingly, it has been proposed that sorting of proteins to the apical membrane in epithelial cells is similar to the sorting mechanisms leading to axonal targeting in neurons and TI-VAMP is implicated in the delivery of membrane carriers to the apical plasma membrane (Dotti and Simons, 1990, Lafont, 1999 #5370).

Furthermore, the role of TI-VAMP-mediated endosomal trafficking in the function of cell adhesion molecules like L1 might not be restricted to regulating the cell surface density of these molecules. Activation of L1 by homophilic interaction triggers a cascade of intracellular signaling events including p60src and MAP kinases (Schaefer et al., 1999; Schmid et al., 2000) see also Fig. 21), important for L1 function (Ignelzi et al, 1994). Importantly, the L1-triggered signaling cascade depends on clathrin-mediated endocytosis (Schaefer et al., 1999) and thus also establishes a role for endosomes in signaling events important for neuronal differentiation. In fact, the regulation of signaling events by endosomal compartments may play key roles in neurite outgrowth *in vivo* as illustrated by a drosophila mutant defective in the gene *spinster.* Spinster localizes to a late endosomal compartment and late endosomes show altered size and distribution in *spinster* flies. This phenotype is associated with a very pronounced synaptic overgrowth (200% increase in synaptic bouton number at the neuro-muscular junction), and an enhanced TGF-ß signaling (Sweeney and Davis, 2002). Synaptic overgrowth of this range has also been observed in the case of overexpression of an ubiquitin hydrolase (DiAntonio et al., 2001).

Clearly, the identification of TI-VAMP as an essential molecular player involved in the trafficking of L1 will greatly facilitate the analysis of the complex function and regulation of this highly important molecule in brain development.

IV.4. TI-VAMP-localization in growth cones depends on actin dynamics

TI-VAMP-localization in axonal growth cones shows a heterogenous appearance. Whereas some growth cones show accumulation of the TI-VAMP compartment in the peripheral, actin-rich domain, others are virtually devoid of TI-VAMP positive membranes. This dynamic behaviour of the TI-VAMP compartment is highly correlated with actin dynamics in axonal growth cones (Fig. 11) and TI-VAMP localization in growth cones depends on the integrity of the actin cytoskeleton (Fig. 12).

The dependence of TI-VAMP localization on actin and the enrichment of the TI-VAMP compartment to actin-rich filopodia in the periphery of growth cones is of great interest. The growth cone, and particularly the peripheral filopodia, constitutes the sensing organ of the axon which reads guidance cues. This is illustrated by the fact that actin-depolymerizing drugs administered *in vivo* prevent filopodia formation in axonal growth cones and induce dramatic pathfinding errors with no apparent effect on neurite elongation (Bentley and Toroian-Raymond, 1986; Chien et al., 1993; Kaufmann et al., 1998). Similar results were obtained *in vitro.* Low concentrations of actin depolymerizing drugs prevent filopodia formation and completely disrupt growth cone turning in a gradient of soluble, attractive cues (Zheng et al., 1996) or in substrate-induced repulsion (Challacombe et al., 1996). In fact, isolated filopodia were described as the fundamental probing unit for neuronal pathfinding, since they represent an autonomous sensing and signalling machinery. (Davenport et al., 1993) The central region of the growth cone then integrates signals received from different filopodia resulting in motility and neurite elongation (Davenport et al., 1993). Interestingly, neurite outgrowth is not significantly inhibited by drug concentrations which inhibit filopodia formation (Dent and Kalil, 2001; Rajnicek and McCaig, 1997; Zheng et al., 1996), but it becomes unpolarized. (Dent and Kalil, 2001) In this study, actin depolymerizing drugs were used at concentrations which were previously shown to have no effect on axonal outgrowth in hippocampal neurons (Dent and

Kalil, 2001; Rajnicek and McCaig, 1997). Thus, the accumulation of the TI-VAMP-positive membrane compartment is presumably not necessary for neurite outgrowth. Unpolarized exocytosis of TI-VAMP vesicles outside the growth cone might be sufficient to supply membrane for growth. Rather, it can be speculated that the actin-dependent accumulation of the TI-VAMP-compartment in the growth cone periphery might be necessary to integrate actin- and membrane-dynamics to enable polarized growth. It will be of great interest to test this hypothesis as a possible involvement of intracellular, growth cone-resident membrane compartments in pathfinding of neurons has not previously been anticipated.

IV.5. Regulation of the TI-VAMP-compartment in growth cones by L1 signalling

L1-mediated adhesion induces a local recruitment of the TI-VAMP compartment to sites of adhesion (Fig. 14, 15, 16). The accumulation of TI-VAMP depends on the adhesive cue, as it is not induced by N-Cadherin-mediated adhesive junctions (Fig. 18). TI-VAMP recruitment is strictly dependent on the actin-cytoskeleton (Fig. 17) and recruitment of membrane by L1-junctions is highly selective for the TI-VAMP-compartment (Fig. 19, 20). Importantly, accumulation of the TI-VAMP-compartment was observed at contact sites in neuronal cultures, suggesting that adhesion-dependend accumulation of the TI-VAMP compartment might indeed occur *in vivo* (Fig. 7, 13). These findings strongly support the hypothesis that the TI-VAMP compartment in growth cones is involved in early signaling events, leading to advancement or retraction upon encountering attractive or repulsive substrates during axonal navigation. Furthermore, they reveal a functional crosstalk between L1-mediated adhesion and TI-VAMP-dependent trafficking. TI-VAMP controls the trafficking of L1 to, and function at, the plasma membrane (first part of this study). In turn, L1-mediated adhesive cues lead to a local recruitment of the TI-VAMP compartment (second part of this study).

The novelty of this finding raises several important questions. Are these vesicles involved in the establishment and/or maintenance of the contacts? Recent results on the regulation of L1 trafficking show that endocytosis of L1 is directly linked to tyrosine dephosphorylation of neuronal L1 on the YRSLE-motif (Schaefer *et al.*,

2002). Interestingly, this dephosphorylation seems to occur locally at sites where L1 is engaged in cell-cell contacts or axonal outgrowth on L1 substrate (Schaefer *et al.*, 2002). The concentration of TI-VAMP vesicles at L1-dependent contacts might therefore provide the trafficking machinery necessary for L1 to recycle locally and thus perform its function.

How does L1-dependent signaling control membrane trafficking? Activation of L1 by homophilic interaction stimulates a signaling pathway involving p60src and activation of src seems to play an essential role in L1 dependent neurite outgrowth (Ignelzi *et al.*, 1994; Schaefer *et al.*, 1999; Schmid *et al.*, 2000). Here, local activation of tyrosine kinases and in particular src-family kinases due to L1-bead binding to growth cones was observed (Fig. 21) indicating that activation of src-family kinases is a very early event in L1-induced signaling. This view is in agreement with studies on apCAM, a cell adhesion molecule of the IgCAM family found in Aplysia. Binding of apCAM-coated beads to growth cones induces local activation of src kinases (Suter and Forscher, 2001). P60src was proposed to phosphorylate L1 on tyrosine 1176 of the YRSLE motif, which inhibits L1-binding to the AP-2 adaptor complex thus inhibiting its endocytosis (Schaefer et al., 2002). It can be speculated that TI-VAMP-mediated transport of L1 to sites of newly formed contacts enhances homophilic L1-ligation and therefore L1-induced activation of src kinases. Thus, a dynamic equilibrium might exist between TI-VAMP-dependent L1-delivery and signaling events regulating the stability or removal of L1 from the plasma membrane. Interestingly, p60src has been localized to endosomes in fibroblasts (Kaplan et al., 1992) and a recent study showed that p60src activity on endosomes is necessary for the stable association of endosomes with actin cables via a RhoD/hDia2C complex (Gasman et al., 2003). Thus, src activity could serve as an integrator for coordinated delivery of L1-containing, TI-VAMP-positive endosomal structures to L1 junctions and L1 stability at the plasma membrane, which would provide the cell with a highly dynamic regulatory mechanism to control adhesion and growth cone movement.

It will be important to identify the molecule(s), which link TI-VAMP-positive organelles to the actin cytoskeleton upon L1 signaling. Scaffolding proteins like Ankyrin and Ezrin, which interact directly with L1, could play a role in recruiting the TI-VAMP-compartment to L1-junctions (Davis and Bennett, 1994; Dickson *et al.*, 2002). Ankyrin B is a scaffolding protein that links L1 to the spectrin-based actin cytoskeleton via dual interaction with L1 and spectrin (Davis and Bennett, 1994).

Similar to Ankyrin, Ezrin interacts directly with L1 and is known to serve as a membrane-cytoskeleton linker (Dickson et al., 2002). Ezrin or other members of the Ezrin-Radixin-Moesin (ERM)-family of proteins are good candidates to mediate early events in L1-dependent adhesion, since they localize to actin rich, peripheral regions in growth cones (Paglini et al., 1998). Future studies should test to what extent the recruitment of TI-VAMP vesicles to L1-dependent contacts depends on any of the proteins mentioned above or whether an as yet unknown mechanism is recruiting and stabilizing TI-VAMP-vesicles.

Furthermore, Rab proteins can be expected to play an important role in the site-directed trafficking unravelled here. As described, members of this family play crucial roles in vesicle targeting and association of organelles with the cytoskeleton (Hammer and Wu, 2002). Rab 5 is a very interesting candidate, since it is expressed in neurons and localizes to multilamellar, endocytic organelles different from synaptic vesicles in brain (Ikin et al., 1996). It was proposed, that Rab5-activity is involved in the regulation of actin-based membrane motility, particularly in highly dynamic processes like neurite outgrowth (Sabo et al., 2003).

Figure 20 suggests that the endoplasmic reticulum could be recruited together with the TI-VAMP-compartment to L1-junctions. A highly dynamic behavior of ER in growth cones has been observed before and it was proposed that local Ca^{2+} release by ER-resident Ca^{2+} channels might be implicated in regulation of the cytoskeleton (Dailey and Bridgman, 1989). Indeed, intracellular release of Ca^{2+} via ER-resident Ca^{2+} channels has been shown to play important roles in growth cone guidance (Xiang et al., 2002) and might contribute to local Ca^{2+} signaling events that are observed upon activation of L1 (Archer et al., 1999). In fact, Ca^{2+} signaling could play a direct role in regulating the recruitment of TI-VAMP vesicles to L1-beads. Ca^{2+} signaling is of major importance *in vivo* for both the regulated secretion of neurotransmitter at synapses (FernandezChacon et al., 2001; Geppert et al., 1994) and for the regulated release of secretory lysosomes during plasma membrane repair (Jaiswal et al., 2002). It will be important to test the specificity of ER recruitment by L1-beads in order to better understand this potentially interesting observation.

IV.6. Specific recruitment of TI-VAMP by L1-, but not N-Cadherin junctions

Both L1- and N-Cadherin-dependent contacts induce strong accumulation of actin-rich structures (Fig. 18). Yet, whereas recruitment of TI-VAMP vesicles is dependent on actin dynamics (Fig. 17), formation of actin rich structures is not sufficent to recruit TI-VAMP vesicles (Fig. 18). Thus, L1 and N-Cadherin seem to induce different signaling events.

Differences in L1- and N-Cadherin-stimulated neurite outgrowth have previously been observed. Whereas blocking endocytosis inhibits L1-dependent neurite outgrowth, no effect was observed on N-Cadherin-mediated neurite outgrowth (Kamiguchi and Yoshihara, 2001). This finding is in agreement with the result shown in Figure 10 demonstrating that N-Cadherin-dependent junctions are independent of TI-VAMP-mediated trafficking. Growth cones grown on N-Cadherin, L1 or Laminin, which stimulates receptors of the integrin family, exhibit different morphologies (Burden-Gulley et al., 1995) and differences in the dynamics of growth cone-substrate interaction were observed depending on the substrate (Drazba et al., 1997). These morphological and mechanistic differences between L1- and N-Cadherin-function are reflected by differences in the molecular composition of the adaptor complexes, which mediate linkage of L1 and N-Cadherin to the actin cytoskeleton. Thus, activation of Cadherins by homophilic interactions induces linkage to the underlying actin cytoskeleton via catenins (Ranscht, 2000), while, as described above, ankyrin and ERM proteins are involved in linkage of IgCAMs to actin.

In contrast, differences in signaling pathways induced by L1 and N-Cadherin are less clear. In fact, both ligation of N-Cadherin and L1 leads to activation of the MAP kinase signaling pathway and inhibition of the MAP kinase pathway interferes with neurite outgrowth on both substrates (Perron and Bixby, 1999; Schaefer et al., 1999; Schmid et al., 2000). L1 and N-Cadherin were suggested to stimulate neurite outgrowth through activation of the FGF Receptor and FGF Receptor-dependent signaling (Williams et al., 1994). The different morphologies of growth cones observed when neurons are grown on L1 or N-Cadherin (Burden-Gulley et al., 1995) most likely result from the action of small GTPases of the Rho family, which are key

regulators of actin filament structures in response to extracellular cues (Skaper et al., 2001). Yet the Rho-family GTPase Rac1 is implicated in the function of both N-Cadherin and L1 (Lambert et al., 2002; Schaefer et al., 1999). Thus, whereas points of conversion in signaling events generated by different adhesive systems apparently exist, the differences providing specific responses are not yet fully understood (Fig. 18; Burden-Gulley et al., 1995)

It is reasonable to assume that the recruitment of the TI-VAMP compartment by L1 is involved in establishing the differences between L1- and N-Cadherin-junctions. In fact, a deeper understanding of the function of the TI-VAMP-recruitment by L1 might provide insights into the different functions of adhesive systems like N-Cadherin and L1 for brain development.

IV.7. Neurite outgrowth and neuronal polarity

A major task to understand neuronal differentiation in more detail is to elucidate the temporal and spatial cues which regulate the delivery and insertion of transport vesicles into specific domains of the plasma membrane. The results presented in in this study suggest that the TI-VAMP compartment undergoes regulated, polarized exocytosis in the growth cone upon L1 ligation. Thus, an intimate link seems to exist between TI-VAMP-dependent exocytotic membrane trafficking involved in neurite outgrowth and adhesion/signaling molecules like L1, which determine neuronal morphogenesis.

What determines sites for exocytosis? Exocytosis of the TI-VAMP compartment depends on the plasma membrane SNAREs Syntaxin 1 and SNAP-25 (Fig. 2). As shown in Figure 22, Syntaxin 1 is diffusely expressed throughout the axonal plasma membrane, thus presumably does not account for the spatial specificity of exocytosis. This observation agrees with earlier reports that Syntaxin 1 and SNAP-25, which are essential for fusion of synaptic vesicles with the plasma membrane, are distributed diffusely throughout the plasma membrane and are not found to be concentrated at sites of synapses (Galli et al., 1995). Similarly, in the budding yeast *S.cerevisiae*, membrane growth produces the daughter cell bud via exocytosis at the tip of the bud. The plasma membrane t-SNAREs Sec9p and Sso1p/2p are essential for this process but are nevertheless localized over the entire

surface of the mother cell and bud (Brennwald et al., 1994). Thus, whereas it is clear that the plasma membrane resident target SNAREs are essential for the polarized delivery of transport carriers, they cannot account for the spatial specificity of exocytotic events during, for example, neurite outgrowth and synaptogenesis.

In yeast a key component to specify the site of exocytosis during bud formation is the exocyst complex, which shows a polarized distribution to the daughter bud. Disruption of components of the exocyst complex results in accumulation of transport vesicles in the bud, suggesting a role for the exocyst in tethering of vesicles to specific sites (TerBush et al., 1996). As suggested by Figure 22, the exocyst could play a similar role in the site-directed exocytosis of the TI-VAMP compartment in neuronal growth cones. As outlined above, the exocyst plays an important role in neurite outgrowth, although the exact function in the generation of neuronal polarity was not established (Murthy et al., 2003). A link between the exocyst and the generation of cell polarity has been demonstrated in mammalian epithelial cells (Grindstaff et al., 1998). Upon formation of cell-cell contacts, the exocyst complex is recruited to sites of cell-cell contact and is essential for the delivery of a basolateral membrane protein, the LDL receptor (Grindstaff et al., 1998). Importantly, the localization of the exocyst complex to the apical junctional complex is dependent on cell-cell adhesion mediated by E-Cadherin. Therefore, an E-Cadherin mediated initial spatial cue can result in the establishment of an exocyst-dependent targeting patch where polarized exocytosis occurs. It can be speculated that L1-ligation might play a role similar to E-Cadherin-activation in defining sites of recruitment for the exocyst, which in turn allow for the site-specific delivery of exocytotic vesicles.

In neuronal cells, the importance of cell adhesion molecules in defining sites of synaptogenesis and maturation in functional synapses has been highlighted by several recent publications. Two unrelated CAMs, neuroligin and SynCAM, were shown to be sufficient to induce morphological and functional presynaptic differentiation in contacting axons, when presented by non-neuronal cells engineered to express these molecules (Biederer et al., 2002; Scheiffele et al., 2000). Analysis of the neuromuscular junction in mice deficient for the neuronal cell adhesion molecule NCAM showed relatively normal synapse formation, but severe deficits in the mechanism of recycling of synaptic vesicles, leading to impaired synaptic release (Polo-Parada et al., 2001). In fact, NCAM might play a role in neurons similar to that

of E-Cadherin in epithelial cells by defining spatial cues for the delivery of transport carriers to sites of synaptogenesis (Sytnyk et al., 2002). NCAM seems to perform this task by directly interacting via spectrin with TGN transport carriers which contain synaptic vesicle proteins (Sytnyk et al., 2002).

The findings presented here have important implications for the understanding of the role of adhesion molecules like L1 in the differentiation of neurons and the development of the brain. It can be proposed that the function of L1 does not solely depend on its capacity to transduce intracellular signals and to mediate cell-to-cell adhesion but also consists in the targeting of exocytotic organelles to the leading edge of growing axons and to sites of contact formation between cells. At the same time, delivery of adhesion and signaling molecules like L1 in a TI-VAMP-dependent manner may stabilize initial contacts and reinforce signaling mechanism leading to stable target recognition and/or directed growth by a positive feedback mechanism (See model 1).

Therefore, neuronal morphogenesis is likely to occur as an integrated mechanism of cytoskeleton and membrane dynamics, which are controlled by morphogenetic cues, such as ligation of the cell adhesion molecule L1.

a) b)

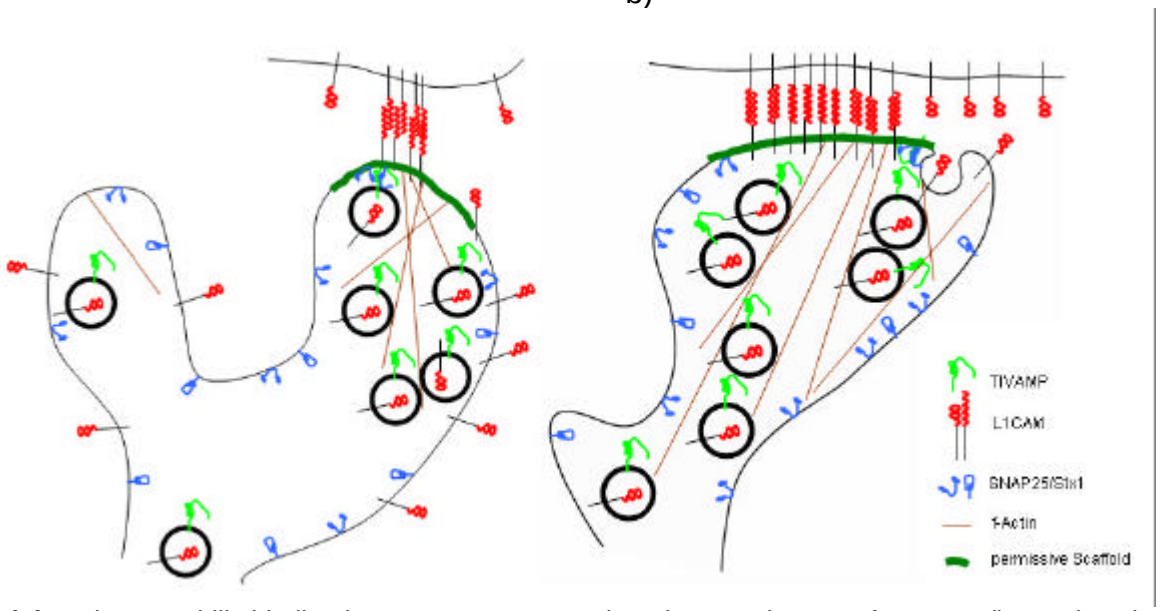

Model 1: a) Homophilic binding between L1 expressed on the growth cone of an axon (bottom) and an adjacent cell (top) leads to conformational change and activation of the L1 molecule. Activation of L1 leads to an assembly of a molecular scaffold including the exocyst, perhaps via src-activation, and reorganization of the actin cytoskeleton. The establishment of this spatial cue allows for the recruitment and accumulation of TI-VAMP-positive vesicles containing L1 at sites of contact formation. SNARE complex formation between TIVAMP and the t-SNARE SNAP25/Stx 1 mediates exocytosis of L1 molecules which will reinforce the initial contact and lead to stable contact formation.
b) Stable contact formation will reinforce L1-induced signaling and thus recruitment of TI-VAMP vesicles. In turn, enhanced recruitment of TI-VAMP-vesicles will stimulate growth towards the attractive substrate. Therefore, a positive feedback mechanism based on L1-signaling and TI-VAMP-mediated trafficking could result in directed growth of the axon or stable target recognition.

V. Litterature

Advani, R.J., B. Yang, R. Prekeris, K.C. Lee, J. Klumperman, and R.H. Scheller. 1999. VAMP-7 mediates vesicular transport from endosomes to lysosomes. *J.Cell Biol.* 146:765-775.

Alberts, P., R. Rudge, I. Hinners, A. Muzerelle, S. Martinez-Arca, T. Irinopoulou, V. Marthiens, S. Tooze, F. Rathjen, P. Gaspar, and T. Galli. 2003. Cross Talk between Tetanus Neurotoxin-insensitive Vesicle-associated Membrane Protein-mediated Transport and L1-mediated Adhesion. *Mol. Biol. Cell*. 14:4207-4220.

Allan, B.B., B.D. Moyer, and W.E. Balch. 2000. Rab1 recruitment of p115 into a cis-SNARE complex: Programming budding COPII vesicles for fusion. *Science*. 289:444-448.

Amigorena, S., J.R. Drake, P. Webster, and I. Mellman. 1994. Transient accumulation of new class II MHC molecules in a novel endocytic compartment in B lymphocytes. *Nature*. 369:113-20.

Antonin, W., D. Fasshauer, S. Becker, R. Jahn, and T.R. Schneider. 2002. Crystal structure of the endosomal SNARE complex reveals common structural principles of all SNAREs. *Nature Struct Biology*. 9:107-111.

Antonin, W., C. Holroyd, D. Fasshauer, S. Pabst, G.F. vonMollard, and R. Jahn. 2000. A SNARE complex mediating fusion of late endosomes defines conserved properties of SNARE structure and function. *Embo J*. 19:6453-6464.

Aravamudan, B., T. Fergestad, W.S. Davis, C.K. Rodesch, and K. Broadie. 1999. Drosophila Unc-13 is essential for synaptic transmission. *Nat.Neurosci.* 2:965-971.

Archer, F.R., P. Doherty, D. Collins, and S.R. Bolsover. 1999. CAMs and FGF cause a local submembrane calcium signal promoting axon outgrowth without a rise in bulk calcium concentration. *Eur J Neurosci*. 11:3565-73.

Atlashkin, V., V. Kreykenbohm, E.L. Eskelinen, D. Wenzel, A. Fayyazi, and G.F. vonMollard. 2003. Deletion of the SNARE vti1b in mice results in the loss of a single SNARE partner, syntaxin 8. *Mol Cell Biol*. 23:5198-5207.

Balch, W.E., W.G. Dunphy, W.A. Braell, and J.E. Rothman. 1984. Reconstitution of the transport of protein between successive compartments of the Golgi measured by the coupled incorporation of N-acetylglucosamine. *Cell*. 39:405-16.

Baumert, M., P.R. Maycox, F. Navone, P. De Camilli, and R. Jahn. 1989. Synaptobrevin: an integral membrane protein of 18,000 daltons present in small synaptic vesicle of rat brain. *EMBO J.* 8:379-384.

Bennett, M.K., N. Calakos, and R.H. Scheller. 1992. Syntaxin: a synaptic protein implicated in docking of synaptic vesicles at presynaptic active zones. *Science*. 257(5067):255-259.

Bentley, D., and A. Toroian-Raymond. 1986. Disoriented pathfinding by pioneer neurone growth cones deprived of filopodia by cytochalasin treatment. *Nature*. 323:712-5.

Bhattacharya, S., B.A. Stewart, B.A. Niemeyer, R.W. Burgess, B.D. McCabe, P. Lin, G. Boulianne, C.J. O'Kane, and T.L. Schwarz. 2002. Members of the synaptobrevin/vesicle-associated membrane protein (VAMP) family in Drosophila are functionally interchangeable in vivo for neurotransmitter release and cell viability. *Proc Natl Acad Sci U S A*. 99:13867-72.

Blasi, J., E.R. Chapman, E. Link, T. Binz, S. Yamasaki, P. De Camilli, T.C. Südhof, H. Niemann, and R. Jahn. 1993a. Botulinum neurotoxin A selectively cleaves the synaptic protein SNAP-25. *Nature*. 365:160-163.

Blasi, J., E.R. Chapman, S. Yamasaki, T. Binz, H. Niemann, and R. Jahn. 1993b. Botulinum neurotoxin C1 blocks neurotransmitter release by means of cleaving HPC-1/syntaxin. *EMBO J.* 12:4821-4828.

Block, M.R., and J.E. Rothman. 1992. Purification of N-ethylmaleimide-sensitive fusion protein. *Methods In Enzymology*. 219:300-309.

Blott, E.J., and G.M. Griffiths. 2002. Secretory lysosomes. *Nat Rev Mol Cell Biol*. 3:122-131.

Bock, J.B., H.T. Matern, A.A. Peden, and R.H. Scheller. 2001. A genomic perspective on membrane compartment organization. *Nature*. 409:839-841.

Bogdanovic, A., N. Bennett, S. Kieffer, M. Louwagie, T. Morio, J. Garin, M. Satre, and F. Bruckert. 2002. Syntaxin 7, Syntaxin 8, Vti1 and VAMP7 form an active SNARE complex for early macropinocytic compartment fusion in Dictyostelium discoideum. *Biochem J*. Pt.

Bonifacino, J.S., and J. Lippincott-Schwartz. 2003. Coat proteins: shaping membrane transport. *Nat Rev Mol Cell Biol*. 4:409-14.

Brennwald, P., B. Kearns, K. Champion, S. Keränen, V. Bankaitis, and P. Novick. 1994. Sec9 is a SNAP-25-like component of a yeast SNARE complex that may be the effector of Sec4 function in exocytosis. *Cell*. 79:245-258.

Bretscher, M.S. 1992. Circulating integrins: alpha 5 beta 1, alpha 6 beta 4 and Mac-1, but not alpha 3 beta 1, alpha 4 beta 1 or LFA-1. *EMBO J.* 11:405-410.

Broadie, K., A. Prokop, H.J. Bellen, C.J. Okane, K.L. Schulze, and S.T. Sweeney. 1995. Syntaxin and synaptobrevin function downstream of vesicle docking in Drosophila. *Neuron.* 15:663-673.

Brose, N. 1999. Synaptic cell adhesion proteins and synaptogenesis in the mammalian central nervous system. *Naturwissenschaften*. 86:516-24.

Brummendorf, T., S. Kenwrick, and F.G. Rathjen. 1998. Neural cell recognition molecule L1: from cell biology to human hereditary brain malformations. *Curr Opin Neurobiol*. 8:87-97.

Buchstaller, A., S. Kunz, P. Berger, B. Kunz, U. Ziegler, C. Rader, and P. Sonderegger. 1996. Cell adhesion molecules NgCAM and axonin-1 form heterodimers in the neuronal membrane and cooperate in neurite outgrowth promotion. *J Cell Biol*. 135:1593-607.

Burden-Gulley, S.M., H.R. Payne, and V. Lemmon. 1995. Growth cones are actively influenced by substrate-bound adhesion molecules. *J Neurosci*. 15:4370-81.

Cao, X.C., N. Ballew, and C. Barlowe. 1998. Initial docking of ER-derived vesicles requires Uso1p and Ypt1p but is independent of SNARE proteins. *EMBO J.* 17:2156-2165.

Cao, X.C., and C. Barlowe. 2000. Asymmetric requirements for a Rab GTPase and SNARE proteins in fusion of COPII vesicles with acceptor membranes. *J Cell Biol*. 149:55-65.

Castellani, V., A. Chedotal, M. Schachner, C. Faivre-Sarrailh, and G. Rougon. 2000. Analysis of the L1-deficient mouse phenotype reveals cross-talk between

Sema3A and L1 signaling pathways in axonal guidance. *Neuron*. 27:237-49.

Challacombe, J.F., D.M. Snow, and P.C. Letourneau. 1996. Actin filament bundles are required for microtubule reorientation during growth cone turning to avoid an inhibitory guidance cue. *J Cell Sci*. 109 (Pt 8):2031-40.

Chavrier, P., and B. Goud. 1999. The role of ARF and Rab GTPases in membrane transport. *Curr Opin Cell Biol*. 11:466-75.

Chen, Y.A., and R.H. Scheller. 2001. Snare-mediated membrane fusion. *Nat Rev Mol Cell Biol*. 2:98-106.

Chien, C.B., D.E. Rosenthal, W.A. Harris, and C.E. Holt. 1993. Navigational errors made by growth cones without filopodia in the embryonic Xenopus brain. *Neuron*. 11:237-51.

Clary, D.O., I.C. Griff, and J.E. Rothman. 1990. SNAPs, a family of NSF attachment proteins involved in intracellular membrane fusion in animals and yeast. *Cell*. 61:709-721.

Coco, S., G. Raposo, S. Martinez, J.J. Fontaine, S. Takamori, A. Zahraoui, R. Jahn, M. Matteoli, D. Louvard, and T. Galli. 1999. Subcellular localization of tetanus neurotoxin-insensitive vesicle-associated membrane protein (VAMP)/VAMP7 in neuronal cells: Evidence for a novel membrane compartment. *J.Neurosci.* 19:9803-9812.

Cohen, N.R., J.S. Taylor, L.B. Scott, R.W. Guillery, P. Soriano, and A.J. Furley. 1998. Errors in corticospinal axon guidance in mice lacking the neural cell adhesion molecule L1. *Curr Biol*. 8:26-33.

Condic, M.L., and P.C. Letourneau. 1997. Ligand-induced changes in integrin expression regulate neuronal adhesion and neurite outgrowth. *Nature*. 389:852-6.

Craig, A.M., R.J. Wyborski, and G. Banker. 1995. Preferential addition of newly synthesized membrane protein at axonal growth cones. *Nature*. 375:592-594.

Dahme, M., U. Bartsch, R. Martini, B. Anliker, M. Schachner, and N. Mantei. 1997. Disruption of the mouse L1 gene leads to malformations of the nervous system. *Nat Genet*. 17:346-9.

Dailey, M.E., and P.C. Bridgman. 1989. Dynamics of the endoplasmic reticulum and other membranous organelles in growth cones of cultured neurons. *J Neurosci*. 9:1897-909.

Darsow, T., S.E. Rieder, and S.D. Emr. 1997. A multispecificity syntaxin homologue, Vam3p, essential for autophagic and biosynthetic protein transport to the vacuole. *J.Cell Biol.* 138:517-529.

Davenport, R.W., P. Dou, V. Rehder, and S.B. Kater. 1993. A sensory role for neuronal growth cone filopodia. *Nature*. 361:721-4.

Davis, J.Q., and V. Bennett. 1994. Ankyrin binding activity shared by the neurofascin/L1/NrCAM family of nervous system cell adhesion molecules. *J Biol Chem*. 269:27163-6.

De Angelis, E., J. MacFarlane, J.S. Du, G. Yeo, R. Hicks, F.G. Rathjen, S. Kenwrick, and T. Brummendorf. 1999. Pathological missense mutations of neural cell adhesion molecule L1 affect homophilic and heterophilic binding activities. *Embo J*. 18:4744-53.

Deitcher, D.L., A. Ueda, B.A. Stewart, R.W. Burgess, Y. Kidokoro, and T.L. Schwarz. 1998. Distinct requirements for evoked and spontaneous release of neurotransmitter are revealed by mutations in the Drosophila gene neuronal-synaptobrevin. *J.Neurosci.* 18:2028-2039.

Dent, E.W., and K. Kalil. 2001. Axon branching requires interactions between dynamic microtubules and actin filaments. *J Neurosci*. 21:9757-69.

Dickson, B.J. 2002. Molecular mechanisms of axon guidance. *Science*. 298:1959-64.

Dotti, C.G., and K. Simons. 1990. Polarized sorting of viral glycoproteins to the axon and dendrites of hippocampal neurons in culture. *Cell*. 62:63-72.

Drazba, J., P. Liljelund, C. Smith, R. Payne, and V. Lemmon. 1997. Growth cone interactions with purified cell and substrate adhesion molecules visualized by interference reflection microscopy. *Brain Res Dev Brain Res*. 100:183-97.

Dulubova, I., S. Sugita, S. Hill, M. Hosaka, I. Fernandez, T.C. Sudhof, and J. Rizo. 1999. A conformational switch in syntaxin during exocytosis: role of munc18. *EMBO J.* 18:4372-4382.

Farsad, K., and P. De Camilli. 2003. Mechanisms of membrane deformation. *Curr Opin Cell Biol*. 15:372-81.

Fasshauer, D. 2003. Structural insights into the SNARE mechanism. *Bba Mol Cell Res*. 18:2-3.

Fasshauer, D., W. Antonin, M. Margittai, S. Pabst, and R. Jahn. 1999. Mixed and Non-cognate SNARE complexes. Characterization of assembly and biophysical properties. *J.Biol.Chem.* 274:15440-15446.

Fasshauer, D., W. Antonin, V. Subramaniam, and R. Jahn. 2002. SNARE assembly and disassembly exhibit a pronounced hysteresis. *Nature Struct Biology*. 9:144-151.

Fasshauer, D., R.B. Sutton, A.T. Brunger, and R. Jahn. 1998. Conserved structural features of the synaptic fusion complex: SNARE proteins reclassified as Q- and R-SNAREs. *Proc.Natl.Acad.Sci.USA*. 95:15781-15786.

FernandezChacon, R., A. Konigstorfer, S.H. Gerber, J. Garcia, M.F. Matos, C.F. Stevens, N. Brose, J. Rizo, C. Rosenmund, and T.C. Sudhof. 2001. Synaptotagmin I functions as a calcium regulator of release probability. *Nature*. 410:41-49.

Filippini, F., V. Rossi, T. Galli, A. Budillon, M. D'Urso, and M. D'Esposito. 2001. Longins: a new evolutionary conserved VAMP family sharing a novel SNARE domain. *Trends Biochem Sci*. 26:407-9.

Forscher, P., and S.J. Smith. 1988. Actions of cytochalasins on the organization of actin filaments and microtubules in a neuronal growth cone. *J.Cell Biol.* 107:1505-1516.

Fukuda, R., J.A. McNew, T. Weber, F. Parlati, T. Engel, W. Nickel, J.E. Rothman, and T.H. Sollner. 2000. Functional architecture of an intracellular membrane t- SNARE. *Nature*. 407:198-202.

Futerman, A.H., and G.A. Banker. 1996. The economics of neurite outgrowth--the addition of new membrane to growing axons. *Trends.Neurosci.* 19:144-149.

Galli, T., T. Chilcote, O. Mundigl, T. Binz, H. Niemann, and P. De Camilli. 1994. Tetanus toxin-mediated cleavage of cellubrevin impairs exocytosis of transferrin receptor-containing vesicles in CHO cells. *J.Cell Biol.* 125:1015-1024.

Galli, T., E.P. Garcia, O. Mundigl, T.J. Chilcote, and P. DeCamilli. 1995. v- and t-SNAREs in neuronal exocytosis: A need for additional components to define sites of release. *Neuropharmacology.* 34:1351-1360.

Galli, T., A. Zahraoui, V.V. Vaidyanathan, G. Raposo, J.M. Tian, M. Karin, H. Niemann, and D. Louvard. 1998. A novel tetanus neurotoxin-insensitive vesicle-associated membrane protein in SNARE complexes of the apical plasma membrane of epithelial cells. *Mol.Biol.Cell*. 9:1437-1448.

Gasman, S., Y. Kalaidzidis, and M. Zerial. 2003. RhoD regulates endosome dynamics through Diaphanous-related Formin and Src tyrosine kinase. *Nat Cell Biol*. 5:195-204.

Geppert, M., Y. Goda, R.E. Hammer, C. Li, T.W. Rosahl, C.F. Stevens, and T.C. Südhof. 1994. Synaptotagmin I: A major Ca^{2+} sensor for transmitter release at a central synapse. *Cell*. 79:717-727.

Gerst, J.E. 2003. SNARE regulators: matchmakers and matchbreakers. *Bba Mol Cell Res*. 18:2-3.

Gonzalez, L.C., W.I. Weis, and R.H. Scheller. 2001. A novel SNARE N-terminal domain revealed by the crystal structure of Sec22b. *J Biol Chem*. 276:24203-24211.

Gotte, M., and D. Gallwitz. 1997. High expression of the yeast syntaxin-related Vam3 protein suppresses the protein transport defects of a pep12 null mutant. *FEBS Lett.* 411:48-52.

Grindstaff, K.K., C. Yeaman, N. Anandasabapathy, S.C. Hsu, E. RodriguezBoulan, R.H. Scheller, and W.J. Nelson. 1998. Sec6/8 complex is recruited to cell-cell contacts and specifies transport vesicle delivery to the basal-lateral membrane in epithelial cells. *Cell*. 93:731-740.

Grosse, G., J. Grosse, R. Tapp, J. Kuchinke, M. Gorsleben, I. Fetter, B. HohneZell, M. Gratzl, and M. Bergmann. 1999. SNAP-25 requirement for dendritic growth of hippocampal neurons. *J.Neurosci.Res.* 56:539-546.

Hammer, J.A., 3rd, and X.S. Wu. 2002. Rabs grab motors: defining the connections between Rab GTPases and motor proteins. *Curr Opin Cell Biol*. 14:69-75.

Hanson, P.I., R. Roth, H. Morisaki, R. Jahn, and J.E. Heuser. 1997. Structure and conformational changes in NSF and its membrane receptor complexes visualized by quick- freeze/deep-etch electron microscopy. *Cell*. 90:523-535.

Hay, J.C., D.S. Chao, C.S. Kuo, and R.H. Scheller. 1997. Protein interactions regulating vesicle transport between the endoplasmic reticulum and Golgi apparatus in mammalian cells. *Cell*. 89:149-158.

Hayashi, T., H. McMahon, S. Yamasaki, T. Binz, Y. Hata, T.C. Südhof, and H. Niemann. 1994. Synaptic vesicle membrane fusion complex: Action of clostridial neurotoxins on assembly. *EMBO J.* 13:5051-5061.

Hibi, T., N. Hirashima, and M. Nakanishi. 2000. Rat basophilic leukemia cells express syntaxin-3 and VAMP-7 in granule membranes. *Biochem Biophys Res Commun*. 271:36-41.

Higgins, D., M. Burack, P. Lein, and G. Banker. 1997. Mechanisms of neuronal polarity. *Curr.Opin.Neurobiol.* 7:599-604.

Hu, C., M. Ahmed, T.J. Melia, T.H. Sollner, T. Mayer, and J.E. Rothman. 2003. Fusion of cells by flipped SNAREs. *Science*. 300:1745-1749.

Huang, K.M., K. D'Hondt, H. Riezman, and S.K. Lemmon. 1999. Clathrin functions in the absence of heterotetrameric adaptors and AP180-related proteins in yeast. *Embo J*. 18:3897-908.

Hunt, J.M., K. Bommert, M.P. Charlton, A. Kistner, E. Habermann, G.J. Augustine, and H. Betz. 1994. A post-docking role for synaptobrevin in synaptic vesicle fusion. *Neuron*. 12:1269-1279.

Ignelzi, M.A., Jr., D.R. Miller, P. Soriano, and P.F. Maness. 1994. Impaired neurite outgrowth of src-minus cerebellar neurons on the cell adhesion molecule L1. *Neuron*. 12:873-84.

Ikin, A.F., W.G. Annaert, K. Takei, P. DeCamilli, R. Jahn, P. Greengard, and J.D. Buxbaum. 1996. Alzheimer amyloid protein precursor is localized in nerve terminal preparations to Rab5-containing vesicular organelles distinct from those implicated in the synaptic vesicle pathway. *J.Biol.Chem.* 271:31783-31786.

Ikonen, E., M. Tagaya, O. Ullrich, C. Montecucco, and K. Simons. 1995. Different requirements for NSF, SNAP, and rab proteins in apical and basolateral transport in MDCK cells. *Cell*. 81:571-580.

Jahn, R., T. Lang, and T.C. Sudhof. 2003. Membrane fusion. *Cell*. 112:519-33.

Jaiswal, J.K., N.W. Andrews, and S.M. Simon. 2002. Membrane proximal lysosomes are the major vesicles responsible for calcium-dependent exocytosis in nonsecretory cells. *J Cell Biol*. 159:625-35.

Jareb, M., and G. Banker. 1997. Inhibition of axonal growth by brefeldin A in hippocampal neurons in culture. *J.Neurosci.* 17:8955-8963.

Kamiguchi, H., and V. Lemmon. 1998. A neuronal form of the cell adhesion molecule L1 contains a tyrosine-based signal required for sorting to the axonal growth cone. *J Neurosci*. 18:3749-56.

Kamiguchi, H., and V. Lemmon. 2000. Recycling of the cell adhesion molecule L1 in axonal growth cones. *J Neurosci*. 20:3676-86.

Kamiguchi, H., and F. Yoshihara. 2001. The role of endocytic l1 trafficking in polarized adhesion and migration of nerve growth cones. *J Neurosci*. 21:9194-203.

Kaplan, K.B., J.R. Swedlow, H.E. Varmus, and D.O. Morgan. 1992. Association of p60c-src with endosomal membranes in mammalian fibroblasts. *J Cell Biol*. 118:321-33.

Kaufmann, N., Z.P. Wills, and D. Van Vactor. 1998. Drosophila Rac1 controls motor axon guidance. *Development*. 125:453-61.

Kayyem, J.F., J.M. Roman, E.J. de la Rosa, U. Schwarz, and W.J. Dreyer. 1992. Bravo/Nr-CAM is closely related to the cell adhesion molecules L1 and Ng-CAM and has a similar heterodimer structure. *J Cell Biol*. 118:1259-70.

Kirchhausen, T. 2000. Three ways to make a vesicle. *Nat Rev Mol Cell Biol*. 1:187-98.

Kleijmeer, M., G. Ramm, D. Schuurhuis, J. Griffith, M. Rescigno, P. Ricciardi-Castagnoli, A.Y. Rudensky, F. Ossendorp, C.J. Melief, W. Stoorvogel, and H.J. Geuze. 2001. Reorganization of multivesicular bodies regulates MHC class II antigen presentation by dendritic cells. *J Cell Biol*. 155:53-63.

Koleske, A.J. 2003. Do filopodia enable the growth cone to find its way? *Sci STKE*. 2003:pe20.

Lafont, F., P. Verkade, T. Galli, C. Wimmer, D. Louvard, and K. Simons. 1999. Raft association of SNAP receptors acting in apical trafficking in Madin-Darby canine kidney cells. *Proc.Nat.Acad.Sci.Usa*. 96:3734-3738.

Lambert, M., D. Choquet, and R.M. Mege. 2002. Dynamics of ligand-induced, Rac1-dependent anchoring of cadherins to the actin cytoskeleton. *J Cell Biol*. 157:469-79.

Lambert, M., F. Padilla, and R.M. Mege. 2000. Immobilized dimers of N-cadherin-Fc chimera mimic cadherin-mediated cell contact formation: contribution of both outside-in and inside-out signals. *J Cell Sci*. 113:2207-19.

Lan, J.Y., V.A. Skeberdis, T. Jover, S.Y. Grooms, Y. Lin, R.C. Araneda, X. Zheng, M.V. Bennett, and R.S. Zukin. 2001. Protein kinase C modulates NMDA receptor trafficking and gating. *Nat Neurosci*. 4:382-90.

Lee, S.H., J.G. Valtschanoff, V.N. Kharazia, R. Weinberg, and M. Sheng. 2001. Biochemical and morphological characterization of an intracellular membrane compartment containing ampa receptors. *Neuropharmacology 2001 NOV;41(6):680-692*.

Lemmon, V., K.L. Farr, and C. Lagenaur. 1989. L1-mediated axon outgrowth occurs via a homophilic binding mechanism. *Neuron*. 2:1597-603.

Lin, C.H., E.M. Espreafico, M.S. Mooseker, and P. Forscher. 1996. Myosin drives retrograde F-actin flow in neuronal growth cones. *Neuron*. 16:769-82.

Lin, C.H., and P. Forscher. 1993. Cytoskeletal remodeling during growth cone-target interactions. *J Cell Biol*. 121:1369-83.

Lin, R.C., and R.H. Scheller. 1997. Structural organization of the synaptic exocytosis core complex. *Neuron.* 19:1087-1094.

Lu, W., H. Man, W. Ju, W.S. Trimble, J.F. MacDonald, and Y.T. Wang. 2001. Activation of synaptic NMDA receptors induces membrane insertion of new AMPA receptors and LTP in cultured hippocampal neurons. *Neuron*. 29:243-54.

Martinez-Arca, S., P. Alberts, and T. Galli. 2000a. Clostridial neurotoxin-insensitive vesicular SNAREs in exocytosis and endocytosis. *Biol. Cell*. 92:449-453.

Martinez-Arca, S., P. Alberts, A. Zahraoui, D. Louvard, and T. Galli. 2000b. Role of tetanus neurotoxin insensitive vesicle-associated membrane protein (TI-VAMP) in vesicular transport mediating neurite outgrowth. *J Cell Biol*. 149:889-899.

Martinez-Arca, S., S. Coco, G. Mainguy, U. Schenk, P. Alberts, P. Bouille, M. Mezzina, A. Prochiantz, M. Matteoli, D. Louvard, and T. Galli. 2001. A common exocytotic mechanism mediates axonal and dendritic outgrowth. *J Neurosci*. 21:3830-8.

Martinez-Arca, S., R. Rudge, M. Vacca, G. Raposo, J. Camonis, V. Proux-Gillardeaux, L. Daviet, E. Formstecher, A. Hamburger, F. Filippini, M.

D'Esposito, and T. Galli. 2003. A dual mechanism controlling the localization and function of exocytotic v-SNAREs. *Proc Natl Acad Sci U S A*. 100:9011-9016.

McBride, H.M., V. Rybin, C. Murphy, A. Giner, R. Teasdale, and M. Zerial. 1999. Oligomeric complexes link Rab5 effectors with NSF and drive membrane fusion via interactions between EEA1 and syntaxin 13. *Cell*. 98:377-386.

McNew, J.A., F. Parlati, R. Fukuda, R.J. Johnston, K. Paz, F. Paumet, T.H. Sollner, and J.E. Rothman. 2000. Compartmental specificity of cellular membrane fusion encoded in SNARE proteins. *Nature*. 407:153-159.

Murthy, M., D. Garza, R.H. Scheller, and T.L. Schwarz. 2003. Mutations in the Exocyst Component Sec5 Disrupt Neuronal Membrane Traffic, but Neurotransmitter Release Persists. *Neuron*. 37:433-447.

Muzerelle, A., P. Alberts, S. Martinez Arca, O. Jeannequin, P. Lafaye, J.-C. Mazié, T. Galli, and P. Gaspar. 2003. Identification of a presynaptic membrane compartment containing Tetanus Neurotoxin-Insensitive Vesicle Associated Membrane Protein in the rat brain. *Neuroscience*.

Nishimura, T., Y. Fukata, K. Kato, T. Yamaguchi, Y. Matsuura, H. Kamiguchi, and K. Kaibuchi. 2003. CRMP-2 regulates polarized Numb-mediated endocytosis for axon growth. *Nat Cell Biol*. 5:819-26.

Nonet, M.L., O. Saifee, H.J. Zhao, J.B. Rand, and L.P. Wei. 1998. Synaptic transmission deficits in Caenorhabditis elegans synaptobrevin mutants. *J.Neurosci.* 18:70-80.

Novick, P., S. Ferro, and R. Schekman. 1981. Order of events in the yeast secretory pathway. *Cell*. 25:461-9.

Novick, P., C. Field, and R. Schekman. 1980. Identification of 23 complementation groups required for post-translational events in the yeast secretory pathway. *Cell*. 21:205-215.

Orci, L., V. Malhotra, M. Amherdt, T. Serafini, and J.E. Rothman. 1989. Dissection of a single round of vesicular transport: sequential intermediates for intercisternal movement in the Golgi stack. *Cell*. 56:357-368.

Osen-Sand, A., J.K. Staple, E. Naldi, G. Schiavo, O. Rossetto, S. Petitpierre, A. Malgaroli, C. Montecucco, and S. Catsicas. 1996. Common and distinct fusion proteins in axonal growth and transmitter release. *J.Comp.Neurol.* 367:222-234.

Overly, C.C., and P.J. Hollenbeck. 1996. Dynamic organization of endocytic pathways in axons of cultured sympathetic neurons. *J Neurosci*. 16:6056-64.

Oyler, G.A., G.A. Higgins, R.A. Hart, E. Battenberg, M. Billingsley, F.E. Bloom, and M.C. Wilson. 1989. The identification of a novel synaptosomal-associated protein, SNAP-25, differentially expressed by neuronal subpopulations. *J.Cell Biol.* 109:3039-3052.

Paglini, G., P. Kunda, S. Quiroga, K. Kosik, and A. Caceres. 1998. Suppression of radixin and moesin alters growth cone morphology, motility, and process formation in primary cultured neurons. *J.Cell Biol.* 143:443-455.

Palade, G. 1975. Intracellular aspects of the process of protein synthesis. *Science*. 189:347-58.

Paquet, M.R., S.R. Pfeffer, J.D. Burczak, B.S. Glick, and J.E. Rothman. 1986. Components responsible for transport between successive Golgi cisternae are highly conserved in evolution. *J Biol Chem*. 261:4367-70.

Parlati, F., T. Weber, J.A. McNew, B. Westermann, T.H. Sollner, and J.E. Rothman. 1999. Rapid and efficient fusion of phospholipid vesicles by the alpha-helical core of a SNARE complex in the absence of an N-terminal regulatory domain. *Proc.Natl.Acad.Sci.U.S.A.* 96:12565-70.

Parton, R.G., K. Simons, and C.G. Dotti. 1992. Axonal and dendritic endocytic pathways in cultured neurons. *J.Cell.Biol.* 119:123-137.

Payne, G.S., and R. Schekman. 1985. A test of clathrin function in protein secretion and cell growth. *Science*. 230:1009-14.

Peretti, D., L. Peris, S. Rosso, S. Quiroga, and A. Caceres. 2000. Evidence for the involvement of KIF4 in the anterograde transport of L1- containing vesicles. *J Cell Biol*. 149:141-52.

Perron, J.C., and J.L. Bixby. 1999. Distinct neurite outgrowth signaling pathways converge on ERK activation. *Mol Cell Neurosci*. 13:362-78.

Pevsner, J., H. Shu-Chan, and R.H. Scheller. 1994. N-sec1: a neural-specific syntaxin-binding protein. *Proc.Natl.Acad.Sci.USA*. 91:1445-1449.

Prochiantz, A. 1995. Neuronal polarity: giving neurons heads and tails. *Neuron.* 15:743-746.

Raiborg, C., T.E. Rusten, and H. Stenmark. 2003. Protein sorting into multivesicular endosomes. *Curr Opin Cell Biol*. 15:446-55.

Rajnicek, A., and C. McCaig. 1997. Guidance of CNS growth cones by substratum grooves and ridges: effects of inhibitors of the cytoskeleton, calcium channels and signal transduction pathways. *J Cell Sci*. 110 (Pt 23):2915-24.

Ranscht, B. 2000. Cadherins: molecular codes for axon guidance and synapse formation. *Int J Dev Neurosci*. 18:643-51.

Richmond, J.E., R.M. Weimer, and E.M. Jorgensen. 2001. An open form of syntaxin bypasses the requirement for UNC- 13 in vesicle priming. *Nature*. 412:338-341.

Rothman, J.E. 1994. Mechanisms of intracellular protein transport. *Nature*. 372:55-63.

Rothman, J.E., and G. Warren. 1994. Implication of the SNARE hypothesis for intracellular membrane topology and dynamics. *Curr.Biol.* 4:220-233.

Sabo, S.L., A.F. Ikin, J.D. Buxbaum, and P. Greengard. 2003. The amyloid precursor protein and its regulatory protein, FE65, in growth cones and synapses in vitro and in vivo. *J Neurosci*. 23:5407-15.

Schaefer, A.W., Y. Kamei, H. Kamiguchi, E.V. Wong, I. Rapoport, T. Kirchhausen, C.M. Beach, G. Landreth, S.K. Lemmon, and V. Lemmon. 2002. L1 endocytosis is controlled by a phosphorylation-dephosphorylation cycle stimulated by outside-in signaling by L1. *J Cell Biol*. 157:1223-32.

Schaefer, A.W., H. Kamiguchi, E.V. Wong, C.M. Beach, G. Landreth, and V. Lemmon. 1999. Activation of the MAPK signal cascade by the neural cell adhesion molecule L1 requires L1 internalization. *J Biol Chem*. 274:37965-73.

Schiavo, G., F. Benfenati, B. Poulain, O. Rossetto, P. Polverino de Laureto, B.R. DasGupta, and C. Montecucco. 1992. Tetanus and botulinum-B neurotoxins block neurotransmitter release by proteolytic cleavage of synaptobrevin. *Nature*. 359:832-835.

Schmid, R.S., W.M. Pruitt, and P.F. Maness. 2000. A MAP kinase-signaling pathway mediates neurite outgrowth on L1 and requires Src-dependent endocytosis. *J Neurosci*. 20:4177-88.

Schmidt, C.E., J. Dai, D.A. Lauffenburger, M.P. Sheetz, and A.F. Horwitz. 1995. Integrin-cytoskeletal interactions in neuronal growth cones. *J Neurosci*. 15:3400-7.

Schoch, S., F. Deak, A. Konigstorfer, M. Mozhayeva, Y. Sara, T.C. Sudhof, and E.T. Kavalali. 2001. SNARE function analyzed in synaptobrevin/VAMP knockout mice. *Science*. 294:1117-22.

Serafini, T., L. Orci, M. Amherdt, M. Brunner, R.A. Kahn, and J.E. Rothman. 1991. ADP-ribosylation factor is a subunit of the coat of Golgi-derived COP-coated vesicles: a novel role for a GTP-binding protein. *Cell*. 67:239-253.

Setou, M., T. Nakagawa, D.H. Seog, and N. Hirokawa. 2000. Kinesin superfamily motor protein KIF17 and mLin-10 in NMDA receptor-containing vesicle transport. *Science*. 288:1796-802.

Sheng, M., and S.H. Lee. 2003. AMPA receptor trafficking and synaptic plasticity: major unanswered questions. *Neurosci Res*. 46:127-134.

Shin, O.H., J.S. Rhee, J. Tang, S. Sugita, C. Rosenmund, and T.C. Sudhof. 2003. Sr2+ binding to the Ca2+ binding site of the synaptotagmin 1 C2B domain triggers fast exocytosis without stimulating SNARE interactions. *Neuron*. 37:99-108.

Skaper, S.D., S.E. Moore, and F.S. Walsh. 2001. Cell signalling cascades regulating neuronal growth-promoting and inhibitory cues. *Prog Neurobiol*. 65:593-608.

Söllner, T., M.K. Bennett, S.W. Whiteheart, R.H. Scheller, and J.E. Rothman. 1993a. A protein assembly-disassembly pathway in vitro that may correspond to sequential steps of synaptic vesicle docking, activation, and fusion. *Cell*. 75:409-418.

Söllner, T., S.W. Whiteheart, M. Brunner, H. Erdjument-Bromage, S. Geromanos, P. Tempst, and J.E. Rothman. 1993b. SNAP receptors implicated in vesicle targeting and fusion. *Nature*. 362:318-324.

Song, H., and M. Poo. 2001. The cell biology of neuronal navigation. *Nat Cell Biol*. 3:E81-8.

Song, J.Y., K. Ichtchenko, T.C. Sudhof, and N. Brose. 1999. Neuroligin 1 is a postsynaptic cell-adhesion molecule of excitatory synapses. *Proc Natl Acad Sci U S A*. 96:1100-5.

Sudhof, T.C. 2002. Synaptotagmins: why so many? *J Biol Chem*. 277:7629-32.

Suter, D.M., L.D. Errante, V. Belotserkovsky, and P. Forscher. 1998. The Ig superfamily cell adhesion molecule, apCAM, mediates growth cone steering by substrate-cytoskeletal coupling. *J Cell Biol*. 141:227-40.

Suter, D.M., and P. Forscher. 1998. An emerging link between cytoskeletal dynamics and cell adhesion molecules in growth cone guidance. *Curr Opin Neurobiol*. 8:106-16.

Suter, D.M., and P. Forscher. 2001. Transmission of growth cone traction force through apCAM-cytoskeletal linkages is regulated by Src family tyrosine kinase activity. *J Cell Biol*. 155:427-38.

Sutton, R.B., D. Fasshauer, R. Jahn, and A.T. Brunger. 1998. Crystal structure of a SNARE complex involved in synaptic exocytosis at 2.4 angstrom resolution. *Nature*. 395:347-353.

Sweeney, S.T., and G.W. Davis. 2002. Unrestricted synaptic growth in spinster-a late endosomal protein implicated in TGF-beta-mediated synaptic growth regulation. *Neuron*. 36:403-16.

TerBush, D.R., T. Maurice, D. Roth, and P. Novick. 1996. The Exocyst is a multiprotein complex required for exocytosis in Saccharomyces cerevisiae. *EMBO J.* 15:6483-6494.

Tessier-Lavigne, M., and C.S. Goodman. 1996. The molecular biology of axon guidance. *Science*. 274:1123-33.

Thelen, K., V. Kedar, A.K. Panicker, R.S. Schmid, B.R. Midkiff, and P.F. Maness. 2002. The neural cell adhesion molecule L1 potentiates integrin-dependent cell migration to extracellular matrix proteins. *J Neurosci*. 22:4918-31.

Tochio, H., M.M.K. Tsui, D.K. Banfield, and M.J. Zhang. 2001. An autoinhibitory mechanism for nonsyntaxin SNARE proteins revealed by the structure of Ykt6p. *Science*. 293:698-702.

Tuma, P.L., and A.L. Hubbard. 2003. Transcytosis: crossing cellular barriers. *Physiol Rev*. 83:871-932.

Turley, S.J., K. Inaba, W.S. Garrett, M. Ebersold, J. Unternaehrer, R.M. Steinman, and I. Mellman. 2000. Transport of peptide-MHC class II complexes in developing dendritic cells. *Science*. 288:522-7.

Ungermann, C., K. Sato, and W. Wickner. 1998. Defining the functions of trans-SNARE pairs. *Nature*. 396:543-8.

Verhage, M., A.S. Maia, J.J. Plomp, A.B. Brussaard, J.H. Heeroma, H. Vermeer, R.F. Toonen, R.E. Hammer, T.K. vandenBerg, M. Missler, H.J. Geuze, and

T.C. Sudhof. 2000. Synaptic assembly of the brain in the absence of neurotransmitter secretion. *Science*. 287:864-869.

Vogt, L., R.J. Giger, U. Ziegler, B. Kunz, A. Buchstaller, W. Hermens, M.G. Kaplitt, M.R. Rosenfeld, D.W. Pfaff, J. Verhaagen, and P. Sonderegger. 1996. Continuous renewal of the axonal pathway sensor apparatus by insertion of new sensor molecules into the growth cone membrane. *Curr Biol*. 6:1153-8.

Volkmer, H., B. Hassel, J.M. Wolff, R. Frank, and F.G. Rathjen. 1992. Structure of the axonal surface recognition molecule neurofascin and its relationship to a neural subgroup of the immunoglobulin superfamily. *J Cell Biol*. 118:149-61.

Ward, D.M., J. Pevsner, M.A. Scullion, M. Vaughn, and J. Kaplan. 2000. Syntaxin 7 and VAMP-7 are soluble N-ethylmaleimide- sensitive factor attachment protein receptors required for late endosome-lysosome and homotypic lysosome fusion in alveolar macrophages. *Mol Biol Cell*. 11:2327-2333.

Washbourne, P., P.M. Thompson, M. Carta, E.T. Costa, J.R. Mathews, G. Lopez-Bendito, Z. Molnar, M.W. Becher, C.F. Valenzuela, L.D. Partridge, and M.C. Wilson. 2002. Genetic ablation of the t-SNARE SNAP-25 distinguishes mechanisms of neuroexocytosis. *Nat Neurosci*. 5:19-26.

Waters, M.G., T. Serafini, and J.E. Rothman. 1991. 'Coatomer': a cytosolic protein complex containing subunits of non-clathrin-coated Golgi transport vesicles. *Nature*. 349:248-251.

Weber, T., B.V. Zemelman, J.A. McNew, B. Westermann, M. Gmachl, F. Parlati, T.H. Sollner, and J.E. Rothman. 1998. SNAREpins: Minimal machinery for membrane fusion. *Cell*. 92:759-772.

Weimbs, T., K. Mostov, S.H. Low, and R. Hofmann. 1998. A model for structural similarity between different SNARE complexes based on sequence relationships. *Tr.Cell Biol.* 8:260-262.

Wettey, F.R., S.F. Hawkins, A. Stewart, J.P. Luzio, J.C. Howard, and A.P. Jackson. 2002. Controlled elimination of clathrin heavy-chain expression in DT40 lymphocytes. *Science*. 297:1521-5.

Williams, E.J., J. Furness, F.S. Walsh, and P. Doherty. 1994. Activation of the FGF receptor underlies neurite outgrowth stimulated by L1, N-CAM, and N-cadherin. *Neuron*. 13:583-94.

Wilson, D.W., C.A. Wilcox, G.C. Flynn, E. Chen, W.J. Kuang, W.J. Henzel, M.R. Block, A. Ullrich, and J.E. Rothman. 1989. A fusion protein required for vesicle-mediated transport in both mammalian cells and yeast. *Nature*. 339:355-359.

Wisco, D., E.D. Anderson, M.C. Chang, C. Norden, T. Boiko, H. Folsch, and B. Winckler. 2003. Uncovering multiple axonal targeting pathways in hippocampal neurons. *J Cell Biol*. 162:1317-28.

Xiang, Y., Y. Li, Z. Zhang, K. Cui, S. Wang, X.B. Yuan, C.P. Wu, M.M. Poo, and S. Duan. 2002. Nerve growth cone guidance mediated by G protein-coupled receptors. *Nat Neurosci*. 5:843-8.

Wu, Q. and T. Maniatis. 1999. A striking organization of a large family of human neural cadherin-like cell adhesion genes. *Cell* **97:** 779–790.

Yagi, T and M. Takechi. 2000 Cadherin superfamily genes: functions, genomic organization, and neurologic diversity Genes&Dev. 14: 1169-80

Yang, B., L. Gonzalez, Jr., R. Prekeris, M. Steegmaier, R.J. Advani, and R.H. Scheller. 1999. SNARE interactions are not selective. Implications for membrane fusion specificity. *J Biol Chem*. 274:5649-53.

Yang, C.M., S. Mora, J.W. Ryder, K.J. Coker, P. Hansen, L.A. Allen, and J.E. Pessin. 2001. VAMP3 null mice display normal constitutive, insulin- and exercise-regulated vesicle trafficking. *Mol Cell Biol*. 21:1573-1580.

Zerial, M., and H. McBride. 2001. Rab proteins as membrane organizers. *Nat Rev Mol Cell Biol*. 2:107-117.

Zheng, J.Q., J.J. Wan, and M.M. Poo. 1996. Essential role of filopodia in chemotropic turning of nerve growth cone induced by a glutamate gradient. *J Neurosci*. 16:1140-9.

Zizioli, D., C. Meyer, G. Guhde, P. Saftig, K. von Figura, and P. Schu. 1999. Early embryonic death of mice deficient in gamma-adaptin. *J Biol Chem*. 274:5385-90.

VI. Deutsche Zusammenfassung

In dieser Arbeit wurde die Rolle des vesikulären SNARE Proteins Tetanus neurotoxin Insensitive VAMP (TI-VAMP, auch VAMP-7 genannt) in der neuronalen Differenzierung untersucht.

TI-VAMP gehört zur Familie der SNARE Proteine, die eine entscheidende Rolle im Membranverkehr eukaryotischer Zellen spielen. Sogenannte vesikuläre oder v-SNAREs wie TI-VAMP sind in vesikulären Transportintermediaten exprimiert, während sich die sogenannten target oder t-SNAREs auf der Zielmembran befinden. Die SNARE-Hypothesis sieht voraus, das die Komplexformation zwischen spezifischen v- und t-SNAREs zur spezifischen Fusion des Transportintermediats mit seiner Zielmembran führt. Auch wenn SNARE-Proteine nur bedingt die Spezifität von Membranfusion bestimmen, sind sie dennoch hervorragende Marker spezifischer Transportwege und genetische Inaktivierung von SNARE Proteinen führt oftmals zu dem Verlust eines spezifischen Transportwegs innerhalb der Zelle. Aus diesem Grund erlaubt das Studium eines bestimmten SNARE Proteins ein tieferes Verständis der Funktion spezifischer Membrantransportwege.

TI-VAMP ist ein ubiquitär exprimiertes v-SNARE, welches in nichtneuronalen Zellen in einem spätendosomalen Kompartiment lokalisiert ist. Es konnte gezeigt werden, das TI-VAMP eine Rolle in der neuronalen Differenzierung spielt, wobei der genaue Membrantransportweg und eventuelle Cargoproteine, die durch diesen Pfad transportiert werden, nicht definiert wurde. Aus diesem Grund sollte in dieser Arbeit der TI-VAMP-vermittelte Transportweg in neuronalen Zellen genauer definiert werden. Ausserdem sollten Cargoproteine identifiziert werden, um die Rolle des TI-VAMP-abhängigen Transports in der neuronalen Differenzierung besser zu verstehen.

Ein zweiter wichtiger Punkt, der in dieser Arbeit näher untersucht werden sollte, war die Frage nach der Regulation des TI-VAMP-vermittelten vesikulären Transports. Die neuronale Differenzierung ist ein Prozess von ausserordentlicher Komplexität. Das Auswachsen von Axonen und Dendriten verläuft entlang genau definierter Bahnen, die durch direkte Zell-Zell-Interaktionen oder Bindung von sekretierten Signalmolekülen an einen Rezeptor vorgegeben werden. Die Signale können entweder anziehender oder abstossender Natur sein, und dementsprechend

wird das wachsende Axon in einen bestimmten Hirnbereich eindringen oder aber ihn meiden. Dieses zielgerichtete Wachstum von Neuriten während der Hirnentwicklung erlaubt letztendlich das komplexe Muster an synaptischen Kontakten im adulten Gehirn. Somit ist klar, dass der Membranverkehr, welcher Wachstum von Neuriten erlaubt, einer strikten Kontrolle unterliegen muss. In dieser Arbeit sollte die Hypothese getestet werden, ob Signalmoleküle, die die axonale Navigation kontrolieren, einen Einfluss auf den TI-VAMP-vermittelten Membranverkehr haben.

Im ersten Teil dieser Arbeit wird gezeigt, das die Expression von TI-VAMP für effizientes Auswachsen von Neuriten notwendig ist. Transfektion der neuronalen Zellinie PC12 mit inhiborischen, kleine RNAs spezifisch für die mRNA Sequenz von TI-VAMP inhibieren die Expression dieses Proteins. Als Folge ist das Auswachsen von Neuriten in der Zellinie PC12 inhibiert. Es kann gezeigt werden, dass TI-VAMP mit target SNARE Proteinen der Plasmamembran und des endosomalen Systems im Gehirn der Ratte interagiert. Ausserdem wird demonstriert, dass TI-VAMP-positive Vesikel direkt mit der Plasmamembran fusionieren. Daher kann davon ausgegangen werden, dass TI-VAMP den Austausch von Proteinen und Lipiden zwischen der Zelloberfläche und einem intrazellulären, endosomalen System vermittelt und dass dieser Transportweg von entscheidender Bedeutung für die neuronale Differenzierung ist.

Das Zell-Zell Adhesionsmolekül L1, welches eine wichtige Rolle in der Gehirnentwicklung spielt, colokalisiert mit TI-VAMP im embryonalen Gehirn, in *in vitro*-kultivierten primären Neuronen sowie in der Zellinie PC12. L1 wird von der Plasmamembran in ein intrazelluläres, TI-VAMP-positives Membrankompartiment aufgenommen. Da Inhibierung der TI-VAMP-Expression eine verminderte Expression von L1 an der Zelloberfläche provoziert, sind die TI-VAMP-positiven Vesikel wahrscheinlich an dem Transport von L1 von einem endosomalen Kompartiment zur Plasmamembran beteiligt. Inhibierung der TI-VAMP-Expression provoziert nicht nur eine verminderte Expression von L1 an der Zelloberfläche, sondern auch die selektive Instabilität von L1-vermittelten adhesiven Kontakten. Gleichzeitig hat die verminderte Expression von TI-VAMP keinen Einfluss auf die Stabilität von N-Cadherin-abhängigen Adhesionsverbindungen. Somit wird in diesem ersten Teil der Arbeit demonstriert, das der TI-VAMP-abhängige Membranverkehr in neuronalen Zellen eine entscheidende Rolle in der neuronalen Differenzierung spielt. Vermutlich ist der TI-VAMP-vermittelte Transport des Zelladhesionsmolküls L1 hierbei von

grosser Bedeutung. L1 spielt eine wichtige Rolle in der neuronalen Diffenzierung, da Mutationen dieses Moleküls zu schweren Missbildungen des Gehirns in Maus und Mensch führt.

Im zweiten Teil dieser Arbeit wird gezeigt, das die Dynamik des TI-VAMP-Kompartiments in Neuronen von dem Aktincytoskelett abhängig ist. Behandlung von Neuronen mit aktindepolymerisierenden Drogen führt zu einer drastischen Delokalisation von TI-VAMP. Somit kann die Dynamik des TI-VAMP-Kompartiments in Neuronen direkt durch die Dynamik des Aktincytoskeletts bestimmt werden. Das Aktincytoskelett spielt eine wichtige Rolle in der axonalen Navigation während der Entwicklung, und seine Dynamik wird durch Navigationssignale bestimmt. In der Tat kann gezeigt werden, dass die lokale Aktivierung des Adhesionsmolekül L1 zu einer gleichzeitigen Akkumulation von Actin und TI-VAMP-positiven Vesikeln führt. Die Akkumulierung der TI-VAMP-Vesikel ist spezifisch für L1-vermittelte adhesive Kontakte und wird nicht durch N-Cadherin-vermittelte Kontakte induziert. Ausserdem ist die Akkumulation intrazellulärer Membranen hochspezifisch für das TI-VAMP-Kompartiment. Es kann gezeigt werden, dass L1-induzierte adhesive Kontakte einen Signaltransduktionsweg aktivieren, welcher Tyrosinphosphorylierungen und Aktivierung von Tyrosinkinasen der src Familie beinhaltet. Es kann davon ausgegangen werden, das die beobachtete Rekrutierung von Aktin und des TI-VAMP-Kompartiments von diesen oder ähnlichen Signaltransduktionsketten abhängt. Somit kann in diesem zweiten Teil der Arbeit gezeigt werden, dass das TI-VAMP-Kompartiment durch Signale wie zum Beispiel die Aktivierung des Adhesionsmolküls L1 reguliert wird, welche das Navigieren von Axonen während der Gehirnentwicklung ermöglichen.

Die Beobachtung, dass die Dynamik des Cytoskeletts und Membranverkehr in koordinierter Weise durch morphogenetische Signale reguliert wird, ist von grossem Interesse. Sie legt nahe, dass Zelladhesionsmoleküle wie L1 eine Rolle in neuronaler Morphogenese nicht nur als Vermittler von Zell-Zell-Adhesion und Regulatoren von Signaltransduktionswegen spielen können, sondern gleichzeitig einen zielgerichteten Transport von Vesikeln zu Adhesionskontakten ermöglichen.

Zusammengefasst wird in dieser Arbeit gezeigt, dass TI-VAMP den intrazellulären Transport von L1 vermittelt und das gleichzeitig L1-vermittelte Adhesion die Dynamik dieses Membrantransportweges kontrolliert. Das funktionelle

Zusammenspiel zwischen Zelladhesion und Membranverkehr, welches hier demonstriert wird, ist vermutlich von grosser Wichtigkeit für die Koordinierung der neuronalen Differenzierung.

"Ich versichere, daß ich die von mir vorgelegte Dissertation selbständig angefertigt, die benutzten Quellen und Hilfsmittel vollständig angegeben und die Stellen der Arbeit - einschließlich Tabellen, Karten und Abbildungen -, die anderen Werken im Wortlaut oder dem Sinn nach entnommen sind, in jedem Einzelfall als Entlehnung kenntlich gemacht habe; daß diese Dissertation noch keiner anderen Fakultät oder Universität zur Prüfung vorgelegen hat; daß sie - abgesehen von unten angegebenen Teilpublikationen - noch nicht veröffentlicht worden ist sowie, daß ich eine solche Veröffentlichung vor Abschluß des Promotionsverfahrens nicht vornehmen werde. Die Bestimmungen dieser Promotionsordnung sind mir bekannt. Die von mir vorgelegte Dissertation ist von Dr Thierry Galli betreut worden."

Teilpublikationen zu einigen der in Abschnitt III beschriebenen Versuchen:

Alberts, P., R. Rudge, I. Hinners, A. Muzerelle, S. Martinez-Arca, T. Irinopoulou, V. Marthiens, S. Tooze, F. Rathjen, P. Gaspar, and T. Galli. 2003. Cross Talk between Tetanus Neurotoxin-insensitive Vesicle-associated Membrane Protein-mediated Transport and L1-mediated Adhesion. *Mol. Biol. Cell*. 14:4207-4220.

Muzerelle, A., **P. Alberts**, S. Martinez Arca, O. Jeannequin, P. Lafaye, J.-C. Mazié, T. Galli, and P. Gaspar. 2003. Identification of a presynaptic membrane compartment containing Tetanus Neurotoxin-Insensitive Vesicle Associated Membrane Protein in the rat brain. *Neuroscience (in press)*.

Martinez-Arca, S., **P. Alberts**, A. Zahraoui, D. Louvard, and T. Galli. 2000. Role of tetanus neurotoxin insensitive vesicle-associated membrane protein (TI-VAMP) in vesicular transport mediating neurite outgrowth. *J Cell Biol*. 149:889-899.

Danksagung

Als erstes möchte ich mich ganz herzlich bei Dr Thierry Galli bedanken. Sein persönliches Engagement, sein Ideenreichtum und seine spontane Art, Dinge in die Wege zu leiten, waren ein entscheidender Bestandteil für den Fortgang dieser Arbeit. Auch möchte ich mich ganz herzlich bedanken für seinen tapferen und phantasievollen Kampf gegen bürokratische Hürden, der meinen Aufenthalt in Paris um vieles erleichtert hat.

Bedanken möchte ich mich bei Professor Jonathan C. Howard, dass er die Verantwortung als Doktorvater dieser Arbeit ohne Zögern übernommen hat und für sein stetes Interesse am Fortgang dieser Arbeit.

Auch bedanke ich mich bei meinen Kollegen der Arbeitsgruppe Galli, Sonja Martinez, Veronique Proux, Rachel Rudge und Fabrice Laroche, für ein anregendes und freundschaftliches Arbeitsklima. Vor allem Rachel gilt mein Dank für ihre geduldige Hilfe bei der inhaltlichen und sprachlichen Korrektur dieser Arbeit.

Des weiteren möchte ich mich natürlich auch ganz herzlich bei allen Mitarbeitern der INSERM Unite 536 und ehemaligen Mitarbeitern am Institut Curie bedanken. Das herzliche Arbeitsklima war unersetzlich für die Freude an dieser Arbeit.

Mein Dank gilt Veronique Marthiens, denn ohne unsere gelegentlichen Gespräche über aktuelle Experimente wäre der Crosstalk vermutlich ein Monolog von TI-VAMP an L1 geblieben; des weiteren mein Dank an die restlichen Mitglieder der Arbeitsgruppe Mege, Julie Gavard und Mireille Lambert, für die grosszügige Bereitstellung von Reagenzien.

Mein Dank gilt auch Bernadette Alincourt und Alain Prochiantz für die Anleitung zum Erlernen der Primärkultur von Neuronen.

Zum Schluss möchte ich mich auch bei Dr Michael Knittler bedanken, der zusammen mit Jonathan den Spass am wissenschaftlichen Arbeiten in mir geweckt hat, und der während meiner Doktorarbeit immer ein offenes Ohr für mich hatte.